POLITECNICO DI TORINO

Facoltà di Ingegneria dell'Informazione

Corso di Laurea in Ingegneria dell'Informazione

Tesi di Laurea

Optical Interconnections based on Microring Resonators

Relatore:
Prof. Fabio Neri

Candidato:
Miquel Garrich

Ottobre 2009

Abstract

The aim of this thesis is to present and analyse optical interconnection architectures based on microring resonators.

The trend of meeting large bandwidth and strict latency requirements in both global on-chip and off-chip communication face critical challenges in maintaining a sustainable performance-per-watt. Optical technologies support the immense bandwidth allowed by wavelength division multiplexed (WDM) while could offer a significant power saving switching capabilities.

Microring resonators have received considerable attention as promising technologies for realizing photonic integrated circuits. Their small footprint and their capacity for processing high-bandwidth WDM data can lead these devices become the key elements for the switch nodes in next-generation telecommunication networks.

This thesis firstly describes the basic principles of operation of a microring resonator defining 1x2 basic switching element (1B-SE). Then, the 2x2 basic SE (2B-SE) based on two 1B-SEs jointly controlled and the new 2x2 mirrored SE (2M-SE) are characterised as atomic building elements for interconnection architectures. The severe asymmetric behaviour presented by those SEs could limit the scalability of classical optical switching fabrics and we aim at balancing the complexity and optical signal level.

In a second stage, the well-known switching theory is revised in order to classify the interconnection architectures according to their characteristics when using that SEs as building element. It is applied an exhaustive procedure to obtain the performance of classical Crossbar and Benes structures and of the newly proposed Mirroring and HBC structures.

Thereafter, using as a starting point for each analysed structure the characterisation previously obtained, the scalability response of larger switching fabrics is explored. Then we define a construction rule for the new proposed architectures of which we assess the complexity in terms of used microrings.

In a third stage, the results of all the architectures presented and analysed before are compared. The different solutions are also discussed to distinguish suitable network structures according to each network size.

In conclusion, this thesis presents, defines, describes and analyses several solutions to the trade-off between complexity and scalability of interconnection architectures when microring resonators are used as basic switching elements. Finally, as future research lines the author suggests a complex microring model, AWG involvement and scheduling algorithms.

This work has been partially supported by the BONE project, a Network of Excellence funded by the European Commission within the 7th Framework Programme. The obtained results have been partially compiled in a publication for the IEEE International Conference on Photonics in Switching 2009, Pisa, Italy.

Contents

1 Introduction **1**

1.1 Optical Microring Resonator 4

1.2 Objectives 5

1.3 Structure of the thesis 6

2 Related theory **9**

2.1 Optical Microring Resonator 9

2.1.1 System characterisation of Microring SE 11

2.1.2 Asymmetry brief 14

2.2 Architectures 14

3 Method and Simulations **19**

3.1 Microring-based switching elements 19

3.1.1 1B-SE, 2B-SE, 2M-SE 19

3.2 Crossbar 23

3.3 Preliminary Considerations 26

3.4 Benes 29

3.4.1 Basic Benes configuration 29

3.4.2 Modified Benes configuration 38

3.4.3 Waksman 48

3.5 Cumulative approach to the analysis 49

3.6 Mirroring 52

3.6.1 Mirrored network 52

3.6.2 Mirrored plane 61

3.7 Benes-crossbar (HBC) 67

4 Results and Discussion **71**
4.1 Benes 71
4.2 Mirroring 76
4.2.1 Mirrored plane 77
4.2.2 Recursive mirroring 80
4.3 Benes-crossbar (HBC) 84
4.3.1 basic HBC 85
4.3.2 mirrored HBC 88
4.4 Clos 92
4.4.1 Clos all crossbar 94
4.4.2 Clos-Benes (HCB) 96
4.4.3 Clos-mirrored Benes (M-HCB) 100
4.5 Vertical Replication 103
4.6 Discussion 108

5 Conclusion **113**
5.1 Main findings 113
5.2 Future research lines 114

Bibliography **115**

Bibliography **117**

Chapter 1

Introduction

The recent emergence of chip multiprocessors (CMPs) that obtain a better performance increasing the number of computational cores has changed the trend in system interconnects and global communications infrastructure. CMP architectures reach high parallel computing and their performance is directly tied to how efficiently the parallelism of the system is exploited and its aggregate compute power used. Therefore, when the number of functional parallel units scales those systems achieve the maximum utilization of compute resources increasing the efficiency of the information exchange among these resources. Thus, the global on-chip communications becomes a very important feature in the ultimate CMP system performance.

The realization of a scalable on-chip and off-chip communication infrastructure faces critical challenges in meeting the enormous bandwidths, capacities, and stringent latency requirements demanded by CMPs maintaining a suitable performance-per-watt. Several evidences on path to multiplication of on-chip processing cores appear in POWER series of IBM [1], Niagara [2] or Intel's 80-core multiprocessor (see Figure 1.1) that delivers a computing performance over 1 TeraFLOP [3]. The importance of improving a low-power communication infrastructure for those next generation multiprocessors lets photonic Networks on Chip (NoC) offer a promising solution [4].

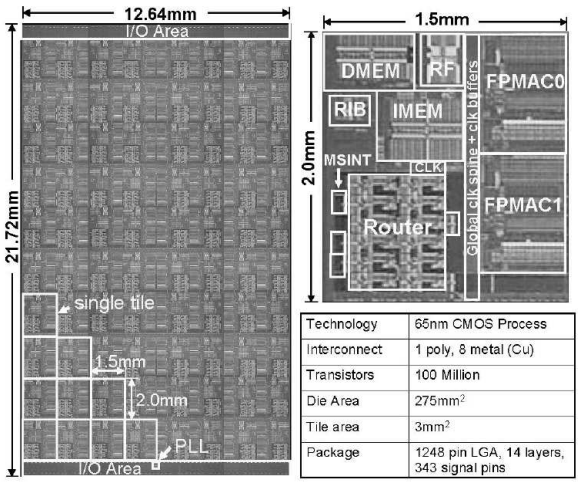

Figure 1.1: Intel's 80-core full-chip and tile micrograph and characteristics [3]

Current integrated photonic technology presents huge advancements in fabrication capabilities of nano-scale devices and precise control over their optical properties. Importantly, these breakthroughs have led to the development of silicon photonic device integration with electronics directly in commercial CMOS [5] (see Figure 1.2). For the first time, we can consider the practical insertion of high-speed optical communications directly between silicon, as the communications infrastructure for CMPs.

Photonic NoCs deliver a huge reduction in power expended on intrachip global communications confirming the unique benefits for future generations of CMPs [6]. Photonic NoCs essentially change the power scalability rules: as a result of the low loss in optical waveguides, once a photonic path is established, the data are transmitted end-to-end without the need for repeating, regeneration or buffering. In electronic NoCs, on the other hand, a message is buffered, regenerated and then transmitted on the inter-router links multiple times en route to its destination. Furthermore, the switching and regenerating elements in CMOS consume dynamic power that grows with the data rate. The power consumption of optical switching elements, conversely, is independent of the bit rate, so high bandwidth messages do not consume additional dynamic power.

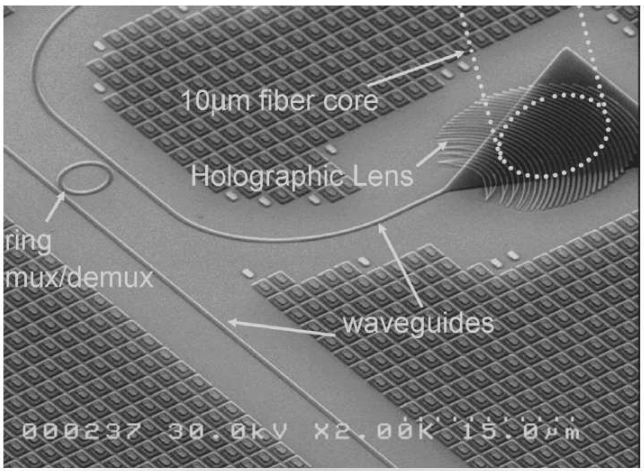

Figure 1.2: Optical fiber connected to waveguides by holographic lens [5]

Optical technology presents design challenges different from those faced by electronic NoC designers. While in CMOS technology buffers and processing resources are abundant and are amply used, they are very difficult to implement in optics. Considering the small chip-scale area, no buffers or all-optical processing can be used. To utilize the advantages of photonics in constructing a NoC, we use a hybrid approach: a network of silicon optical switching elements and waveguides is used for mass message transmission, and an electronic network, with the same topology, is used for distributed control and short message exchange. This hybrid micro-architecture combines a circuit-switched network with an electronic packet-switched control network as models used in [4], [6], [7] and [8].

In conclusion, physical layer arrangement of the photonic components is an important consideration for the performance of the network. Moreover, implementing non-blocking photonic switching architectures can increase the utilization, and confirm the benefits that can be achieved by bringing photonics into the chip.

1.1 Optical Microring Resonator

The silicon-on-insulator (SOI) technology is attractive for realizing photonic integrated circuit-based interconnection networks due to high index contrast and complementary metal-oxide-semiconductor compatibility [5] [9] [10]. Thus, microring resonators present attractive building blocks, having exhibited complex passive filters [11], as well as electrooptic and all-optical modulators [12] performing a limited power dissipation. With the growing need for short-range optical interconnect technology at the board-to-board or chip-to-chip levels, it is expected that microrings will play an important role in the photonics device trend for the next decade.

In order to give a brief introduction to the microring resonator, we mention several basic characteristics. The main feature of the ring resonator is its transfer function identical to that one of the Fabry-Perot cavity, and it has been demonstrated a technique of comb switching by using a single ring resonator for WDM applications [12]. The ring resonator has a relatively small free spectral range (FSR) corresponding approximately to the wavelength spacing used in dense-WDM (0.8 nm), and can simultaneously switch on and off a large number of wavelength channels. Moreover, it has also been proved that a single microring resonator achieve all-optical switching of 20 continuous-wave wavelength channels simultaneously [10].

Regarding to physical design, A microring resonator consists of a circularly-bent waveguide which joins up with itself to form a ring, whose diameter is typically 10-1000 times the wavelength, depending on the refractive indices of the materials that comprise the waveguide (index contrast). Usually, one or two straight waveguides are near the microring, which serve as input and output pathways for the light. Since in the most of the cases two waveguides will be near the microring, means that there are four available ports for the input/output of the optical signals as we can observe in Figure 1.3. The microscopic microring depicted in Figure 1.3 presents a slight model as the considered in this work, where the ring is coupled to two straight waveguides with the same cross section, one acting as an input port and through port, and the other acting as a drop port. Despite having another input/output at the drop port waveguide, it will not be considered.

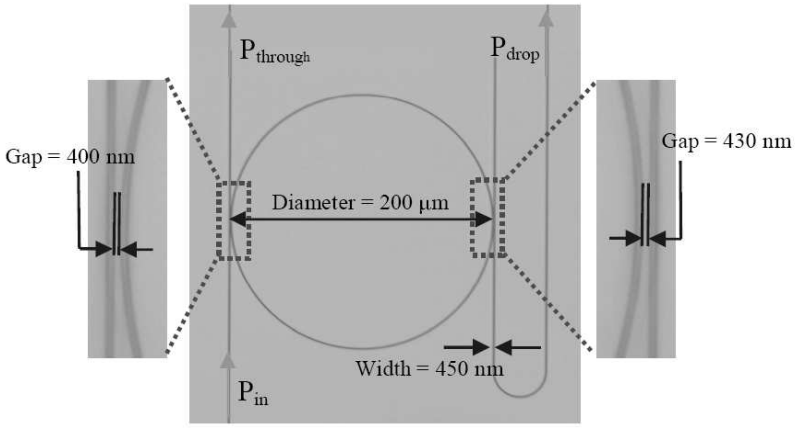

Figure 1.3: Microscopic picture of a single microring resonator [12]

The microring resonator analysed in *All-optical compact silicon comb. switch* [12] and depicted in Figure 1.3 is tuned by pumping optical pulses as in [10] or [13]. But the performed transfer function can also be shifted by carrier injection using p-i-n junctions as in [9], [4], [19] or [20]; or by thermal tuning [14] [18].

1.2 Objectives

The main objective of this work is to present and analyse optical interconnection architectures based on microring resonators. In order to reach this goal, two collateral objectives need to be carried out:

- For one side, it will be firstly presented the microring resonator model used and its scalability, emphasising those characteristics that make this switching element (SE) change the point of view of classical interconnection networks.

- For the other side, becomes an objective characterise several switching architectures, i.e., using classical metrics (as complexity), recalling well-known routing algorithms and construction rules.

Once the most important parts of the main objective will be executed separately, we will face the global goal, that is evaluate interconnection architectures using microring resonators. Again, the objective will be faced in two steps as follows:

- A new procedure to perform the characterisation will be presented being necessary a new metric to compare different networks from the microring resonator characterisation point of view.

- Finally, we should compare all the interconnection architectures analysed mapping them and presenting the most advantageous solutions able to balance the trade-off complexity and scalability.

1.3 Structure of the thesis

In order to reach those objectives previously presented, this work devotes first and second chapters to do an overview of current technology and theory basics, letting the last three chapters face the goals mentioned.

1 Introduction

In this chapter the reader has been introduced to the present technology, mentioning advances in CMP, CMOS and integration of photonics into NoC. Microring resonator is presented giving several characteristics, basic principles of operation and *tuning* alternatives letting the reader slightly infer the technological motivation of this work.

2 Related theory

The first part of this chapter is devoted to present an accurate microring resonator model that is slightly used to define the 1x2 basic switching element (SE) in the following chapter three. At this point it is made especial emphasis to those characteristics that make this SE change the point of view of classical interconnection networks.

Secondly, well-known switching theory is provided, i.e., basic construction rules, complexity and routing algorithms. Those theory basics is taken into account on following analysing steps.

3 Method and simulations

This chapter firsts describes the behaviour of the 1x2 basic switching element (1B-SE) used. Then, are characterised the basic 2x2 basic SE (2B-SE) based on two 1B-SEs jointly controlled and the newly proposed 2x2 mirrored SE (2M-SE) as atomic building elements for the interconnection architectures. It is focused the severe asymmetric behaviour presented by those SEs that could limit the scalability of classical optical switching fabrics. It is applied an exhaustive procedure to obtain the performance of either classical small Crossbar and Benes structures. Moreover, are explained several examples of specific matching requests for those networks. Finally, newly proposed small Mirroring and HBC structures are characterised and exemplified.

4 Results and discussion

This forth chapter uses as a starting point for each analysed structure the previously small characterisation obtained. Then, are explored the scalability response of larger switching fabrics. Are described the construction rules applied to reach those higher network sizes indicating at the same time the complexity and, obviously, the performance achieved. Nevertheless if necessary, it is subdivided that building procedure, scalability and cost into slight different versions of the initial network structures. Thus, we close the scalability response characterisation of each network presenting its corresponding plot and obtained values. Then, an overall comparison and discussion between all the obtained results is made.

5 Conclusion

This final chapter firstly summarises our work done in the area and points out the relevant findings. And secondly, future research lines are suggested e.g., complex microring model, AWG involvement, scheduling algorithms and layout design.

Chapter 2

Related theory

This second chapter firstly presents an accurate microring resonator model. Several characteristics are considered to define the 1x2 basic switching element (SE) in the following chapter three. At this point it is made especial emphasis to those characteristics that make this SE change the point of view of classical interconnection networks.

2.1 Optical Microring Resonator

It is important to recall the similarity between the transfer function of the microring resonator and that one of the Fabry-Perot cavity. Figure 2.1 shows the transmission spectra of a microring resonator, we can observe the most flat behaviour of the power delivered from the input port to the through port, but for those optical frequencies that *resonate* with the microring, most of the power is delivered to the drop port. In fact, light traveling in the input waveguide whose wavelength is a divisor of the optical path length L can couple into the ring and form a standing wave pattern in the ring resonator we say that this wavelength is *on-resonance* with the ring. Light of wavelengths far from the resonance wavelengths does not see the ring and simply travels in the straight waveguide from input port to the through port without being coupled into the ring [15]. In any case, the selectivity and flatness of the spectral response may be improved by cascading more rings in series or in parallel, whose study exceeds objective of this work.

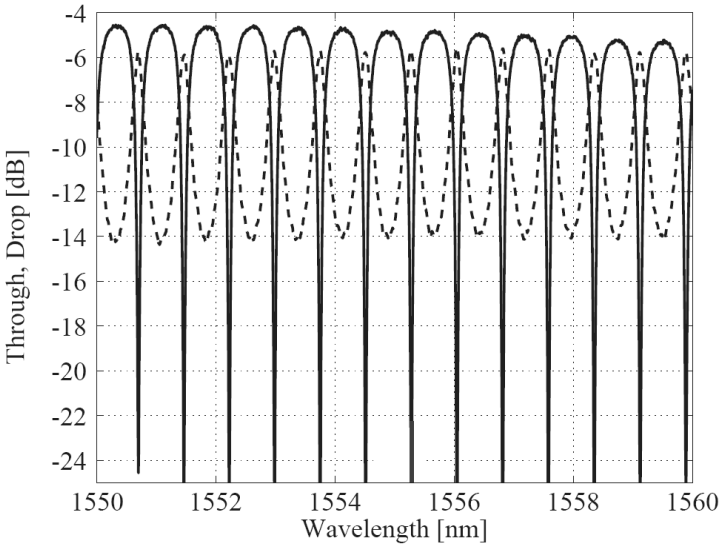

Figure 2.1: Transmission spectra of the ring resonator [15]. Trough port in continue line and drop port in dashed line

The transfer function presented in Figure 2.1 (through port identified by continue line, drop port by dashed line) depends on the diameter of the microring and the refractive index contrast. For instance, work presented on [14] uses rings having 20-μm diameter corresponding to an 8-nm free-spectral-range (FSR) (that is 10 channels in a 100 GHz spaced WDM system), in [13] are used 100-μm diameter rings that imply a 1.6-nm FSR, and in [15] is presented an example of a single ring filter with a radius 312-μm corresponding to a FSR=100GHz. Nevertheless, in those examples mentioned, different index contrast are used, satisfying the following expression:

$$FSR \equiv \frac{c}{n_{group} 2\pi R} \tag{2.1}$$

Where R is the microring radius, and n_{group} is the waveguide group refractive index. Due to chromatic dispersion the group refractive index is wavelength dependent according to the relation $\Delta n_{group} = c\beta_2 \Delta w$ where β_2 is the cromatic dispersion and takes into account both the material and the waveguide contribution.

Figure 2.2b shows a waveguide-coupled double microring resonators with selectively integrated p-i-n diodes and being **I** Input port; **T**: Throughput port; and **D**: Drop port. Nevertheless, the study of the double microring resonator exceeds the objective of this work, but the aim of Figure 2.2b and its scanning electron micrograph 2.2a is to present a microring tuned by carrier injection using p-i-n junctions [9].

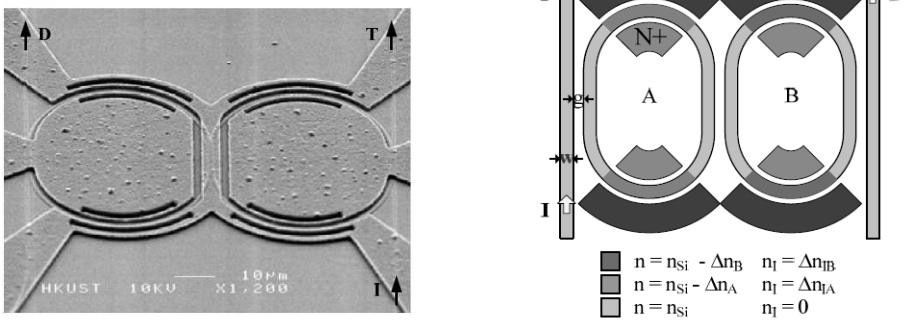

(a) Micrograph of a couple microring resonators electrooptic switch in SOI [9]

(b) Schematic of the double microring resonators in [9]

Figure 2.2: Double microring silicon electrooptic switch

Therefore, when the *tuning* of the microring resonators is made by carrier injection using p-i-n junctions as in [9], [19] or [20], it has been experimentally demonstrated a switching time of 30 ps [4]. In those other cases where the shifting of the transfer function is made by pumping optical pulses as in works [10] or [13], the switch has a switching time of less than 1 ns [12]. Finally, the lowest performed switching time is exhibit by thermal tuned rings [14] or [18].

2.1.1 System characterisation of Microring SE

Describing the microring resonator from the physical model point of view is not a main objective of this work. Nevertheless, we discuss several physical characteristics to give the background necessary to study scalability of microring based interconnection architectures [19].

In our characterisation, we consider the signal transmission on a wavelength that matches with the maximum of the through port of the transfer function (see Figure 2.1) when the ring is non-tuned. By tuning the ring and shifting the transfer function (for instance by carrier injection [9]), our wavelength considered matches with the maximum drop port.

Figure 2.3 depicts the two possible states of the 1x2 microring based switching element.

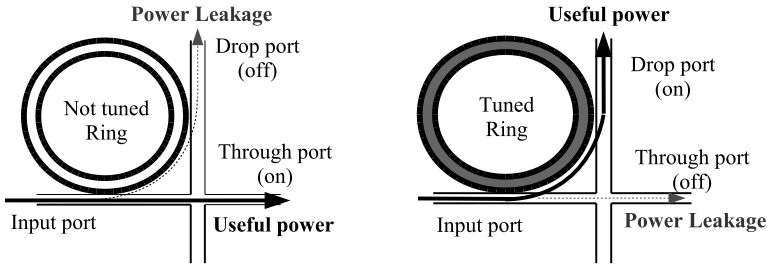

(a) 1x2 microring based not tuned state

(b) 1x2 microring based tuned state

Figure 2.3: Microring switching element 1x2 in its two possible states

From one side, Figure 2.3a depicts the non-tuned state. We can observe the signal entering the input port and going out by the through port. In this state, the signal wavelength matches with the maximum **through** in the transfer function (see Figure 2.1). Reaching this the maximum of the transfer function of the ring, the signal reaches the through out port with negligible losses 0.1dB[10](*power through ON*). At the same time, a small part of the useful signal is deflected to the drop port (matching the minimum of the **drop** curve of the transmission spectra). This power leakage suffers a high penalty due to coupling the ring (called *power drop OFF*).

From the other side, Figure 2.3b shows the tuned state of the ring. In this state, the signal wavelength matches with the maximum of the **drop** curve in the transfer function (see Figure 2.1). Now, the useful power obtained at the drop port (called *power drop ON*) is lower than the previously *power through ON*. Experimental measurements report that coupling the ring in order to reach the drop port costs non negligible attenuation 2.3dB[10]. At the same time, a higher value of power leakage is obtained at the trough port (called *Power through OFF*) since the signal does not couple the ring.

Summarising,

$$power\ through\ ON\ >\ power\ drop\ ON$$
$$\text{and}$$
$$power\ through\ OFF\ >\ power\ drop\ OFF$$

Figure 2.4 depicts the two possible states of the 2x2 microring based switching element.

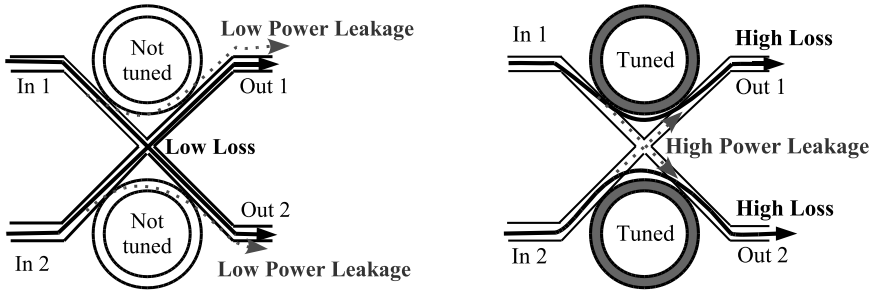

(a) 1x2 microring based not tuned state (b) 1x2 microring based tuned state

Figure 2.4: Microring switching element 1x2 in its two possible states

Now, when using a 2x2 basic switching block made with two jointly controlled 1B-SE, two possible states can be provided, *cross* (in1 → out2, in2 → out1) and *bar* (in1 → out1, in2 → out2). Useful power and leakage power issues are considered for each state:

Figure 2.4a depicts the *cross* state,

- Both useful signals (from input port one and input port two respectively) take negligible losses reaching the maximum of the **through** transfer function. Thus, at each corresponding output we get *power through ON* defined for the 1x2 switching element. Hence, we consider this state as low-losses state.

- From the crosstalk point of view, power leakage from each input reaches its corresponding output degenerating the signal. We can observe that *power drop OFF* is obtained at output one from input one, and at output two from input two respectively. Hence, we consider this state as low crosstalk state.

Figure 2.4b shows the *bar* state,

- Both useful signals take higher losses (compared with *cross* state) reaching the maximum of the **drop** transfer function. Thus, at each corresponding output we get *power drop ON* for both signals. Hence, we consider this state as high-losses state.

- From the crosstalk perspective, power leakage from each input reaches its corresponding output degenerating the signal. We can observe that *power through OFF* is obtained at output two from input one, and at output two from input one respectively. Hence, we consider this state as high crosstalk state.

2.1.2 Asymmetry brief

We have seen the high asymmetrical behaviour presented by microring based switching elements. This intrinsic loss and crosstalk asymmetry could limit the number of successive switching elements achieved. *Scalability* will be considered, for the rest of this work, as the number of high loss/crosstalk states a signal is able to reach.

Therefore, we aim at face this asymmetric issues by designing suitable switching architectures. With this proposal, we define quite simply microring-based Switching Elements (SEs). In next Section 3.1 will be defined three type of SEs highlighting the losses of the useful signal (see Figures 3.1, 3.2 and 3.3).

2.2 Architectures

In this second part of this chapter two, well-known switching theory is provided [16] [17]. From the more generic networks, we recall Clos network, and its matrix used to represent the paths set; then, we recall strictly non blocking condition; and finally, the rearrangeable non blocking condition to present Benes network and its construction rule.

Clos network

Figure 2.5 depicts a three-stage Clos network where in the i-th stage m_i is the number of inputs per module, n_i is number of outputs per module and r_i is the total number of modules. Each module of those r_i belonging to that stage, has and identifier, e.g., $M_i = \{1,2,\ldots,r_i\}$. We assume that only exists one connection between two modules in successive stages, that is no dilated links:

$$r_1 = m_2, r_2 = n_1 = m_3, r_3 = m_2$$

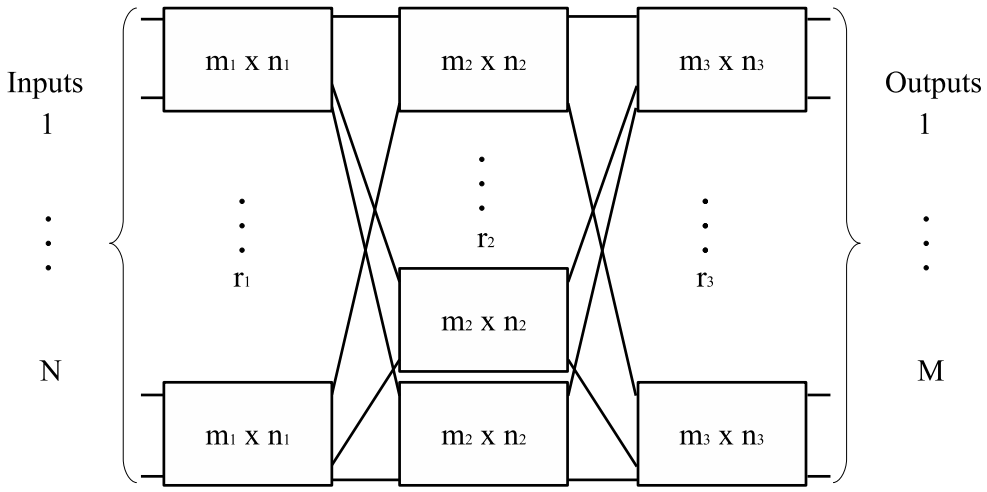

Figure 2.5: Clos network with $N = m_1 r_1$ and $M = r_3 n_3$

Paull's matrix and algorithm

Paull s matrix $(P)$is used to describe the state of the active connections present in a Clos network. In fact, that is switching configurations of all the middle-stage modules. Paull's matrix is characterised by the following points:

- $P = [P_{ij}]$ is a $r_1 \times r_3$ size matrix.
- Each P_{ij} element of the matrix is a set of module identifiers $M_2 = \{1,2,\ldots,r_i\}$ belonging to the second stage (because M_2 for this specific case).

- If one of those module identifiers (k) is in a position of the matrix, that is $k \in P_{ij}$, means that module k is connecting first stage module i with third stage module j.
- Feasibility conditions:
  - Each row with at most m_1 symbols.
  - Each column with at most n_3 symbols.
  - Each element with at most $min\{m_1,n_3\}$ symbols.
  - Each $k \in M_2$ appears at most once for each row and column.

Paull's algorithm is an incremental algorithm, used to add one connection at one time and eventually reconfigure the network. Because of the previously Clos network assumptions considered, and the Paull's matrix construction, we know that: the number of connections in the first-stage cannot exceed the number of the matrix inputs (rows), the number of connections in the last-stage cannot exceed the number of the matrix outputs (columns), and both numbers cannot exceed the number of paths that is equal to the number of middle-stage modules. Furthermore, each symbol cannot appear more than once in a row or in a column, since only one link connects matrices of adjacent stages (no dilated links condition).

Strictly non blocking (SNB) condition

Clos theorem: A Clos network is SNB if and only if the number of second stage switches r_2 satisfies:

$$r_2 \geq m_1 + n_3 - 1$$

In particular, a symmetric network with $m_1 = n_3 = n$ is SNB if and only if

$$r_2 \geq 2n - 1$$

We can proof the Clos theorem assuming that module i of the first-stage should be connected to module j of the third-stage. Hence, a new symbol should be added in P_{ij} of PaullŠs matrix P. In the worst case, there are already $m_1 - 1$ symbols in the i-th row of P and $n_3 - 1$ symbols in the j-th

column. Because of the building definition of the Paull's matrix, they are all distinct. Hence, to find a new symbol available in the middle-stage, it should be $r2 > (m1 - 1) + (n3 - 1)$ which implies $r2 \geq m1 + n3 - 1$.

Rearrangeable non blocking (RNB) condition, Benes network

Slepian-Duguid Theorem: A Clos network is RNB if and only if the number of second stage switches r2 satisfies:

$$r2 > max\{m_1,n_3\}$$

In particular, a symmetric network with $m_1 = n_3 = n$ is SNB if and only

$$r2 > n$$

Benes construction rule

Figure 2.6 shows the construction rule applied to obtain a Benes network.

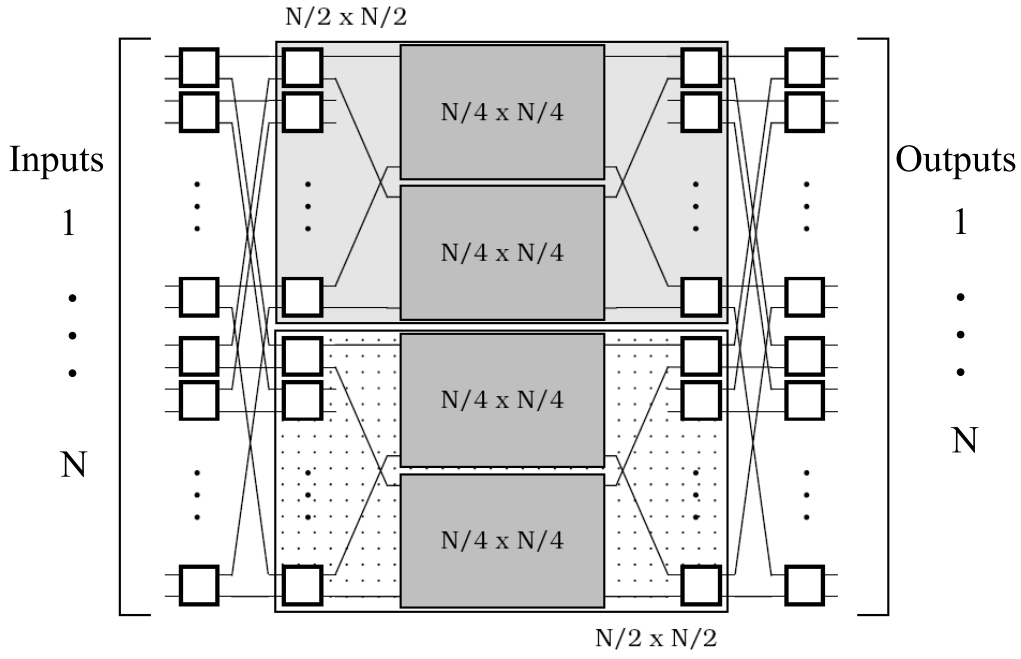

Figure 2.6: Recursive network construction rule

The starting point is to consider a $N \times N$ Slepian-Duguid network with $n_1 = m_3 = 2$. Then, we have $N/2$ switching elements of size 2×2 in the first and third stage and two $N/2 \times N/2$ matrices in the second stage suitably connected to guarantee full connectivity. Now, each of the two $N/2 \times N/2$ matrices is again built as a three-stage structure with 2×2 elements at the edges. This procedure is iterated until the second stage matrices have size 2×2.

We obtain for a Benes network a number of rows $= N/2$ and a number of stages $= 2\log_2 N - 1$ (columns). Hence, the number of SE:

$$Number\ of\ SE = 2\log_2 N - \frac{N}{2}$$

Looping algorithm

Looping algorithm is used to set-up a matching request through a Benes network identifying all the states of the SEs. In fact, it is equivalent to Paull's algorithm using a particular sequence of switching requests.

1. **Loop start**: We select in the first stage the unconnected busy input of an already connected SE, otherwise we select a busy inlet of an unconnected SE; if there is no input to select, the algorithm ends.

2. **Forward connection**: We connect the selected input to the requested output through the only accessible subnetwork if the SE is already connected to the other subnetwork, or through a randomly selected subnetwork if the SE is not yet connected; if the other output of the element just reached is busy, we select it and go to step 3; otherwise we go to step 1.

3. **Backward connection** Connect the selected output to the requested network input through the subnetwork not used in the forward connection; if the other input of the SE just reached is busy and not yet connected, we select it and we go to step 2; otherwise we go to step 1.

Chapter 3

Method and Simulations

The performance of different small switching fabrics using microring resonators as atomic element in the Switching Elements (SE) construction will be described in this chapter. In Section 3.1 all the possible basic building SEs are presented. In Section 3.2 the well known Crossbar switching architecture will be presented and characterised. After that, in 3.4 the Benes network and several slight modifications are analysed with an heuristic procedure. Finally, in Sections 3.6 and 3.7 new construction patterns and architectures (Mirroring and HBC) are presented.

3.1 Microring-based switching elements

3.1.1 1B-SE, 2B-SE, 2M-SE

The different classes of Switching Elements (SE) are described now to provide the background necessary in the analysis of the switching architectures that will be proposed.

Figure 3.1 shows the first simple structure for a 1x2 microring based SE (called 1B-SE). Optical signals entering the input port can be deflected either to the drop port, when the ring is properly tuned to the input signal wavelength (for instance by carrier injection [9]), or to the through port in the normal non-tuned ring state.

This 1B-SE presents an asymmetric behaviour, and as we have seen in Section 2 experimental measurements [9],[10] show that input signals coupled into the ring (to exit by the drop port) suffer larger power losses than signals routed to the through port.

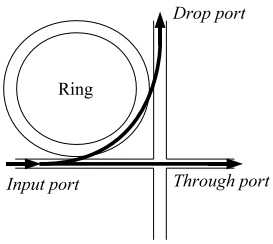

Figure 3.1: A 1x2 Basic SE (1B-SE) made with a microring

A first behaviour description can be done at this point in order to characterise the 1B-SE:

- *High-Loss State* (HL State or HLS): The SE is connecting Input port with the Drop port. In this state, the microring is suitably tuned to route the optical signal through the Drop port. For the rest of this work signal *turn* when uses the ring because of its physical resemblance with light path. In the HLS signals suffer a higher attenuation (2.3dB[10]) than in the complementary State.

- *Low-Loss State* (LL State or LLS): The SE is connecting Input port with Through port. In this state, the microring is not tuned to let the signal go through the straight waveguide. The signal takes negligible losses (0.1dB[10]) avoiding couple the ring and without the need to change two times the waveguide.

Figure 3.2 shows a SE made by two single 1b-SE. By looking at this SE construction, it can be seen that for the Ring 1 the Out port 1 acts as Drop port, and Out port 2 as Trough port. But for the Ring 2, the Out port 1 behaves as its Through port, and the Out port 2 as its Drop port. Two microrings are controlled simultaneously, providing two asymmetric states as in the case of 1B-SE.

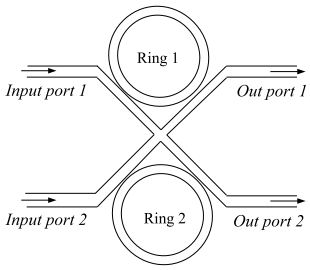

Figure 3.2: A 2x2 Basic SE (2B-SE) made with two microrings

The states of the 2x2 Basic SE (see Figure 3.2) are described in the following:

- *Bar State* (HL State or HLS): The SE is connecting Input port 1 with Output port 1, and Input port 2 with Output port 2. While those paths are set, it is said with some generality, that the SE is in the High Loss State. As it can be seen, each Ring deflects its corresponding input signal to its respective Drop port. Power Losses are higher in this state because of the signal deflection by one (suitably tuned) microring, that is suffer one HLS of its equivalent 1B-SE.

- *Cross State* (LL State or LLS): The SE is now connecting Input port 1 with Output port 2, and Input port 2 with Output port 1. On the contrary, we can say it is in the well performance position or Low-Loss State. So that microring lets each signal go from its Input port to their equivalent Through ports without the coupling penalty or losses. Indeed, the power penalty is in this Cross State is negligible due to the similarly of joining two LLS of 1B-SE.

The newly proposed SE shown in Figure 3.3 is called 2x2 Mirrored Switching Element (2M-SE). The aim in consider this new element is to have an additional tool in our network construction with a complementary behaviour. By cross-connecting the Input ports, the 2M-SE swaps the performance of its *Cross State* and *Bar State* with respect to the 2B-SE. So in order to formalise and finish the description of all our SEs used in next sections, this 2M-SE can be logically modelled as follows:

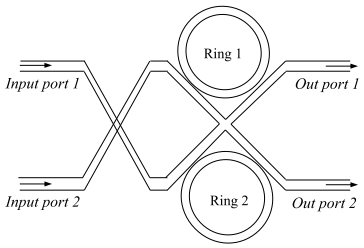

Figure 3.3: A 2x2 Mirrored SE (2M-SE) made with two microrings

- *Bar State* (LL State or LLS): The SE is connecting Input port 1 with Output port 1, and Input port 2 with Output port 2. Now there is no need to deflect each corresponding input signal to the Drop port, because they are directed to the Trough port of the corresponding 1B-SE. Power Losses are lower in this state due to the fact that each Ring is in its equivalent LL State (letting the signal go through the straight waveguide).

- *Cross State* (HL State or HLS): On the contrary, the inside 2x2 microring block needs to tune each Ring to connect Input port 1 with Output port 2, and Input port 2 with Output port 1. So each input signal will suffer the coupling effect. Indeed, the power penalty is in this Cross State higher due to the similarly of joining two HLS of 1B-SE.

In order to see the scalability of the three SEs shown in Figures 3.1, 3.2 and 3.3 several Interconnection Architectures will be analysed using several notation rules. It will be denoted as H the number of Switching Elements in High Loss State crossed by an input signal in order to reach the requested output, or satisfy the optical connection. And finally, as an illustrative notation, Figure 3.4 defines the 1B-SE, 2B-SE and 2M-SE figures used in structures with a higher complexity.

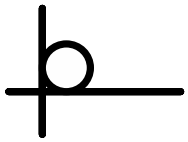

(a) 1B-SE in a small representation

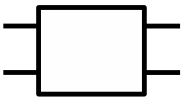

(b) 2B-SE depicted as a small white box

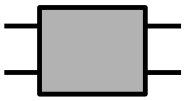

(c) 2M-SE depicted as a small grey box

Figure 3.4: SEs' pictures used in next sections

3.2 Crossbar

This section is the first of five sections in which different architectures are analysed through different points of view. As a starting point, the Crossbar interconnection pattern will be described and characterised.

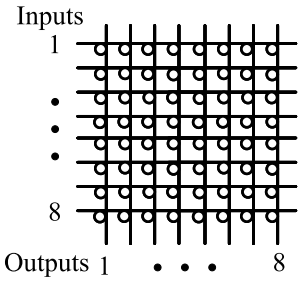

Figure 3.5: Example of a 8x8 crossbar structure

The crossbar architecture considered here in Figure 3.5 is made by integrating 1B-SE (Figure 3.1) in a grid of crossing straight waveguides. Depending on the characteristic of those microrings used as 1B-SE, two different objectives[18] can be achieved with this type of network structure.

1. Wavelength Resonant Router (λ-ReR): In this configuration the Free Spectral Range (FSR) of each microring is at least equal to the channel spacing multiplied by the number of WDM channels. Each single 1B-SE deflects the input channel at a specific wavelength to the output if is the resonating wavelength of that node. Instead, if that channel do not resonate, the signal propagates unaffected to the next 1B-SE.

2. Cross-connect Resonant Router (X-ReR): In this configuration every building block has a FSR equal to the WDM channel spacing considered. If the 1B-SE resonant wavelengths match the WDM channel wavelengths, all the channels are routed from the row to the crossing column. So that is couple all the input signal to the corresponding output selected by the 1B-SE. In fact, because one of our firsts assumptions done in Section 1.1 (single wavelength operation), this is the best way to model the structure in our scalability analysis.

It is important to notice that the number of Switching Elements crossed in HLS is always one for all the possible connections or paths. That SE in HL State used by every connection is the needed to route the overall matching request. It is easy to observe that no simulation or heuristic analysis is necessary in this case. Despite that, we consider two examples to show in a simple way how this network satisfies specific matching requests.

The first example (shown in Figure 3.6) corresponds to a 4 ports Crossbar network. The set of paths to route are named *Matching(N=4)* and the network must be configured by coupling those signals to the microrings belonging to the column i (Input) and row j (Output).

Matching(N=4)	
Input $i \rightarrow$ Output j	SEs in HLS
$1 \rightarrow 3$	1
$2 \rightarrow 4$	1
$3 \rightarrow 2$	1
$4 \rightarrow 1$	1

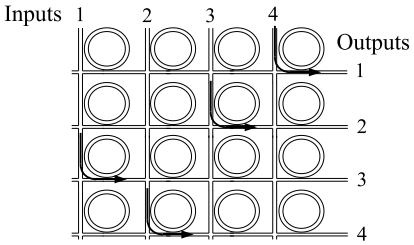

Figure 3.6: Example of a requested matching implementation in a 4x4 Crossbar network

This second example (shown in Fig. 3.7) instead corresponds to a 8 connections case in a 8 ports Crossbar network. The set of paths to route are now named *Matching(N=8)* and the network must be configured again by coupling those signals to the microrings belonging to the column i (Input) and row j (Output). The aim of these examples is to introduce a particular case

for this network that is also going to be useful in different future switching architectures.

Matching(N=8)	
Input $i \rightarrow$ Output j	SEs in HLS
$1 \rightarrow 5$	1
$2 \rightarrow 7$	1
$3 \rightarrow 2$	1
$4 \rightarrow 1$	1
$5 \rightarrow 8$	1
$6 \rightarrow 4$	1
$7 \rightarrow 3$	1
$8 \rightarrow 6$	1

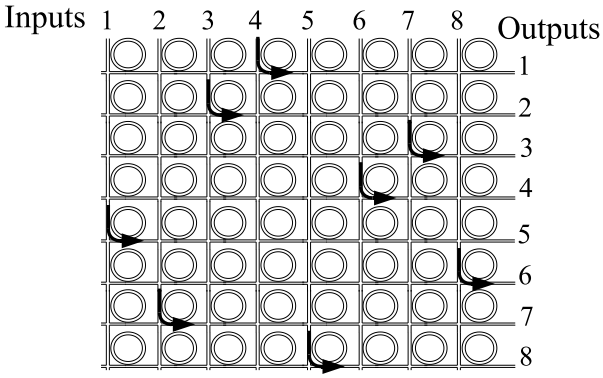

Figure 3.7: Example of a requested matching implementation in a 8x8 Crossbar network

Thus by extrapolating the behaviour noticed in both previous examples, we can formulate the Equation 3.1 that models the crossbar architecture in numbers of HLS SE used by each single connection in all the matching. From the scalability point of view this is the best performance achievable due to its low loss conditions and small crosstalk effect.

$$H_{Xbar}(N) = 1 \tag{3.1}$$

On the other hand, crossbar structure shows one of the highest network building cost in terms of microrings used that will be considered in this work.

The cost obtained is due to the number of crosspoints in a square structure where each crosspoint is dedicated to a specific Input/Output connection.

$$C_{Xbar}(N) = N^2 \tag{3.2}$$

The main idea of this section has been present the well-known crossbar network as an upper bound in two different senses: a good $H(N)$ behaviour, but also a expensive $C(N)$ building cost. From now the aim is to find the structures belonging to the non-blocking class that exhibit a good compromise between performance and cost. And the way to explore that trade-off between those magnitudes will be finding well-known *Multistage* solutions.

3.3 Preliminary Considerations

The starting point of this section is the description of several metrics used and the procedure to do the exhaustive characterisation of different *Multistage* networks that are going to be analysed. First, two metrics implicitly related to the network are presented. Then, several operations with their value and their contain will be done in each case to perform the heuristic study.

Metrics and operations

In the following we describe two important metrics for the characterisation of a *Multistage* network:

- *States* (Equation 3.3): All the possible different configurations in which the network is able to be set up. All those configurations are conformed by all the combinations of the SEs in one of their State (HL or LL). In fact, this metric is strictly related to the network cost because depends on the number of SEs that contains.

$$Number\ of\ States(SE) = 2^{(Number\ of\ SE)} \tag{3.3}$$

- *Matchings* (Equation 3.4): All the possible N Input and Output pairs that can be set in a NxN network. Matchings are all the possible permutations of N.

$$Number\ of\ matchings(N) = N! \tag{3.4}$$

At this point we do two different operations with these two network metrics presented above. The fist operation is establish the relation that follows:

- Correlation between matchings and states: For each possible State corresponds an unique matching satisfies it but not vice versa. So that all the matchings are fully characterised by finding all their possible States. The characterisation is illustrated in Figure 3.8. Thus from the definition of *Surjective function*, there is at least one element in the Domain (*States*) such that satisfies $f(S_j) = M_i$ for all the elements in the Image (*Matchings*).

$$\forall M_i \in Matchings\ :\ \exists S_j \in States,\ f(S_j) = M_i$$

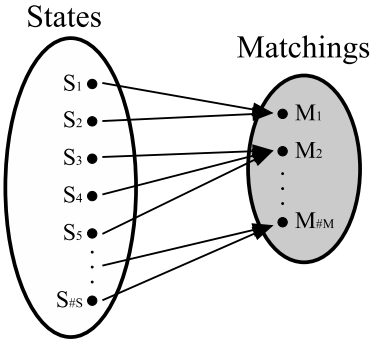

Figure 3.8: Detail of the surjective relation between network configurations (States) and Matchings

- *Degree of Freedom*: In order to see how this correspondence behaves, a ratio between Eq. 3.3 and Eq. 3.4 is calculated in several cases, and which value give us the existing degree of freedom, from now on $D(N)$ (Eq.3.5). This second operation refers to the value of these magnitudes but not their content.

$$D(N) = Degree\ of\ Freedom(N) = \frac{2^{(Number\ of\ SE)}}{N!} \tag{3.5}$$

Procedure

1. In our analysis the starting point is related with the network *States*, the first metric presented. All possible cases in which we can find the network are generated and stored, and they are used in the beginning of the exhaustive analysis.

2. All the possible matchings for the network are now taken into account. As we have seen, that number of matchings is all the possible permutations of the N input-output pairs and in this step they are also generated and stored.

3. By using an exhaustive search, all matchings get fully characterised by finding all their possible corresponding States and indexing them. This step of the procedure requires a high computational cost, and in fact, is the one that limits the size of the networks able to be characterised.

4. Selection of one state for each matching: For each matching we look for the path with the maximum number of turns (*HLS* SEs used) in each state of those chosen. Thus we can select the configuration which has a minimum worst case value of number of turns. Then, by looking for that $Min(Max(\text{Number of turns}))$ between all the matchings of the network we get the final number of *turns* or $H(N)$ (as the example given in Eq.3.1).

   Despite all these considerations in this step of the procedure, it is important to mention that we can find matchings having more than one corresponding state with equal behaviour in terms of HLS worst path. In those cases, due to the assumption of their equivalent result, one of the states will be randomly considered as the corresponding for the matching, letting the others be able to compose the input variables in other studies (i.e. frequency HLS).

The main idea of this procedure explained is modify the relation rule between states and matchings from surjective to bijective. As we can see in Figure 3.9, now every matching is identified by a single network State. Thus all the matchings can be classified by its worst path set of the selected State configuration.

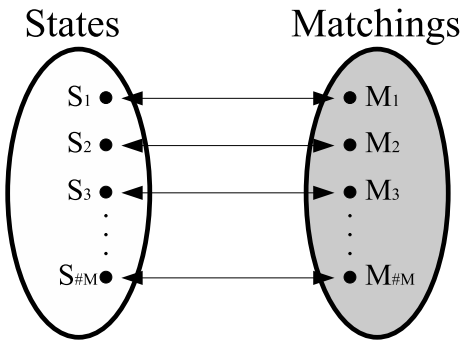

Figure 3.9: Detail of the established bijective relation between States and Matchings

3.4 Benes

3.4.1 Basic Benes configuration

N=4 basic Benes

A basic Benes network is analysed in this section (see Figure 3.10a). It is applied the procedure described before in Section 3.3 in order to classify all the possible matchings of the network. Table 3.1 shows the possible types of matching that can be found in this 4x4 basic Benes network to comprehend this first application of the exhaustive search. Two different correspondences can characterise a matching in this network structure. The case that appears a higher times (16) is when a matching can be routed with two different network states, and the other case occurs when we can route a matching with four different network configurations (an example of this case is considered). Then, the final bijective relation should be a choose between one state of two or four depending on the matching. Despite establishing that relation rule, it

is important recall that when matchings have more than one corresponding network state with equal behaviour in terms of HLS worst path, one of those states will be considered as the image for the bijective function, letting the others be stored as alternative solutions.

Matchings		States for each matching	Subtotal states
	16	2	32
	8	4	32
Total	24	-	64

Table 3.1: Types of correspondences between matchings and states in the 4x4 basic Benes network

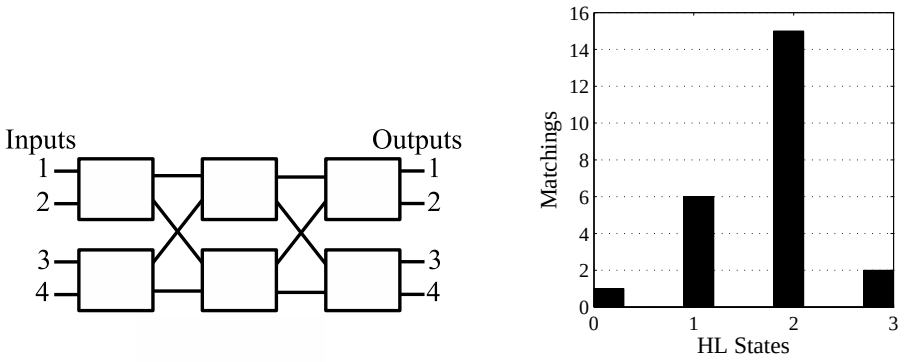

(a) 4x4 basic Benes network

(b) The 24 matchings classified by number of turns

Figure 3.10: Basic Benes 4x4 characterisation

Regarding to the result of the histogram 3.10b that characterises the network, we can see that most of the matchings have at least a worst case connection that goes through two SE in HL State. We also can observe that there are two matchings that have at least one path with the number of turns equal to three, that is numerically equal to the number of stages of this network. Thus, this N=4 sized network has the following number of turns (H) and cost (C):

$$H_{b.Benes}(4) = 3$$
$$C_{b.Benes}(4) = N(2\log_2 N - 1) = 12$$

To comprehend the behaviour of this network we make an analysis of the High-Loss State (HLS) SE location. By naming all the composing SE, averaging all the matchings and possible considered solutions, the histogram in Fig.3.11b shows us the HLS distribution through all the network.

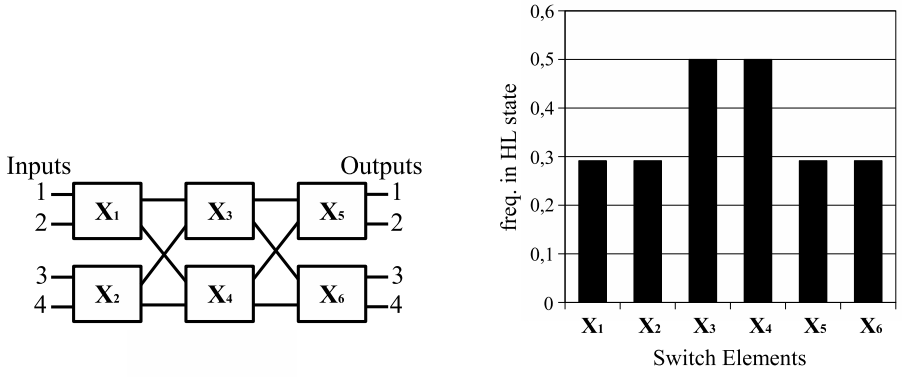

(a) SEs named for a 4x4 Benes (b) The average bar state for each SE

Figure 3.11: Benes 4x4 turns distribution

As we can observe in histogram 3.11b the HLS occurs often in the middle stage (SEs X_3 and X_4). In fact, these two SEs are directly involved in the worst case paths considered before. Thus in the aim to improve the overall performance of this network several modifications will be done in that zone.

Lets recall the example presented in Section 3.2 to show a specific case in the procedure applied to obtain these histograms showed in Figs. 3.10b and 3.11b.

So in order to route the *Matching(N=4)* that contains the connection requests: $1 \rightarrow 3$; $2 \rightarrow 4$; $3 \rightarrow 2$ and $4 \rightarrow 1$; four different network configurations can be considered. In fact, we can say that this case belongs to the group of eight matchings that have a surjective relation of four. For one side, it is easy to see the similarity between cases 3.12a and 3.12b because they have only one SE in HLS. By looking in more detail at those network configurations, we can observe that paths $3 \rightarrow 2$ and $4 \rightarrow 1$ need to go through that SE in HLS, whereas paths $1 \rightarrow 3$ and $2 \rightarrow 4$ go through all the network passing by all the SEs in LL State. So in fact we can say these two first cases are equivalent from the performance point of view. By the other side, we have cases 3.12c and 3.12d where paths $3 \rightarrow 2$ and $4 \rightarrow 1$ still need to go through

one SE in HLS but now the other two connections ($1 \rightarrow 3$ and $2 \rightarrow 4$) have to cross two SEs in HLS. These two network configurations are again similar from the performance point of view but worse than a and b. So by identifying this matching with network configurations 3.12a or 3.12b (one of these two cases in a bijective way) we can say that belongs to the group of six "1 HL State" in the histogram 3.10b.

Matching(N=4)	Number of HLS			
Input $i \rightarrow$ Output j	3.12a	3.12b	3.12c	3.12d
$1 \rightarrow 3$	0	0	2	2
$2 \rightarrow 4$	0	0	2	2
$3 \rightarrow 2$	1	1	1	1
$4 \rightarrow 1$	1	1	1	1

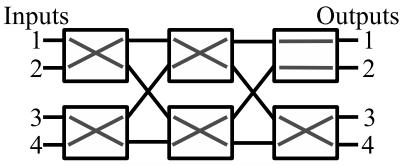

(a) First possible configuration

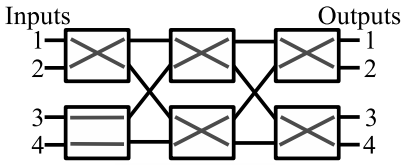

(b) Second possible configuration

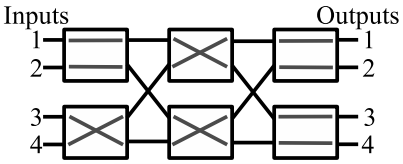

(c) Third possible configuration

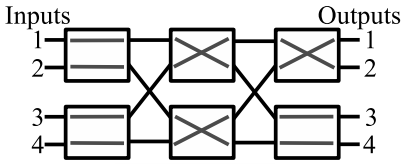

(d) Fourth possible configuration

Figure 3.12: The four possible network configurations that route the required matching

Regarding the proceeding to obtain the histogram 3.11b, and attending to this example in particular, we consider the solutions 3.12a and 3.12b as the configurations that identify this matching. In this case, we can say that in this case SEs X_2 and X_5 are in HL State in the 50% of the time whereas all the others (SEs X_1,X_3,X_4 and X_6) are always in LL State.

We can find three different examples establishing the bijective relation between network states $\leftrightarrow$ matchings. The first one occurs when there is only one network State that may be chosen to characterise a matching; in

this case, we can say that SEs are 100% LLS or 100% in HLS. The second type of example that we can find is the one where (as in the example shown) two different network States are equal, from the performance point of view, to satisfy a specific matching. The third example occurs when four network States have an equivalent behaviour to solve the matching requested; obviously, we do the average (%) of the SE States in those four cases to do the identification of these type of matchings. And finally, by doing the average between all the matchings of all the percentages found applying the procedure explained we get the histogram presented in Fig.3.11b.

To conclude the characterisation of this 4x4 basic Benes network, we calculate the equation 3.5:

$$D(N=4) = \frac{2^{((Number\ of\ SE)=6)}}{(N=4)!} = \frac{2^6}{4!} = 2{,}6\hat{6}$$

We can infer from that degree of freedom that at least there are two network States that we can choose from in most of the cases. We got a $2{,}6\hat{6}$ because the average of those other cases where (as in the example shown) four configurations can hold a requested matching.

N=8 basic Benes

The 8x8 basic Benes network is now analysed in Figure 3.13 from the same point of view as the 4x4 case, and using the same procedure. The construction rule applied is the explained before in Section 2.2 and it guarantees that we have a rearrangeable non-blocking network. Thus is important to notice that now we have a 5 stage network given because the size $N = 8$ and the construction rule.

In this 8x8 Benes characterisation (hist 3.13b) we can observe that the most of the matchings need at least one connection to pass through three SEs in HL State. About six thousand matchings need at least one path to go through two or four SEs in HLS respectively; only one hundred can be satisfied with one SE in HLS (at most for all the connections); and obviously, only one matching can be routed with no SE in HLS (that is all the SEs in

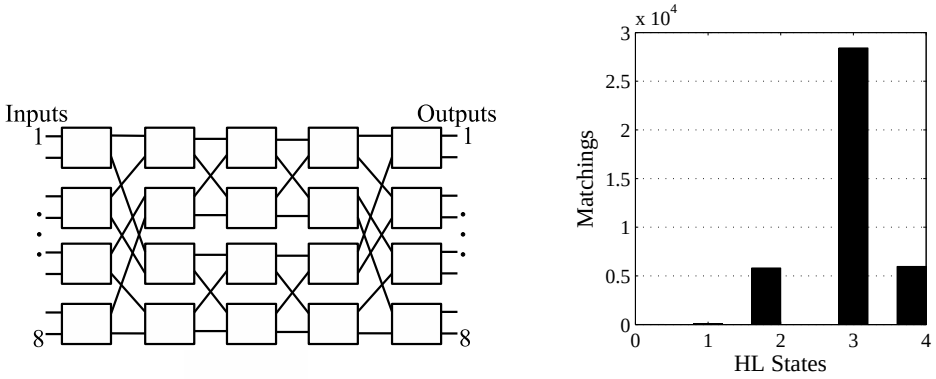

(a) 8x8 basic Benes network

(b) All the matchings classified by number of turns

Figure 3.13: Basic Benes 8x8 characterisation

LLS to hold all the connections with a *max* number of SEs in HLS equal to zero).

Besides all those observations we can infer an important conclusion, that is the absence the worst case matching equal to the network's depth ($S = 5$). Thus in this case the network has:

$$H_{basicBenes}(N = 8) = 4$$
$$C_{basicBenes}(N = 8) = N(2\log_2 N - 1) = 40$$

In fact, this result is related to the heuristic analysis used, and the idea explained in sec 3.4 related to the number of States and number of matchings (equations 3.3 and 3.4 respectively). So we calculate the *Degree of freedom* for this case.

First of that calculation, we retake from Section 2.2 the number of SE in a 8x8 Benes network. Thus we have four rows and five columns that give twenty as the total number of SE.

$$D(N = 8) = \frac{2^{((Number\ of\ SE)=20)}}{(N = 8)!} =\simeq 26$$

This higher value of *Degree of freedom* compared with the one obtained in the 4x4 basic Benes network is the numerical explanation of the avoidance of the worst case matching which is numerically equal to the network's depth in terms of number of turns hold.

Figure 3.14 shows the HL State of all the SEs in the network in order to continue the characterisation of this 8x8 basic Benes structure. As we can see, middle stage (SEs 9, 10, 11 and 12) has a the higher frequency of SEs in HLS being near the 50% of the cases in the bad performance position. Observing the other SEs, we can say that the distribution is almost flat with a frequency between 0.3 and 0.4 over 1. The need to distribute that penalty load between all the rest of the network will be the aim in next sections.

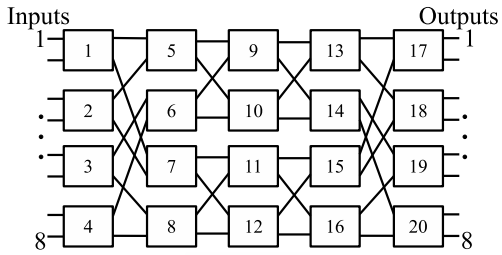

(a) SEs named for a 8x8 Benes

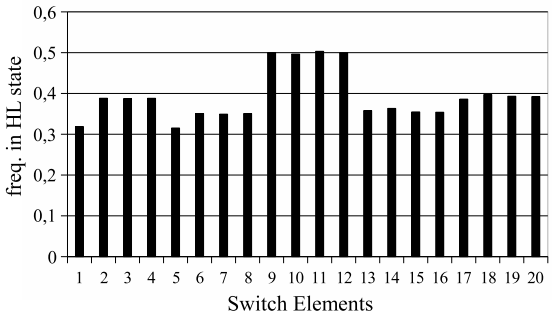

(b) The average bar state for each SE

Figure 3.14: Basic Benes 8x8 HLS distribution

Due to the number of configurations considered for each matching, the procedure applied to obtain this HLS distribution through the switching architecture is slightly different from the one used in the $N = 4$ case. In fact, as we can see in Table 3.2 there are seven different types of matchings that we can find attending to that number of available network configurations: 8, 16, 32, 40, 64, 128 and 256 (instead the 2 or 4 in the $N = 4$ case). In average, we get the *Degree of freedom*$\simeq$ 26, and obviously, the more configurations we have the higher part of them are equal and satisfactory from the performance point of view.

Matchings		States for each matching	Subtotal states
128		256	32768
512		128	65536
2816		64	180224
2048		40	81920
12288		32	393216
14336		16	229376
8192		8	65536
Total	40320	-	1048576

Table 3.2: Types of correspondences between matchings and states in the 8x8 basic Benes network

Regarding to these high number of configurations per matching, the procedure applied in the 8x8 basic Benes case to obtain histogram 3.14b is the following:

1. Store all the suitable network configurations in the smaller cases (i.e. until matchings with 32 states) and a considerable part in the larger cases.

2. Consider different bijective relations between all the best network states for each matching (i.e. one thousand relations in our case)

3. Average all the SEs' states between all those network configurations considered in the previous step.

Lets recall the example used in Section 3.2 (Crossbar 8x8) in order to conclude this N=8 basic Benes study. *Matching(N=8)* belongs to the sixth group of matchings classified in Table 3.2 (14336 matchings that have 16 network configurations each). In this example we consider half of the total network states, four equivalent configurations in Figure 3.15 and four alternative routing solutions in Figure 3.16.

We can infer from the first four pictures (from 3.15a to 3.15d) and from Table 3.3 that the worst connection needs to pass through **three** SE in HLS. Otherwise, from pictures 3.16a to 3.16d and from the last columns in Table 3.3 we can observe that the worst path pass through **four** SE in

Matching(N=8)	Number of HLS							
Input $i \rightarrow$ Output j	3.15a	3.15b	3.15c	3.15d	3.16a	3.16b	3.16c	3.16d
$1 \rightarrow 5$	0	2	0	2	2	2	4	4
$2 \rightarrow 7$	2	2	2	2	2	2	2	2
$3 \rightarrow 2$	3	3	3	3	3	3	3	3
$4 \rightarrow 1$	3	3	3	3	3	3	3	3
$5 \rightarrow 8$	3	3	3	3	3	3	3	3
$6 \rightarrow 4$	1	1	1	1	3	3	3	3
$7 \rightarrow 3$	2	0	2	0	4	4	2	2
$8 \rightarrow 6$	2	2	2	2	4	4	4	4

Table 3.3: Eight network configurations summarised (portion of existing 16)

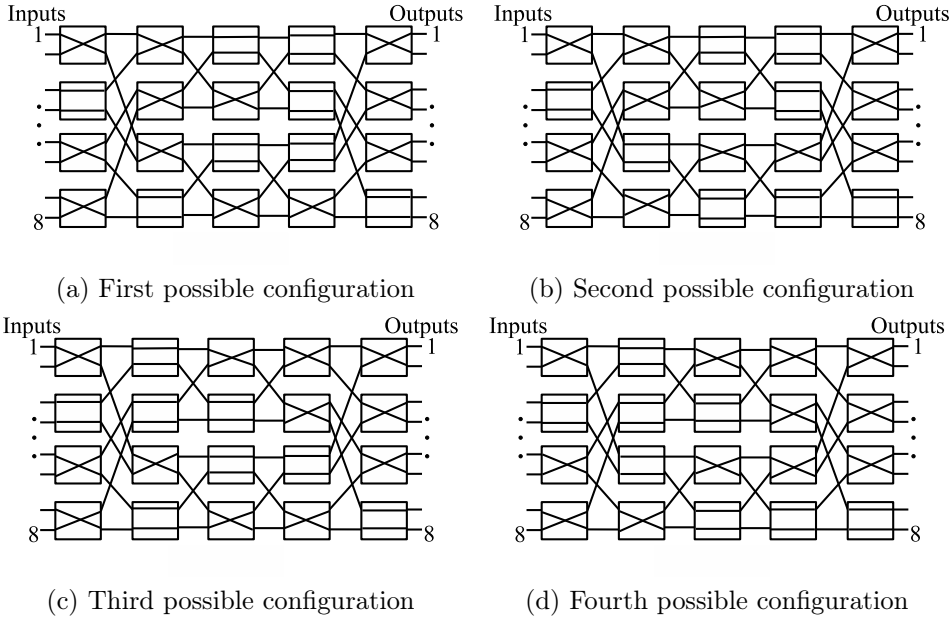

(a) First possible configuration

(b) Second possible configuration

(c) Third possible configuration

(d) Fourth possible configuration

Figure 3.15: Four equivalent network configurations (portion of existing 16) that can route the required matching

HLS. This difference in the behaviour of the eight cases considered (in two groups of four) allows the first four network configurations be as the states that compose the bijective relation for this matching.

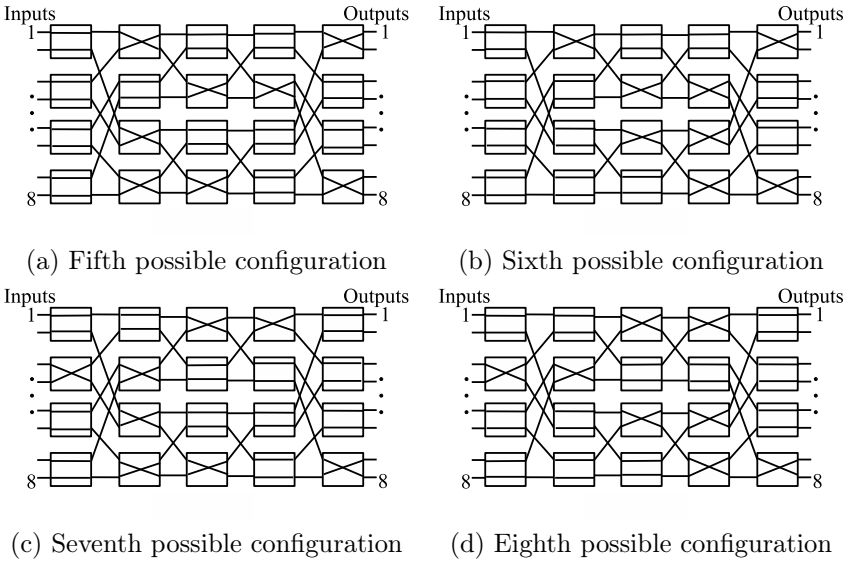

(a) Fifth possible configuration (b) Sixth possible configuration

(c) Seventh possible configuration (d) Eighth possible configuration

Figure 3.16: Four alternative equivalent network configurations (portion of existing 16) that can route the required matching

3.4.2 Modified Benes configuration

N=4 modified Benes

With the aim of improving the network's performance and the observations of HLS frequency in the analysed basic Benes networks, we consider at this point switching fabrics made by combining 2B-SE (2x2 Basic Swithing Elements) and 2M-SE (2x2 Mirrored Switching Elements). The starting point is the $N = 4$ Benes structure, now applying different construction patterns by changing their SEs types or by modifying the connections. In fact, we can say in advance that during this Section 3.4.2, the network cost $C_{b.Benes}(N = 4)$ and the *Degree of freedom* $D(N = 4)$ will remain equal as N=4 basic Benes network while the metric $H(N)$ will be improved.

We can set different networks changing each X_i in Figure 3.17 from 2B-SE to 2M-SE. As it will be shown later, changing $X_i \mid i \in \{1,2,5,6\}$ only implies a permutation of the surjective correspondence between matchings and network States With that effect, the overall performance remains exactly the same as in Figure 3.10.

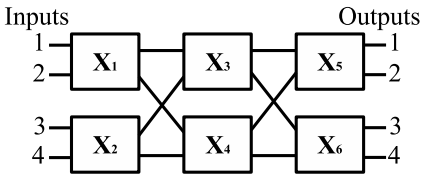

Figure 3.17: SEs named for a 4x4 Benes

As we can see in Figure 3.18 the improvement in the network comes when X_3 or X_4 are changed from 2B-SE to 2M-SE because their symmetry load in the network. In fact, as we have seen in the basic Benes turn distribution (Figure 3.11), there is a higher use of HLS in the middle stage. Thus the next step is the analysis of a structure where the middle stage has a SE with a mirrored configuration (2M-SE) and the other a basic behaviour (2B-SE).

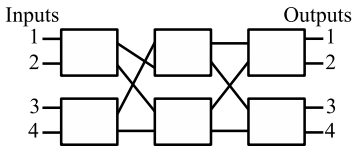

(a) Modified Benes 4x4 network swapping intermediate connections

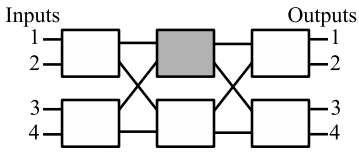

(b) Modified Benes 4x4 network with mirrored SE in middle stage

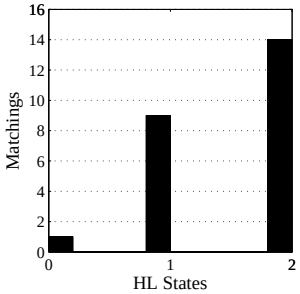

(c) The 24 matchings of the Modified 4x4 Benes network classified by their number of turns

Figure 3.18: Inverted 2nd stage 4x4 characterisation

In order to achieve that overall benefit in the performance, we present two equivalent constructions. The first (shown in Figure 3.18a) consist in a swap of the inputs in the X_3 Switching Element. Figure 3.18b depicts the alternative construction, that is build the network considering X_3 as a 2M-SE, and in fact, swapping its inputs inside the SE box.

There are no matchings having a worst connection that need to go trough three SE in HL State as we can observe in the histogram 3.18c. By doing this modification, also increases from 6 to 9 the number of matchings that only need to take at least for one of their connections one SE in HLS. And finally, as in the basic Benes structure, there is only one matching that can be routed without taking SEs in HLS, that is, taking all the SEs in LLS. Summarising,

$$H_{mod.Benes}(N = 4) = 2$$

It is important to notice that the *opposite behaviour* of a SE given by the Mirrored box (2M-SE) can be achieved by swapping the inputs **or the outputs** of the first defined 2B-SE (as we can see in Figure 3.19). This is the main reason to explain the same result obtained by changing $X_{\{1\ or\ 2\}}$ or $X_{\{5\ or\ 6\}}$ from 2B-SE to 2M-SE. The results are almost the same and they do not present an improvement because they can be obtained in a similar way by modifying the notation of the inputs or the outputs.

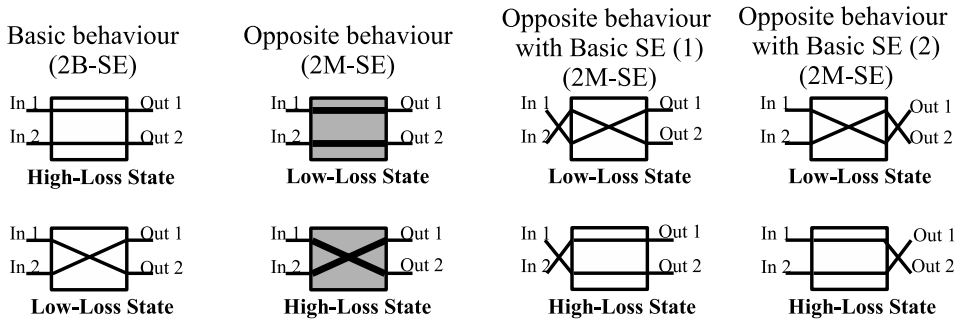

Figure 3.19: Detail of SE opposite behaviour

Thus to continue the characterisation of the structure presented in Figure 3.18a (equivalent to Figure 3.18b), the average distribution of SE in HLS is

shown in histogram 3.20b. As we can observe, with the modification done, the distribution of HLS is almost well balanced between all the SEs. Now, there is no stage in the network that needs to hold the most of the load in terms of SEs in HLS. In fact, we can say that all the existing matchings can be routed with the SEs only around 30% of the cases in HLS, being the other 70% of the time in the good performance state.

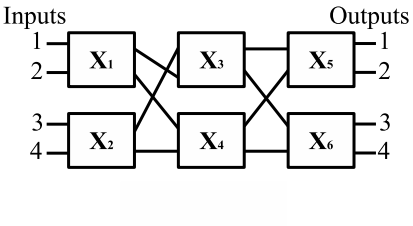

(a) SEs named for a 4x4 with inverted 2nd stage

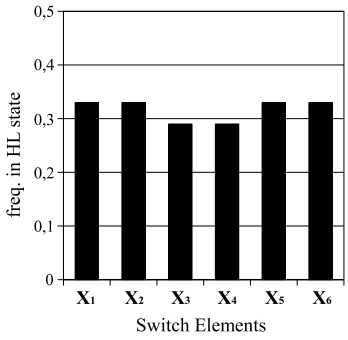

(b) The average bar state for each SE

Figure 3.20: Inverted 2nd stage 4x4 turns distribution

In order to conclude the study of this new N=4 modified Benes structure, we recall the *Matching(N=4)* example considered twice before. Table 3.4 shows the SEs crossed in HLS for each connection in eight network configurations equivalent per pairs. Because the equivalence between Figures 3.18a and 3.18b, we can depict in two different ways the same solution (one for each illustration nomenclature).

As in the example before (see Figure 3.12) we can separate in two pairs the network configurations able to route this matching. For one side we get 3.21a and 3.21b (or their equivalent in 2M-SE notation 3.22a and 3.22b) that have a worst connection that needs to go through two SE in HLS. For the other side, configurations 3.21c and 3.21d (or their equivalent in 2M-SE notation 3.22c and 3.22d) have a worst path that needs to pass three SEs in HLS. With these observations, we get that anyone of the two first network states (or their equivalent) are the chosen to identify this matching in the bijective relation.

Matching(N=4)	Number of HLS			
Input $i \rightarrow$ Output j	3.21a / 3.22a	3.21b / 3.22b	3.21c / 3.22c	3.21d / 3.22d
$1 \rightarrow 3$	0	0	3	3
$2 \rightarrow 4$	1	1	2	2
$3 \rightarrow 2$	2	1	2	1
$4 \rightarrow 1$	1	2	1	2

Table 3.4: Eight network configurations equivalent per pairs

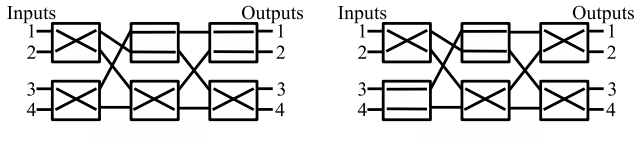

(a) First possible configuration

(b) Second possible configuration

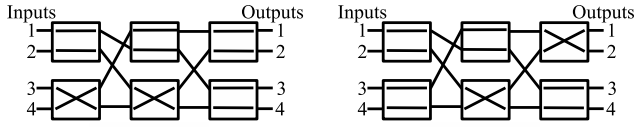

(c) Third possible configuration

(d) Fourth possible configuration

Figure 3.21: The four possible network configurations that can route the required matching

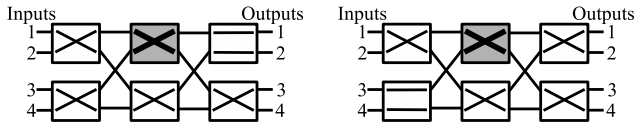

(a) First possible configuration

(b) Second possible configuration

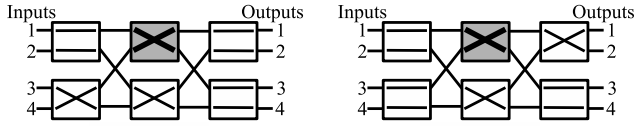

(c) Third possible configuration

(d) Fourth possible configuration

Figure 3.22: The four possible network configurations that route the required matching depicted with 2M-SE in the second stage

N=8 modified Benes networks

The aim of this Section is to improve the value of $H(N)$, knowing that the network cost $C_{modBenes}(N = 8)$ and the *Degree of freedom* $D(N = 8)$ will remain equal as N=8 basic Benes network. That is:

$$C_{modBenes}(N = 8) = N(2\log_2 N - 1) = 40$$

$$D_{modBenes}(N = 8) = \frac{2^{((Number\ of\ SE)=20)}}{(N = 8)!} = \frac{2^{20}}{8!} \simeq 26$$

First N=8 modified Benes

As we have seen in Section 3.4.2, the performance can be improved by swapping the connections in the middle stage. That idea is applied in this section (see Figure 3.23a that performs as the histogram 3.23b). By comparing it with the first 8x8 basic Benes structure analysed with this procedure in Figure 3.13 we can observe that the matchings that need a path with four SE in HLS get almost reduced, from the six thousand to near two hundred. In fact, this is the best improvement of this network, and the aim will be try to route all the matchings with a worst connection cases having maximum three. About the rest of the characterisation, we can see that the most of the matchings are needing again at least one connection to pass through three SEs in HL State; the six thousand matchings that hold a path with two HLS get doubled up to twelve thousand; and the ones that have a worst connection equal to one or zero remain almost equal.

The main idea beyond this structure presented in Figure 3.23a is change the middle part of the network into a structure where the constrained matchings that force several paths to take three HLS in three stages disappear. As we can infer from 3.24a (equivalent construction as 3.23a), the inside black box that contains the three middle stages in the upper and the lower half respectively performs as the histogram 3.18c, that is having worst path cases with number of SE taken in HLS equal to **two**. In the first analysed 8x8 basic Benes structure (Figure 3.13), that part of the network was performing with worst connection cases routed through **three** SEs in HLS (histogram 3.10b). So that is the fact that offers a performance benefit in this case.

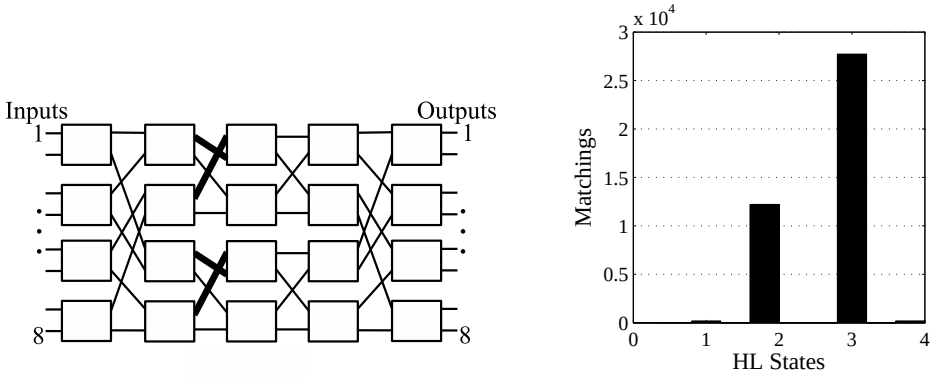

(a) 8x8 Benes Network with inverted 2x2 connections in the middle stage

(b) All the matchings classified by number of turns

Figure 3.23: Modified Benes 8x8 characterisation

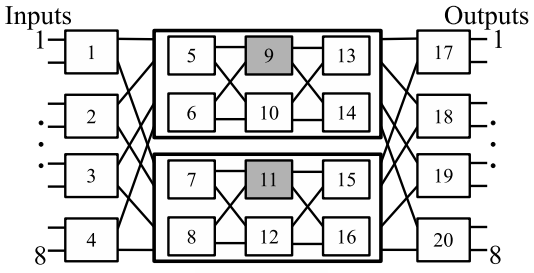

(a) 8x8 Benes Network with 2M-SE in the middle stage (equivalent as Figure 3.23a)

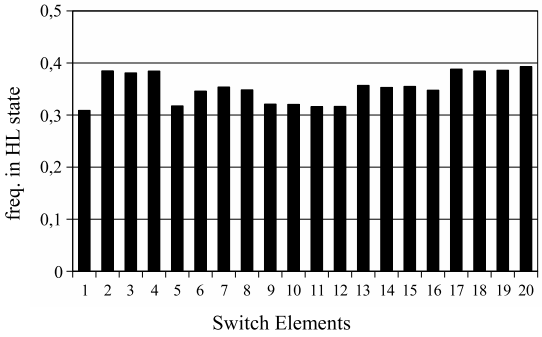

(b) The average HLS for each SE

Figure 3.24: Modified Benes 8x8 (equivalent) and HLS distribution

Histogram 3.24b shows the distribution of the SEs in HLS through all the network states that compose the bijective relation with matchings in this 8x8 modified Benes network. We can observe by comparing this result with

the obtained in the 8x8 basic Benes network (histogram 3.13b) the reduction of the load in terms of HLS in SEs 9, 10, 11 and 12. There are no SEs that need to be configured in the bad performance position 50% of the cases, now several SEs are almost 40% of the cases in HLS. Can be seen that SEs number 1 and 5 have also a lower frequency of HLS than the others (except the middle stage SEs) due to the freedom given by the $D(N = 8)$ and also because the storing procedure used.

Second N=8 modified Benes

At this point, the benefit of inverting or swapping the connections in the inside stages is used in an intuitive way by presenting a second N=8 modified Benes network shown in Figure 3.25a. A small improvement is obtained (see histogram 3.25b) by flipping the inside 4x4 Benes structure respect the first 8x8 modified Benes. In fact, this construction is equivalent as the one that should be generated if we change both SEs 9 and 12 from 2B-SE to 2M-SE in 8x8 basic Benes network with all the SEs identified.

As we can see, with this second modification in the $N = 8$ Benes Network a slightly improvement in the overall performance is achieved. The number of matchings that need two SEs in HLS for at least one connection is increased in two thousand (see changes from histograms 3.23b to 3.25b). Obviously, this implies a reduction of two thousand of the cases that have to hold connections with three SEs in HLS. And in fact, the remaining matchings that need a path to go through four SEs in HLS makes us consider this improvement as a better performance in average, but not in those worst connections of several matching cases.

Histogram 3.26 shows the HLS distribution in average for this second modification network case. By comparing it with the immediately previous 3.24b, we can observe a slight improvement of the HLS load in the middle stage (SEs 9, 10, 11 and 12).

Thus, we can conclude this second modified 8x8 Benes network commenting the slight benefit in the two performance points of view (worst connection per matching classification and average HLS) that presents flipping the inside 4x4 Benes structure with respect of the first N=8 modified Benes.

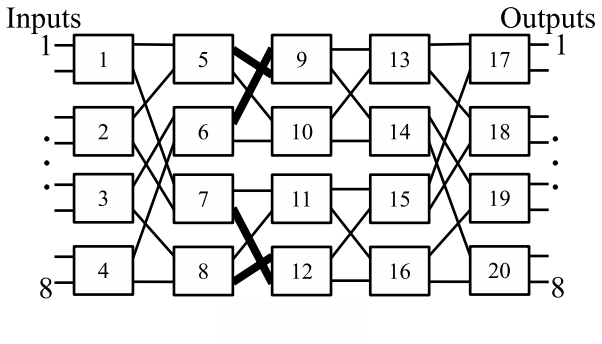

(a) 8x8 Benes Network with inverted and flipped inputs in SEs 9 and 12

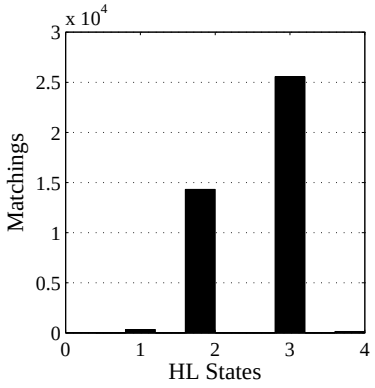

(b) All the matchings classified by number of turns

Figure 3.25: Modified and inverted Benes 8x8 characterisation

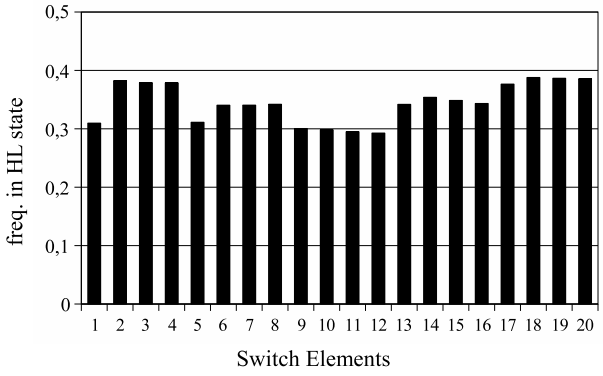

Figure 3.26: The average HLS for each SE in network 3.25a

Third N=8 modified Benes

In order to close the N=8 modified Benes networks, several alternative constructions (see Figures 3.27 and 3.28) are presented and analysed with the same exhaustive procedure. Because the likely results between them, and the fact that no one is able to avoid those worst matchings that need connections that hold four SEs in HLS, the results are also shown numerically.

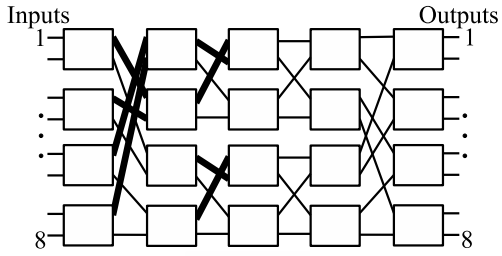

(a) 8x8 Benes Network with flipped inputs in SEs 9 and 11, and flipping several connections from the first stage to the second stage

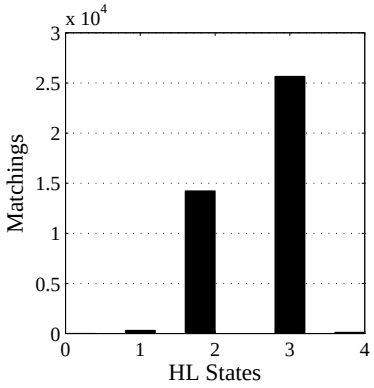

(b) All the matchings classified by number of turns

Figure 3.27: Third modified Benes 8x8 characterisation

Fourth N=8 modified Benes

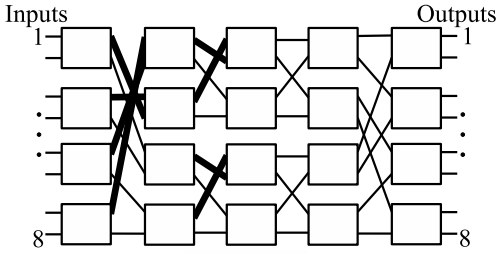

(a) 8x8 Benes Network with flipped inputs in SEs 9 and 11, and flipping several connections from the first stage to the second stage (ver.2)

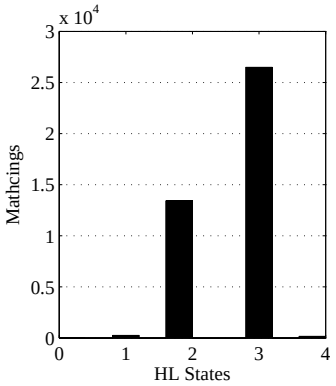

(b) All the matchings classified by number of turns

Figure 3.28: Fourth modified Benes 8x8 characterisation (ver.2)

SEs in HLS for at least one connection	matchings
0	1
1	318
2	14320
3	25658
4	113

Table 3.5: Third modified Benes 8x8 values

SEs in HLS for at least one connection	matchings
0	1
1	254
2	13415
3	26485
4	165

Table 3.6: Fourth modified Benes 8x8 values

3.4.3 Waksman

Another network structure is analysed by using the same exhaustive procedure. Waksman Network (Figure 3.29a) has two mainly beneficial characteristics:

- Lower complexity: Since one SE is removed in every construction step, the total cost of the Network is closer to the theoretical asymptotic optimum. We can see it in the network cost calculation:

$$C_{Waksman}(N = 4) = 2N \log_2 N - 2N + 2 = 10$$

- Easier configuration algorithm: By removing one SE in each construction step, the freedom of choosing in at the beginning of the algorithm disappears. This fact implies starting the looping from a "pre-set SE" and also brings several information of the network configuration in advance.

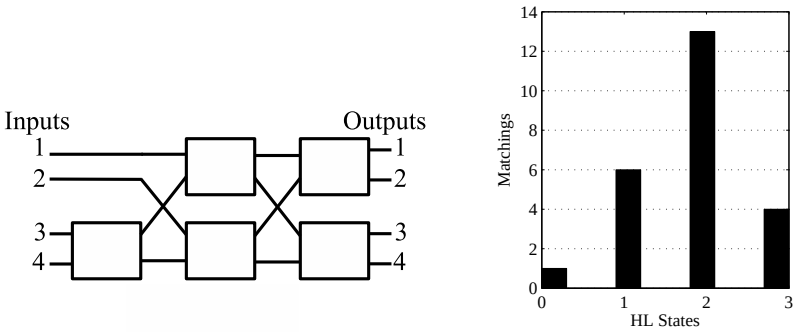

(a) 4x4 Waksman network

(b) The 24 matchings classified by HLS

Figure 3.29: 4x4 Waksman characterisation

In histogram 3.29b we can see that the performance of this Waksman network is not improved even considering the comparison with Figure 3.10 (basic Benes network) and obviously also with the achieved in the Modified Benes network (Figure 3.18). Therefore we still have $H_{Waksman}(N = 4) = 3$

From an intuitive point of view, part of the study of different Switching Architectures answers to the intuitive idea that a missing SE will cause a reduction of the number of HLS required for all the matchings. It is been proved that is absolutely the opposite, the constraint states grow because of that less freedom given by the network structure. Thus we calculate the *Degree of freedom*:

$$D_{Waksman}(N = 4) = \frac{2^{((Number\ of\ SE)=5)}}{(N = 4)!} = 1{,}3\hat{3}$$

By using the same idea as from going to 4x4 basic Benes (see Figure 3.10) to 4x4 inverted 2nd stage network (see Figure 3.18) the following network is analysed. It can bee seen in Figure 3.30b a small improvement in the performance but it does not achieve the elimination of the matchings that have $H_{Waksman}(N = 4) = 3$.

3.5 Cumulative approach to the analysis

Until now, all the characterisations are made using the procedure described at the beginning of the Section 3.4. In fact, as we have seen several times

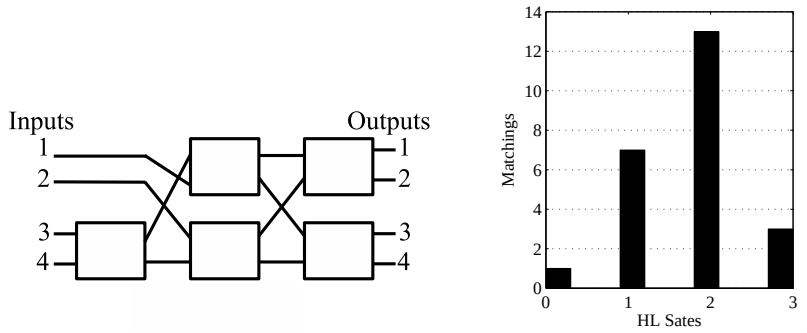

(a) 4x4 modified 2nd stage Waksman network

(b) The 24 matchings classified by number of turns

Figure 3.30: 4x4 modified 2nd stage Waksman characterisation

through this chapter, having metrics depending on $2^{N \log N}$ or $N!$ make hard to continue with the same procedure. As we can see for size N=16 basic Benes network:

$$Number\ of\ SE(N=8) = \frac{C(N=8)}{2} = N(\log_2 N - 1/2) = 56$$

$$Number\ of\ States(SE) = 2^{(Number\ of\ SE)} = 7{,}52 \cdot 10^{16}$$

$$Number\ of\ matchings(N=16) = N! = 2{,}09 \cdot 10^{13}$$

$$D_{Benes}(N=16) = \frac{2^{56}}{16!} \simeq 3.444$$

Attending to these high values, this subsection introduces a little modification on the procedure. It is considered a middle stage box (from now *preset box* p.box) in order to perform the behaviour of the solution obtained in the Section 3.4.2 Figure 3.18. As we can see in Figure 3.31a, the network analysed is the same as Figures 3.23a and 3.24a, now simplifying the middle structure to achieve a faster exhaustive analysis for higher values of N.

Regarding the preset box, it is important notice that is has been reduced the number of available solutions in the bijective relation that compose histogram 3.18c. In fact, network 3.18a (N=4 modified Benes) has several matching cases that have more than one corresponding state with equal behaviour in terms of HLS worst path. Therefore, modifying the correspondence between states and matchings depending on the case we get the

result for the N=8 modified Benes presented in histogram 3.23b (done by the exhaustive analysis). Now, the correspondence becomes absolutely bijective, classifying the 24 matchings with 24 network states and disabling all the freedom choosing states with equal behaviour in terms of HLS worst path.

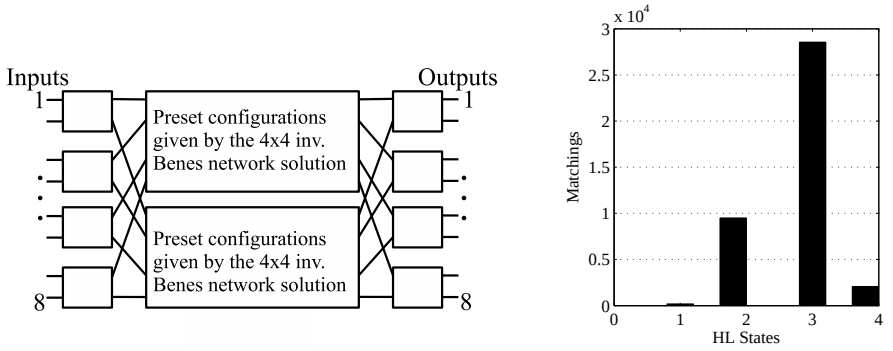

(a) 8x8 Benes Network with preset middle stages

(b) All the matchings classified by number of turns

Figure 3.31: Basic Benes 8x8 characterisation

This approach seems to less effective due to the less *Degree of freedom* in the inner stages commented before. In fact, that metric for the first heuristic procedure was:

$$D_{Benes}(N=8) = \frac{2^{((Number\ of\ SE)=20)}}{(N=8)!} \simeq 26$$

But now, knowing that the number of network states is:

$$Number\ of\ States(SE,p.box) = 2^{(Number\ of\ SE)} \cdot (States\ p.box)^2 = 2^8 \cdot 24^2 = 147.456$$

We get that now the *Degree of freedom* using p.box result is:

$$D_{p.Benes}(N=8) = \frac{147.456}{(N=8)!} \simeq 3{,}65$$

Therefore, this justifies the faster procedure achieved in the exhaustive analysis meanwhile a less accuracy in the result is obtained.

3.6 Mirroring

This section firstly analyses the well-known network structures presented before in Section 3.4 (4x4 and 8x8 basic Benes) now entirely built with 2M-SE. Then, two different approaches are considered: the first uses the offered performance of this structure adding a routing plane called *mirrored plane*, and the second approach uses four routing planes instead of two.

3.6.1 Mirrored network

N=4 mirrored Benes

Figure 3.32a depicts a N=4 basic Benes network structure where all its SEs are 2M-SE (called N=4 mirrored Benes). Analysing the network with the same procedure as the applied previously, we get histogram 3.32b that classifies the 24 matchings equally as in the basic Benes case. Thus we can observe that most of the matching cases (15) need the worst connection to be routed through two SEs in HLS, six matchings have a worst path that require one HLS, two matchings define the $H_{mirrBenes}(N = 4) = 3$, and finally, only one matching can be routed with all the SEs in LLS (zero HLS).

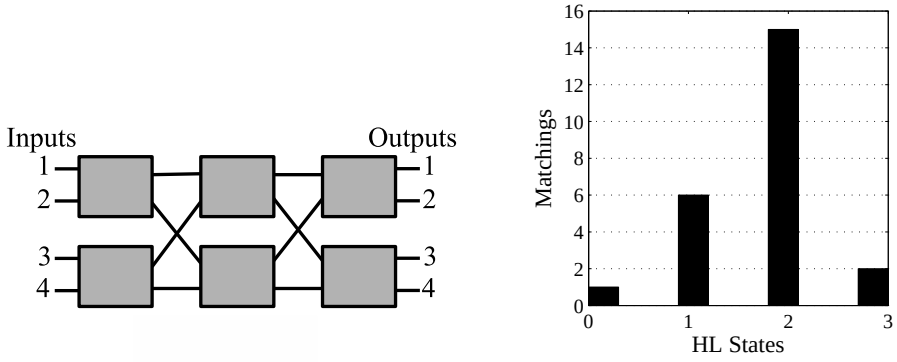

(a) N=4 basic mirrored Benes network

(b) All the matchings classified by number of turns

Figure 3.32: Basic mirrored Benes 4x4 characterisation

Table 3.7 gives the corresponding number of network states i which a matching can be suitable routed. We can see that the classification result is

exactly the same as the shown before in Table 3.1 (N=4 basic Benes network). It is important remark that the matchings contained in each group are not equal as the cases in the previous table, despite the total number is the same.

Matchings		States for each matching	Subtotal states
16		2	32
8		4	32
Total	24	-	64

Table 3.7: Types of correspondences between matchings and states in the 4x4 mirrored Benes network

Therefore, observing the total number of matching cases and the total number of network configurations, we continue the characterisation calculating two important metrics of the network: $C_{mirrBenes}(N = 8)$, because the number of SEs is used for the network cost calculation (and also used for the total number of network states) and the *Degree of freedom*, related to the total number of network states and to the total number of matching cases.

$$C_{mirrBenes}(N = 4) = N(2\log_2 N - 1) = 12$$

$$D_{mirrBenes}(N = 4) = \frac{2^{((Number\ of\ SE)=6)}}{(N = 4)!} = \frac{2^6}{24} = 2{,}6\hat{6}$$

At this point, the identification of those SEs in the network that have the highest frequency in terms of HLS do not gives important analysis information. In fact, we continue recalling the example *Matching(N=4)* used before in order to present intuitively the important mirroring property.

Matching(N=4)	HLS mirrored network				HLS basic network			
Input $i \rightarrow$ Output j	3.33a	3.33b	3.33c	3.33d	3.12a	3.12b	3.12c	3.12d
$1 \rightarrow 3$	3	3	1	1	0	0	2	2
$2 \rightarrow 4$	3	3	1	1	0	0	2	2
$3 \rightarrow 2$	2	2	2	2	1	1	1	1
$4 \rightarrow 1$	2	2	2	2	1	1	1	1

Table 3.8: SEs in HLS for all the paths of *Matching(N=4)* in networks 3.33 and 3.12

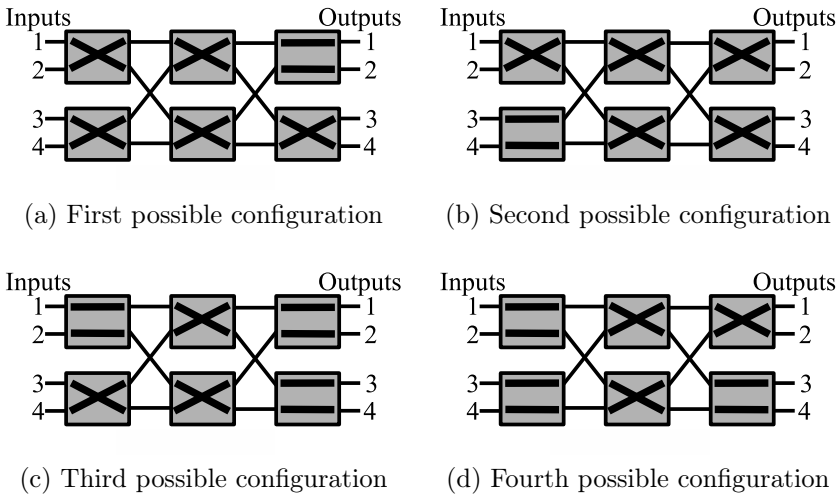

(a) First possible configuration (b) Second possible configuration

(c) Third possible configuration (d) Fourth possible configuration

Figure 3.33: The four possible network configurations that route the required matching in this 4x4 mirrored Benes network

Table 3.7 shows the SEs used in HLS for the *Matching(N=4)* routed through the four network configurations depicted in Figure 3.33. In addition, the four right columns show again the HLS used in the configurations that routed the *Matching(N=4)* with the 4x4 basic Benes network. The aim of this Table 3.7 is to give an easy comparison between those solutions. Analysing in more detail the mirrored configuration, we can observe for one side the similarity between cases 3.33a and 3.33b because they have to take three SE in HLS for paths $1 \rightarrow 3$ and $2 \rightarrow 4$ and two HLS for $3 \rightarrow 2$ and $4 \rightarrow 1$. By the other side, we have cases 3.33c and 3.33d where paths $3 \rightarrow 2$ and $4 \rightarrow 1$ still need to go through two SE in HLS but now the other two connections ($1 \rightarrow 3$ and $2 \rightarrow 4$) have to cross only one SE in HLS. Then, in this example we have that network configuration cases a and b perform worse than c and d, so we identify this matching case with 3.33c or 3.33d in the bijective relation of this network.

Once we have seen the first half of the example presented in Table 3.8, having this switching fabric the same connection pattern as network 3.10a (N=4 basic Benes) and taking into account, from Section 3.1, that 2M-SE (grey boxes) have an *opposite behaviour* respect 2B-SE, we can infer the following points:

- The network configurations that route the required matching are the same as in the example of Figure 3.12. Therefore when we have the same type of fabric, required paths (matching requested) and the connection pattern, we need to have the same network states.

- This example illustrates the fact that changing all the SEs from 2B-type to 2M-type in a network structure (with *opposite behaviour*) does not give the possibility to modify its matchings histogram with any symmetrical or "opposite" operation, movement or transformation. Moreover, entire worst penalty cases remain but the individual matching performance changes. This can be justified recalling the asymmetry of finding the minimum number of HLS between the worsts connections in each network configuration for all the existing matching cases.

- It is important to notice that for connections that do not pass through any SE in HLS in the example depicted in Figure 3.12 now go through three SEs in HLS, connections that take one HLS now use two SEs in HLS and vice versa (meaning that connections passing through three SEs in HLS now do not pass any one in this example (Figure 3.33) and connections using two HLSs now take only one SE in HLS). From another point of view, we can start from this example in Figure 3.33 and go to example presented in Figure 3.12 applying the same procedure, as follows:

HLS count basic Benes $\leftrightarrow$ HLS count mirrored Benes for each connection case
$0 \leftrightarrow 3$
$1 \leftrightarrow 2$
$2 \leftrightarrow 1$
$3 \leftrightarrow 0$

Table 3.9: Mirroring connection penalty transformation for this N=4 Benes case

Generalising the operation presented in Table 3.9, the number of SEs in HLS used by a single connection through a network is as follows:

$$HLS_{mirr}(S) = S - HLS_{basic} \tag{3.6}$$

and its opposite: $HLS_{basic}(S) = S - HLS_{mirr}$

Where S is the number of stages in the considered network, HLS_{basic} is the number of SEs in HLS used for a single connection and HLS_{mirr} is the number of SEs in HLS passed by that single connection using the same route in the equivalent mirrored network.

N=8 mirrored Benes

The 8x8 mirrored Benes network is now analysed in Figure 3.34. We can observe that it presents absolutely the same behaviour as its equivalent N=8 basic Benes network (see Figure 3.13 in Section 3.4). Thus we still find the most of the matchings (near 28,5 thousand) need at least one connection to pass through three SEs in HLS and we can observe that two thousand matching cases that need again at least one path to go through four SEs in HLS.

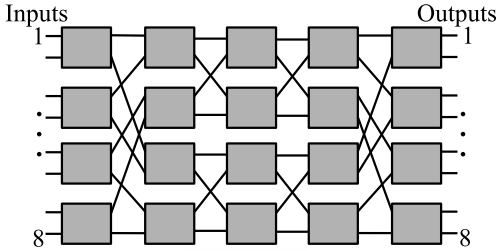

(a) N=8 basic mirrored Benes network

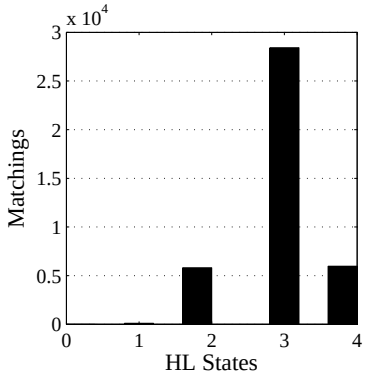

(b) All the matchings classified by number of turns

Figure 3.34: Basic Mirrored Benes 8x8 characterisation

Therefore, metrical values of this network remain equal as in the first well-characterised 8x8 basic Benes:

$$H_{mirrBenes}(8) = 4$$

Given by those two thousand matching cases that need at least one path to go through four SEs in HLS appearing in the histogram 3.34b.

$$C_{mirrBenes}(8) = N(2\log_2 N - 1) = 40$$

Because of having the same number of States and number of matchings (equations 3.3 and 3.4 respectively) the *degree of freedom* for this case remains as:

$$D(8) = \frac{2^{((Number\ of\ SE)=20)}}{(N=8)!} \simeq 26$$

Types of correspondences between matchings and states for this N=8 mirrored Benes network presented in Table 3.10 remain equals as those shown in Table 3.2 (N=8 basic Benes network). Despite that equally numerical value, the matching cases contained in each group are different between basic and mirrored networks.

Matchings		States for each matching	Subtotal states
128		256	32768
512		128	65536
2816		64	180224
2048		40	81920
12288		32	393216
14336		16	229376
8192		8	65536
Total	40320	-	1048576

Table 3.10: Types of correspondences between matchings and states in the 8x8 mirrored Benes network

Lets recall the example *Matching(N=8)* in order to conclude this N=8 mirrored Benes study. Table 3.11 shows the connections required, recalls the number of HLS in the basic Benes network (Table 3.3) and presents the result obtained for this new N=8 mirrored Benes (Figures 3.35 and 3.36). In fact, we can analyse this specific case separating those characteristics that remain equal as the seen in the basic Benes example presented in Figures 3.15 and 3.16 from those others that become different because of the use of 2M-SE.

Matching(N=8)	Number of HLS in basic Benes network							
Input $i \rightarrow$ Output j	3.15a	3.15b	3.15c	3.15d	3.16a	3.16b	3.16c	3.16d
$1 \rightarrow 5$	0	2	0	2	2	2	4	4
$2 \rightarrow 7$	2	2	2	2	2	2	2	2
$3 \rightarrow 2$	3	3	3	3	3	3	3	3
$4 \rightarrow 1$	3	3	3	3	3	3	3	3
$5 \rightarrow 8$	3	3	3	3	3	3	3	3
$6 \rightarrow 4$	1	1	1	1	3	3	3	3
$7 \rightarrow 3$	2	0	2	0	4	4	2	2
$8 \rightarrow 6$	2	2	2	2	4	4	4	4

	Number of HLS in mirrored Benes network							
	3.35a	3.35b	3.35c	3.35d	3.36a	3.36b	3.36c	3.36d
$1 \rightarrow 5$	5	3	5	3	3	3	1	1
$2 \rightarrow 7$	3	3	3	3	3	3	3	3
$3 \rightarrow 2$	2	2	2	2	2	2	2	2
$4 \rightarrow 1$	2	2	2	2	2	2	2	2
$5 \rightarrow 8$	2	2	2	2	2	2	2	2
$6 \rightarrow 4$	4	4	4	4	2	2	2	2
$7 \rightarrow 3$	3	5	3	5	1	1	3	3
$8 \rightarrow 6$	3	3	3	3	1	1	1	1

Table 3.11: Eight basic Benes network configurations and eight mirrored Benes network configurations summarised (portion of existing 16)

From one side, we have that remain:

- *Matching(N=8)* routed through this N=8 mirrored Benes network still belongs to the sixth group of matchings (14336 that have 16 network configurations each). We consider again half of the total network states, four equivalent configurations in Figure 3.35 and four alternative routing solutions in Figure 3.36. Therefore, as it has also seen in the example *Matching(N=4)* mirrored Benes, building the network with 2M-SE instead of 2B-SE do not change the number of network states able to route a requested matching.
- Those network configurations that route the matching requested are equal as the depicted in Figures 3.15 and 3.16. Because of that, we can reiterate that when we have the same type of fabric, required paths and the connection pattern, we need to have the same network states.

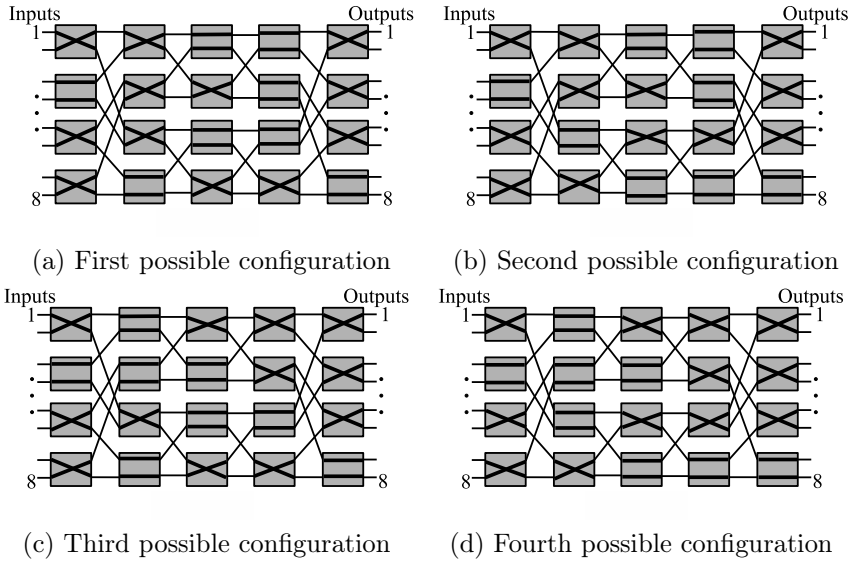

(a) First possible configuration (b) Second possible configuration

(c) Third possible configuration (d) Fourth possible configuration

Figure 3.35: Four equivalent network configurations (portion of existing 16) that can route the required matching

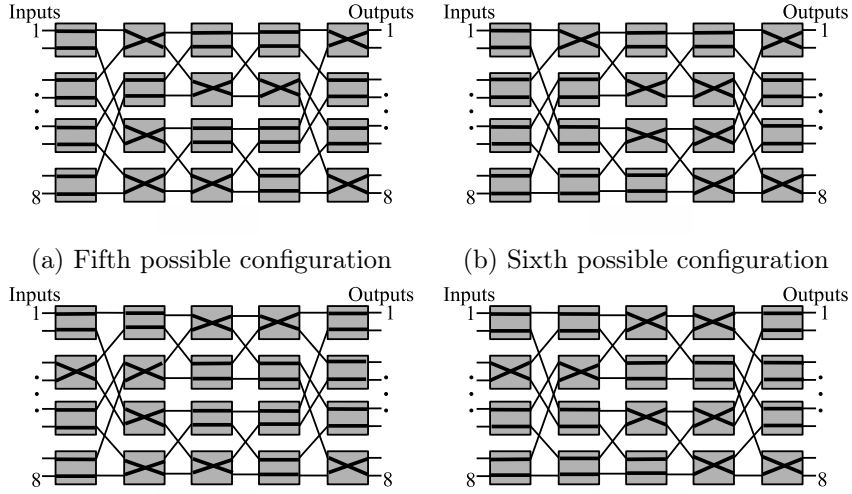

(a) Fifth possible configuration (b) Sixth possible configuration

(c) Seventh possible configuration (d) Eighth possible configuration

Figure 3.36: Four alternative equivalent network configurations (portion of existing 16) that can route the required matching

From the other side, we have that now:

- First half of Table 3.11 recalls the number of HLS in the basic Benes network for the example *Matching(N=8)* (Table 3.3) in order to give

a fast comparison with the new number of HLS in the mirrored Benes networks presented in the second half. We get that the best configuration to route the matching through this mirrored Benes network still implies a worst case connection that pass **three** SE in HLS. This point is mentioned between the different characteristics because we can not guarantee this behaviour. Moreover, the modification of the bijective relation between network states $\leftrightarrow$ matchings, implies to obtain a different value for the number of HLS used for the worst connection.

- Related to that modification of the bijective function, we can infer from the first four pictures in Figure 3.35 and from the values in columns from 3.35a to 3.35d in Table 3.11 that the worst connection needs to pass through **five** SE in HLS. Otherwise, from values in columns 3.36a to 3.36d we can observe that the worst path pass through **three** SE in HLS. This difference in the behaviour of the eight cases considered (in two groups of four) allows now the second four network configurations be as the states that compose the bijective relation for this matching.

- As it happens with *Matching(N=4)* routed with the mirrored Benes network, we can easily obtain the new number of HLS used by each connection applying the operation showed in table3.12 also defined by Equation 3.6, that is:

$$HLS_{mirr}(S) = S - HLS_{basic}$$
$$\text{and } HLS_{basic}(S) = S - HLS_{mirr}$$

To conclude this Section **3.6.1.Mirrored network** where has been presented and analysed N=4 and N=8 mirrored Benes networks, we have to mention that next steps are focused to take the maximum benefit of the mirroring property. That is offer for every single connection in a required matching the possibility to be routed through a basic network and through a mirrored network.

HLS count basic Benes ↔ HLS count mirrored Benes for each connection case
0 ↔ 5
1 ↔ 4
2 ↔ 3
3 ↔ 2
4 ↔ 1
5 ↔ 0

Table 3.12: Mirroring connection penalty transformation for this N=8 Benes case

3.6.2 Mirrored plane

The aim at this point is use Equation 3.6 (mirroring property) to find structures where $H(N)$ become lower than those values obtained in previous sections. We present two exhaustive network characterisations where connections can be routed through total basic planes, total mirrored planes or partial basic/mirrored.

Mirrored plane of all the network

Figure 3.37 uses the exhaustive procedure applied also in previous cases to characterise the network 3.37a in histogram 3.37b. We can separate the construction of the network described in three different points as follows:

1. We first need a *plane selector* (as depicted in the right part of the Figure 3.37a) in order to let each connection be able to select the best performing plane. Thus, because of having two planes in this construction, we need two microrings to make the signal pass to the best one required.

2. At the middle of the network, we have:

   (i) In the upper plane a N=8 basic Benes network as the characterised in Figure 3.13. As we have seen in the characterisation of this network separately, it has a $H_{basicBenes}(N = 8) = 4$. Importantly

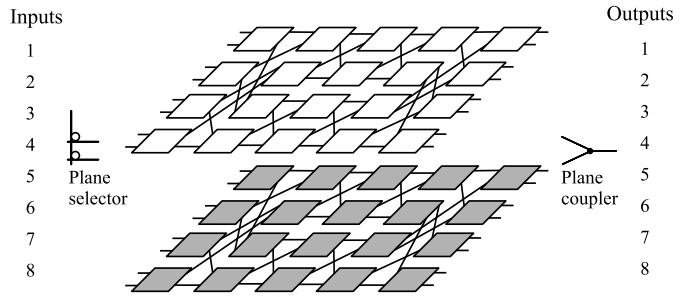

(a) Two planes with 8x8 basic and mirrored Benes networks respectively

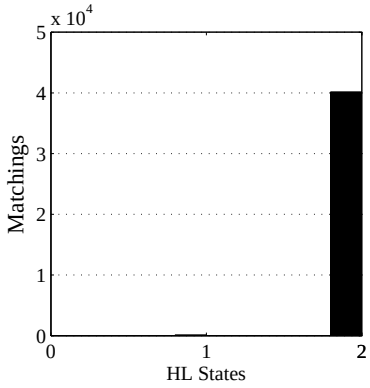

(b) All the matchings classified by number of turns

Figure 3.37: Two planes network with 8x8 basic and mirrored Benes characterisation

enough, worst connection cases can reach up to five HLS (numerically equal as the network depth S) if we apply a routing algorithm that does not take into account the HLS used. It is important to notice that, regarding to the mirrored plane, here each single connection passes through the following number of *turns*:

$$HLS_{basic}(S) = S - HLS_{mirr}$$

(ii) In the lower plane a N=8 mirrored Benes network as the characterised in Figure 3.34. We have also seen with the exhaustive analysis that $H_{mirrBenes}(N = 8) = 4$. Moreover, as in the basic Benes network (upper plane), if we apply a routing algorithm that does not take into account the number of HLS used worst

connection cases can reach up to five SEs in HLS. Despite that fact, because of having a completely different bijective function, every single connection is able to choose between this mirrored plane where:

$$HLS_{mirr}(S) = S - HLS_{basic}$$

3. Once we have routed the connection through the best performing plane, we need to let it reach the output. In fact, this final part of the construction does not need an "active selection" due to the fact that this operation has been done at the beginning. Therefore, just coupling those connections coming from upper and lower plane for each output we passively obtain the expected result. The element used to perform that operation is the *plane coupler* depicted at the right part of the network 3.37a.

Histogram 3.37b shows the exhaustive analysis of this structure characterised above. We can observe that huge part of all the existing matchings have a worst connection routed through two SEs in HLS. In fact, because of letting each connection choose between the two planes, the result will always be to select the plane with less than half of the depth in number of SEs in HLS. Thus having an odd number of stages, we can say in advance that the resulting number of *turns* is $H(N = 8) = 2$ being confirmed with the histogram.

The final number of H for this structure must contain the additional *plane selector* set at the beginning of the network for each input. Nevertheless there is no need to consider an additional penalty at the end of the network, due to the fact that the *plane coupler* does not add HLS. Thus the final performance of this structure is:

$$H_{2pl\ Benes}(N = 8) = 3$$

We can easily obtain the cost of this structure considering the contribution of two addends: one for the selectors, and another as twice the plane cost:

$$C_{2pl\ Benes}(N = 8) = 2 \cdot N + 2 \cdot N(2 \log_2 N - 1) = 96$$

As a final metric, we recall the calculation of the *degree of freedom* taking into account that now we let each of the eight connections be able to choose between two planes. Therefore, the formula for D is increased with a factor 2^8. Nevertheless, because of considering two planes both with the same network state does not add any additional factor.

$$D_{2pl\ Benes}(N=8) = \frac{2^8 \cdot 2^{((Number\ of\ SE)=20)}}{(N=8)!} = \frac{2^{28}}{8!} \simeq 6.657{,}63$$

In conclusion, D for a multiple plane structure gives less relevant information than for a single plane.

Partial planes basic and mirrored

Figure 3.38 is divided in network 3.38a and its histogram 3.38b. With this four-plane structure, we present another characterisation trying to explore another benefit of the mirroring property. As in the two-plane structure, we can describe the network construction in three different points as follows:

1. We first need a higher *plane selector* (as depicted in the right part of the Figure 3.38a) in order to let each connection be able to select the best performing plane. Thus, because of having four planes in this construction, we need four microrings at each input.

2. Now, at the middle of the network, we have:

   (i) The top plane is a N=8 basic Benes network as the upper one forming the two-plane structure previously presented. Then regarding to the mirrored plane, here each single connection passes through the following number of *turns*:

   $$HLS_{basic}(S) = S - HLS_{mirr}$$

   (ii) The second plane is the first of two devoted to the search of more benefit using different 2B and 2M SEs combinations. The main idea is offer for each connection two additional mirrored planes but different from those situated at the top and at the bottom of the structure respectively. We can observe that half of the twenty

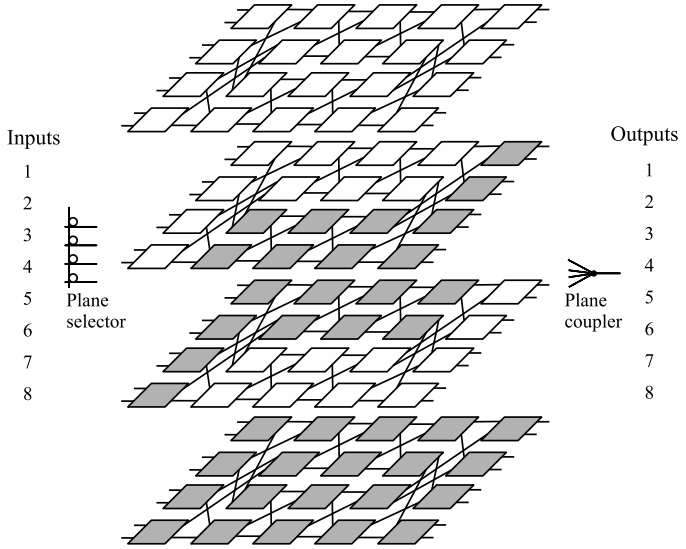

(a) Four planes with 8x8 basic, mirrored and partial basic/mirrored Benes networks respectively

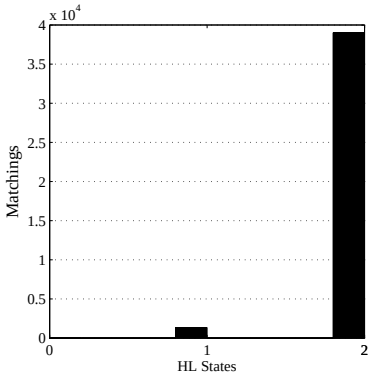

(b) All the matchings classified by number of turns

Figure 3.38: Four planes network with 8x8 basic, mirrored and partial basic/mirrored Benes characterisation

SEs are 2B-type (all first stage and upper middle SEs) while the other half belongs to the 2M-type (lower middle SEs and all last stage). Then, regarding to the third plan we can guarantee that:

$$HLS_{b/m}(S) = S - HLS_{m/b}$$

(iii) The third plane complements the previous described ands is also devoted to the search of more benefit using different 2B and 2M

SEs combinations. Now we have half of the twenty SEs 2M-type (all first stage and upper middle SEs) while the other half 2B-type (lower middle SEs and all last stage). And because of this "symmetry" in the construction:

$$HLS_{m/b}(S) = S - HLS_{b/m}$$

(iv) The lowest plane is a N=8 mirrored Benes network as the lower one forming the two-plane structure previously presented. Then regarding to the basic plane, each single connection passes through the following number of *turns*:

$$HLS_{mirr}(S) = S - HLS_{basic}$$

3. Finally, there is also here no need to have an "active selection" due to the fact that this operation has been done at the beginning. Therefore, we just couple those connections now coming from four different planes for each output passively. The element used to perform that operation is now a *plane coupler* (from four to one) depicted at the right part of the network 3.38a.

Histogram 3.38b shows the exhaustive analysis of this structure characterised above. We can observe a slight reduction of the huge part of matchings that have a worst connection routed through two SEs in HLS. the number of matchings that have a worst connection passing through only one SE in HLS has increased because of having two additional planes. Therefore, this structure performs in average better than the two-plane presented in Figure 3.37a but still has the number of *turns* as $H(N = 8) = 2$.

The final number of H for this structure must contain again the additional *plane selector* set at the beginning of the network for each input. Nevertheless there is no need to consider an additional penalty at the end of the network, due to the fact that the *plane coupler* does not add HLS. Thus the final performance of this structure is:

$$H_{4pl\ Benes}(8) = 3$$

We can easily obtain the cost of this structure considering the contribution of two addends: one for the selectors, and another as four times the plane

cost. We observe that implies twice the value of the previous two-plane structure:

$$C_{4pl\ Benes}(8) = 4 \cdot N + 4 \cdot N(2\log_2 N - 1) = 192$$

In conclusion, we do not obtain any benefit with the addition of those partial basic/mirrored planes. In fact, this four-plane structure should be best exploited considering a different network configuration at each plane able to guarantee several best paths of each required matching. That procedure could be only achieved applying a modification of the routing algorithm making more difficult the overall network control. Moreover, that hypothesis impossibilities using the mirroring property (Equation 3.6), which requires the same network state at each plane in order to offer the correct alternative path.

3.7 Benes-crossbar (HBC)

The aim of this section is to present several alternative interconnection architectures in order to offer more resources to the compromise between HLS used and building cost of the network.

Now we focus the reduction of the SEs in HLS used at the middle part of the network. Concretely, we have seen in Sections 3.4 and 3.6 (Benes and mirrored respectively) that either in a N=4 basic Benes or a N=4 modified Benes or also in a N=4 mirrored Benes, we do not reach to have only one SE in HLS as the worst case for all the matchings. Because of that, we now present an architecture that satisfies the lowest penalty achievable at the middle part of the structure. Therefore, after that middle construction successive stages are made with benes recursively construction pattern.

As a first approach, in Figure 3.39a we explore in the same way as Benes cases, exhaustively all the configuration States in which the possible matchings and can be satisfied. We observe that in the most of the cases two and a maximum of three HL States will be necessary to route a connection set (one HLS mandatory in the middle crossbar; and one or two in the first and last stage). In fact, the histogram 3.39b is fully described in the following:

- One HLS: Only 576 matchings can be hold with all the connections taking one SE in HL State. That number connection sets is related to the number of matchings that a 4x4 network is able to hold by definition, so considering that the SEs in the first and last stages are all in Low Loss State, the two middle 4x4 crossbars are able to route $24 \times 24 = 576$ together.

- Two HLS: If the matching that we want to require to the network do not belongs to the set of 576 explained above, at least one SE in HL State is needed in the first or last stage in order to reach that demand. Thus at the moment that one path has two SEs in HLS, it changes the maximum of that matching.

- Three HLS: As a slightly variation of the case of two HLS, we can say that exists one path that requires HLS in the first and the last stages, modifying the maximum of that matching into three. It is important to say that, being this the worst case of the overall performance, the unavoidable case of matchings holding connections of four HLS does not appear in this construction pattern.

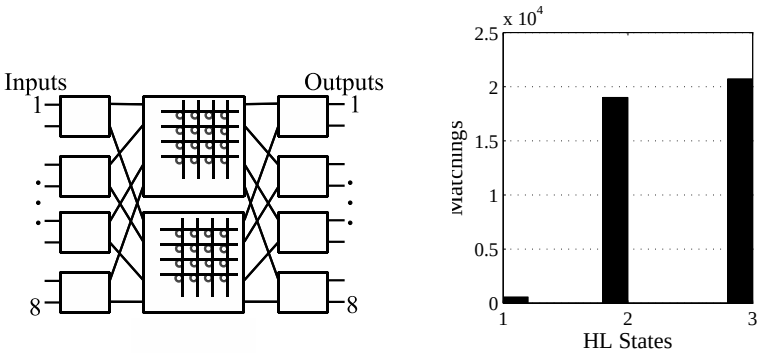

(a) 8x8 Benes network with preseted middle stage

(b) All the matchings classified by number of turns

Figure 3.39: Basic Benes 8x8 characterisation

Regarding to the value of the metrics for this $N = 8$ network, we obtain:

$$H_{HBC}(8) = 3$$

The cost of this structure can be obtained as the contribution of two addends: one for the two middle crossbars, and another as twice a first or last stage of a N=8 Benes network:

$$C_{HBC}(8) = 2 \cdot (\tfrac{N}{2})^2 + 2 \cdot N = 48$$

Finally, the *degree of freedom* for this case knowing that in the numerator we have three factors: twice the 24 different matchings that can be routed at each crossbar and the states of eight SEs. Nevertheless, the denominator remains with the eight factorial existing matchings. We obtain:

$$D_{HBC}(8) = \frac{2^8 \cdot 24 \cdot 24}{8!} = \simeq 3.66$$

In conclusion, hybrid Benes-crossbar combination offers a good promising performance considering the small number of worst case turns obtained despite having a low degree of freedom. Higher size N HBC networks are introduced in next Section 4.3 considering as a starting point the exhaustive analysis presented here.

Chapter 4

Results and Discussion

In this chapter we explore the scalability response of large switching fabrics using SEs made with microring resonators. The starting point for each analysed structure is its simulation result obtained in Chapter 3. Then, we describe the construction rule applied to reach higher N network sizes allowing at the same time deduce the final number of *turns* $H(N)$ and the cost $C(N)$. Nevertheless if necessary, we will subdivide in each section the construction rule, scalability and cost into slight different versions of the starting network structure. Thus, we close the scalability response characterisation of each network presenting its corresponding plot and obtained values.

The main part of the chapter (first five sections) is dedicated to realise the scalability response analysis of different network structures. Finally, an overall comparison and discussion between all the obtained results is made in Section 4.6.

4.1 Benes

The aim of this section is to characterise Benes network by its cost C and scalability H for a higher number of ports than the cases seen in Section 3.4. First, we recall the results obtained in that section for network sizes four and eight. Thereafter, applying the recursive network construction seen in Section 2.2 we formulate equations for C and H, in order to conclude the characterisation showing their growing behaviour.

Simulation results

Figure 4.1 shows a summary of all the results obtained for the N=4 Benes networks exhaustive characterisations presented in Section 3.4. We can observe in network 4.1a two SEs named that need to be modified in order to obtain the 4x4 slight different Benes networks analysed. Thus, describing them from the worst to the best performance reached we have:

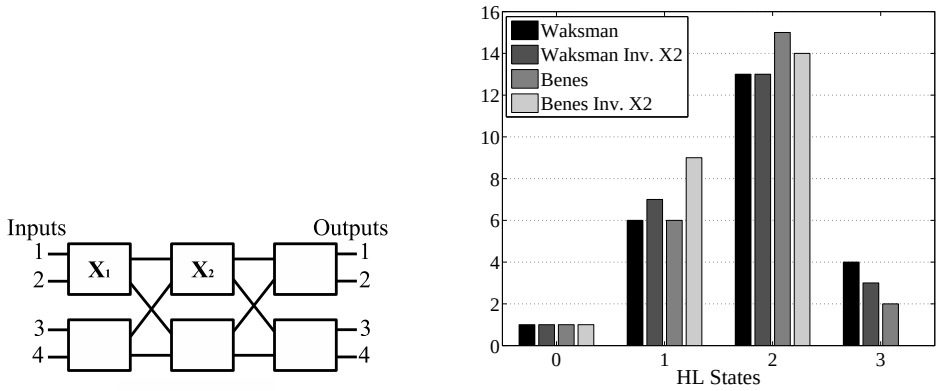

(a) 4x4 Benes network with two SEs named

(b) The behaviour of the four 4x4 Networks considered

Figure 4.1: Comparison of the different four 4x4 Networks

1. Waksman network is obtained by setting SE X_1 = Bar for all the states. The performance exhibited is the worst of all the four N=4 networks compared having four matchings with at least one path passing three SEs in HLS. We can also observe two characteristics shared for all the compared fabrics: that the most of the matchings contain a connection taking two SEs in HLS (between 13 and 15 of the existing 24) and the fact that there is only one matching able to be routed without taking all SEs in LLS.

2. Modified Waksman network is obtained from 4.1a setting X_1 = Bar and inverting X_2, that is consider a 2M-SE instead of a 2B-SE. By inverting the behaviour of that middle SE, we get a slight benefit in

the network behaviour comparing it with Waksman network previously seen.

3. Network 4.1a has a basic Benes structure if all the SEs are 2B-SE and without modifying any intermediate connection. Despite it has the highest number of matchings with a connection routed through two SE in HLS, this Benes structure still needs support three SEs in HLS for two matching cases.

4. Modified Benes network seen in Section 3.4.2 can be obtained inverting the behaviour of X_2, that is considering a 2M-SE instead of a 2B-SE. This network exhibits the best performance of the four compared in Figure 4.1. Its highest number of matchings (9) that can be routed with at least one connection passing only one SE in HLS allows avoid those worst cases with three HLS for several routed paths. We can formulate his result with the expression $H(3) = 2$.

Let us recall the results obtained for the N=8 Benes networks exhaustive characterisation presented in Section 3.4 summarising them in Figure 4.2. Now we can observe in network 4.2a two middle structures squared and four SEs named that need to be modified in order to obtain 8x8 slight different networks. Thus, describing them from the one with worst to the best performance reached we have:

1. Network 4.2a presents a basic Benes structure considering all the SEs as 2B-SE and if we don not modify any connection. We can observe that its performance is the worst of those compared attending to the high number of matchings with at least one path passing four SEs in HLS.

2. We get a preset middle stage Benes network by fixing the routing solutions in *Middle Stages 1* and *Middle Stages 2*. As we have seen in Section 3.6, the routing solution that compose that middle stage dashed boxes is the bijective function corresponding to the modified Benes network. Therefore, we obtain a better performance than the one achieved in the basic structure but due to the decreased degree of freedom we do not reach the same improvement as

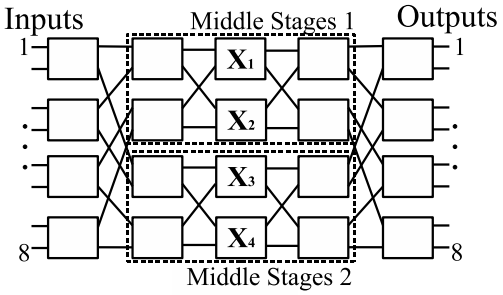

(a) SEs and middle stages named for a 8x8 Benes structure

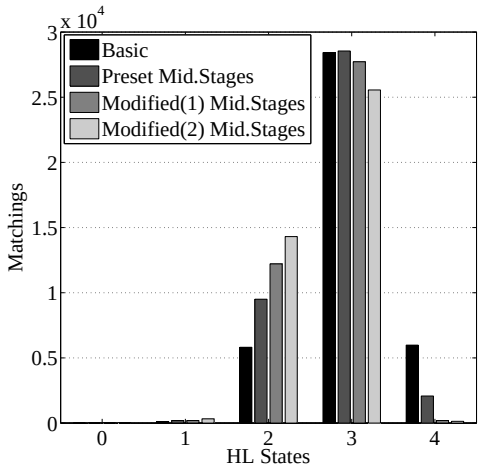

(b) The behaviour of the four 8x8 Networks considered

Figure 4.2: Comparison of the different four 8x8 Networks

3. We obtain the **first N=8 modified Benes** characterised in section 3.4.2 considering X_1 and X_3 as 2M-SE instead of 2B-SE.

4. And finally, the best performance achieved between all N=8 Benes structures is the performed by the **second N=8 modified Benes** characterised in section 3.4.2 considering X_1 and X_4 as 2M-SE instead of 2B-SE.

Histogram 4.2b recalls the results obtained for the four networks. We can observe that the maximum number of turns that characterise each network is $H(8) = 4$ for all the cases.

Scalability $H(N)$ and cost $C(N)$

If we apply one of the routing algorithms explained in Section 2.2, we can not guarantee for a specific matching the best selection of all the routes in terms of number of SEs in HLS. In fact, $H(3) = 2$ and $H(8) = 4$ can be achieved only if we store all the routing solutions for all the existing matchings, that is all the bijective function between network states $\leftrightarrow$ matchings. Therefore, when we use a well-known routing algorithm that do not takes into account the number of turns, we consider the worst equal to the number of stages of the Benes network.

$$H_{Benes}(N) = 2\log_2 N - 1 \tag{4.1}$$

Regarding the network cost, we need to count the result obtained when applying the Benes network construction rule.

$$C_{Benes}(N) = 2 \cdot N\log_2 N - N \tag{4.2}$$

Network accomplishment (achievement)

Figure 4.3 shows graphically the result for $H_{Benes}(N)$ and $C_{Benes}(N)$.

From one side, the cost of the Benes network (see Figure 4.3a) scales as $\sim N\log_2 N$. Because of that, we can observe a severe reduction when comparing it with the cost growing pattern of the crossbar network (that scales as $\sim N^2$). For instance, the difference reached in $N = 256$ size is more than one order of magnitude and increases for higher network sizes.

From the other side, Figure 4.3b shows graphically the growing number of turns of the Benes network. H increases as $\sim 2\log_2 N$ due to the number of stages used to build the network. From the scalability point of view, this is the poorest performance achievable. For instance, a path should go through 15 SEs in HLS when $N = 256$.

In conclusion, considering this Benes network and recalling the crossbar network presented in Section 3.2, two bounds can be defined:

- Multi-stage netwrok, complexity effective but with a growing H number of turns.

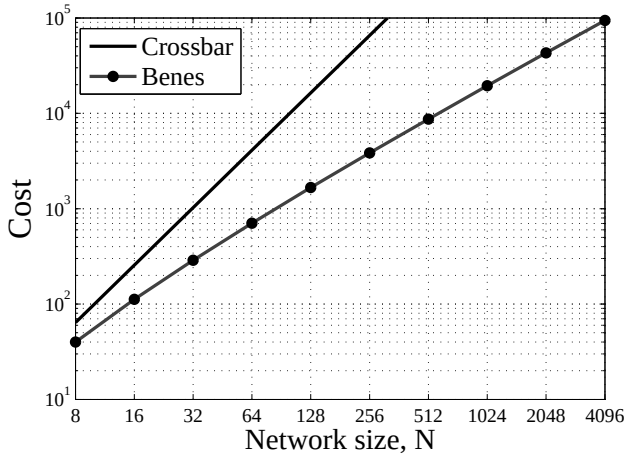

(a) Cost function of Benes network

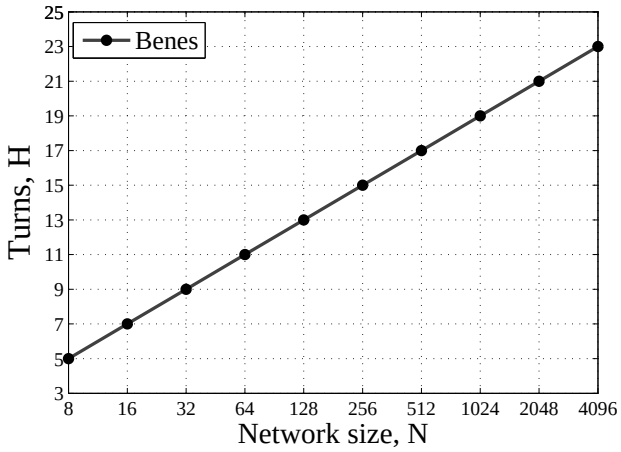

(b) Number of turns H of Benes network

Figure 4.3: Scalability characterisation of Benes network

- Single-stage network, whith a much more expensive but constant number of turns $H(N) = 1$.

4.2 Mirroring

In this section we firstly present a summary of the results obtained for small N sizes. Then, we aim at defining two different construction rules based on the mirroring concept presented in Section 3.6. The first construction rule

offers a complete mirrored plane, and approach uses *recursively* the mirrored structure in each step of the network construction rule.

Simulation results

In Section 3.6 we have presented a network completely built with 2M-SEs (mirrored network) obtaining:

- $H_{mirrBenes}(N = 4) = 3$ and $C_{mirrBenes}(N = 4) = 12$ for a N=4 mirrored network in Figure 3.32.
- $H_{mirrBenes}(N = 8) = 4$ and $C_{mirrBenes}(N = 8) = 40$ for a N=8 mirrored network in Figure 3.34

That exhaustive characterisations and their examples have been the starting point to define a two-plane structure (one basic and one mirrored). Nevertheless, we have not obtained a performance improvement adding partial basic/mirrored planes. Thus, we focus on two slightly different applications of the two-plane solution in the following: first, a complete mirrored plane at the end of the network construction, and second, an alternative mirrored plane at each building step of the construction rule.

4.2.1 Mirrored plane

Construction rule

Figure 4.4 depicts the construction rule applied. We first build a basic Benes network of the required size as in the previous section (recalling the recursive definition in Section 2.2). Then, we duplicate that network building another topologically equivalent exploiting 2M-SEs. Finally, plane selectors and plane couplers are added in order to choose the best plane for every single connection.

Scalability $H(N)$ and cost $C(N)$

From the scalabiltiy point of view, this architecture is able to reduce the number of turns to the half due to the mirroring property presented in Section 3.6, Equation 3.6:

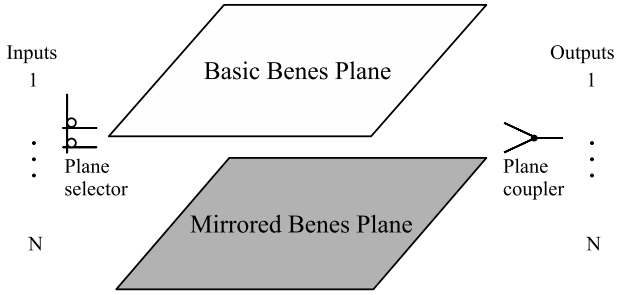

Figure 4.4: Mirrored architecture

$$HLS_{mirr}(S) = S - HLS_{basic}$$

and its opposite: $HLS_{basic}(S) = S - HLS_{mirr}$

Each plane presents a symmetric behaviour for the number of turns exhibited for each connection. Thus, because of the selection of the path with the lower number of HLS between those networks, we can formulate the following expression:

$$H_{mirrBenes}(N) = \lfloor \frac{2\log_2 N - 1}{2} \rfloor + 1 \tag{4.3}$$

Where the floor function shows the fact that we are reducing to the half a odd number of stages (and taking the lower number). Finally, an extra turn is caused by the plane selector at the beginning.

Regarding to the complexity point of view, adding a mirrored plane implies to double the cost of the network. Thus, we consider twice the basic Benes cost and the addition of two microrings for each plane selector:

$$C_{mirrBenes}(N) = 2(2 \cdot N\log_2 N) \tag{4.4}$$

Network accomplishment (achievement)

Figure 4.5 shows graphically the performance achieved for high network sizes.

Figure 4.5a depicts the growing behaviour for crossbar, Benes and mirrored Benes networks. As we expected, mirrored Benes exhibits the double complexity than basic Benes. Nevertheless, it is important to notice that for

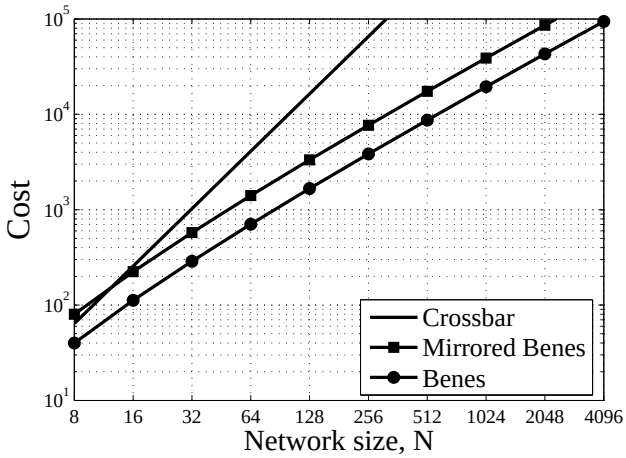

(a) Cost function of crossbar and mirrored Benes networks

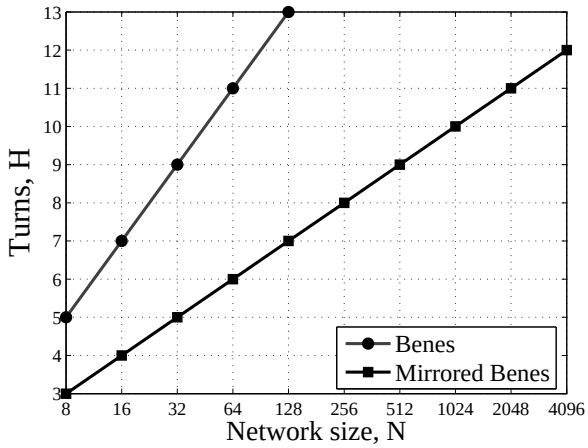

(b) Number of turns H of Benes network

Figure 4.5: Scalability characterisation of Benes network

$N \geq 32$ sizes, mirrored solution is cost advantageous compared with crossbar solution. Moreover, as the architecture increases, the difference becomes increased.

Figure 4.5b depicts the previous expression seen for $H_{Benes}(N)$ and $H_{mirrBenes}(N)$. Now the number of turns are reduced to the floor half plus one. Therefore, that implies a less growing behaviour of the HLS impairment. It is important to mention that setting a constant number of turns, this structure reaches a feasible $N^2/2$ network size. For instance, setting $H = 7$ we can go from

$N = 16$ to $N = 64$ and setting $H = 11$ we can increase from $N = 64$ to $N = 2048$.

In conclusion, we have presented the first middle solution between the trade-off complexity/scalability. This mirrored solution doubles the cost of the Benes network but is still much lower than crossbar complexity. At the same time, it reduces to the half plus one the number of turns, but do not reaches the crossbar constant number of turns $H(N) = 1$. Finally, it is important to mention that building a mirrored plan does not increase the complexity of the control algorithms. Since both planes will be configured with the same network state to route a matching request (as in examples seen in Section 3.4 and 3.6).

4.2.2 Recursive mirroring

Construction rule

Figure 4.6 shows an alternative recursive construction rule in order to reach a higher N size network performing a low $H(N)$ penalty. The idea applied is that every path can be routed in two different networks (basic and mirrored) now at each building step instead of selecting between two completely built networks. Therefore, once a building step is made, that inside box becomes the base for higher Benes networks.

In order to make understandable the way for going from Figure 4.6 to Equation 4.5 we enumerate the sequential procedure of the construction rule:

- Lets consider a $N = 16$ network.

1. The first step is to replicate the $N' = 8$ basic network of size $\left(\frac{N}{2}\right)$ with 2M-SEs. That is, build the mirrored plane.

2. Insert N' plane selectors (with two microrings each) in order to select one of the two planes built in the previous step. Thus we also add N' plane couplers (without microrings) at the end.

- At this point, we have built a $N' = 8$ mirrored network. The goal is reach the $N = 16$ mirrored network, thus Equation 4.5 starts from next step three.

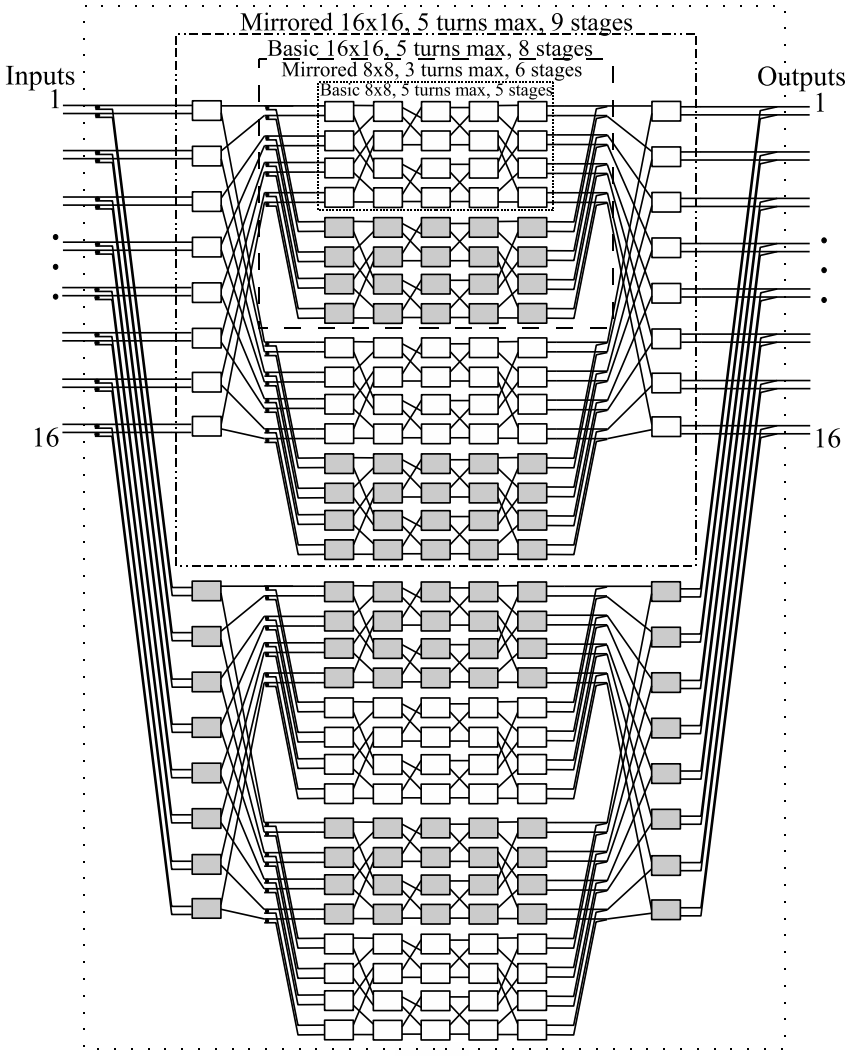

Figure 4.6: Recursive procedure to build a lower penalty network. In white, those SE who have the *basic behaviour*, and in grey, those other ones that have *opposite behaviour*

3. With sixteen 2B-SEs (N) (two microrings each) we build the 16x16 new basic network.

4. Now that we have a N=16 basic network, we apply the same procedure as step one. That is, replicate the network changing all the 2B-SE for 2M-SE and vice versa in order to build the mirrored plane.

5. Finally, we reapply the step two adding now 16 (N) plane selectors (with

two microrings each) in order to choose the best path at the beginning of the structure. Therefore, as every time we add plane selectors, now we also add N plane couplers (without microrings) at the end.

Scalability $H(N)$ and cost $C(N)$

The network cost for this recursive mirroring construction is expressed as follows:

$$C(N) = N + 2(2N + 2C\left(\frac{N}{2}\right)) \tag{4.5}$$

$$C(N) = 5N + 4C\left(\tfrac{N}{2}\right))$$

$$C(N) = 5N + 4\left(5\tfrac{N}{2} + 4C\left(\tfrac{N}{4}\right)\right) = 5N + 2 \cdot 5N + 2^4 C\left(\tfrac{N}{4}\right)$$

$$C(N) = 5N + 2 \cdot 5N + 2^4\left(5\tfrac{N}{4} + 4C\left(\tfrac{N}{8}\right)\right) = 5N + 2 \cdot 5N + 2^2 \cdot 5N + 2^6 C\left(\tfrac{N}{8}\right)$$

$$C(N) = 5N \cdot \textstyle\sum_{i=0}^{k-1} 2^i + 2^{2k} C\left(\frac{N}{2^k}\right)$$

$$\text{So we get that } C(N) = 5N \cdot \left(2^k - 1\right) + 2^{2k} C\left(\tfrac{N}{2^k}\right);$$

With $\frac{N}{2^k} = 8$ as a starting point and $C(8) = 88$ because of the microrings used at points **1.** and **2.** in order to build the $N' = 8$ mirrored network.

$$C(N) = 5N \cdot \left(2^{log_2 \frac{N}{8}} - 1\right) + 2^{log_2 \frac{N}{8}} \cdot C(8) = \tfrac{5}{8}N^2 - 5N + \left(\tfrac{N}{8}\right)^2 \cdot 88$$

So finally,

$$C_{rec\ mirr}(N) = N\left(2N - 5\right) \tag{4.6}$$

Regarding to the number of turns of this construction rule, he have to consider separately HLSs coming for the 2B-type or 2M-type SEs from those HLSs counted from the plane selectors. Thus, we apply the mirroring property to turns presented in 2x2 SEs and we consider as a constant addition (not subjected to mirroring property) the turns due to plane selectors. Consequently, we can observe in Figure 4.6:

1. **Basic 8x8** box has five stages, and without considering a routing algorithm that takes into account the number of HLS per path, that part of the network presents a five turns max.

2. **Mirrored 8x8** box has a total of six stages, where five belong to the 2x2 SE type and one has the plane selector function. Thus, applying mirroring property to the five-stage part, we reduce from a maximum of five HLS to a maximum of two. Then, just adding the selector, we obtain three turns max.

3. **Basic 16x16** box presents seven stages 2x2-type and one selector (8 stages total). Thus we have three turns max from previous point (**2.**) and because the addition of two stages 2x2-type we obtain 5 turns max total.

4. **Mirrored 16x16** box has also seven stages 2x2-type and two selectors (9 stages). We can infer the total number of turns from two equivalent points of view:

   - Seven stages subjected to mirroring property exhibit a total of three maximum number of turns. Moreover, adding the two stages devoted to plane selectors, we obtain a total of five turns max.
   - Recalling the obtained three turns total from point **2. Mirrored 8x8**, we apply mirroring to those two stages added at point **3.** obtaining an additional turn from 2x2 SEs-type. Then, adding the first selector used to mirror, we obtain the total of five max turns.

5. **Basic and mirrored 32x32**. In the following, the construction rule will perform recursively points **3.** and **4.**, that is adding two maximum turns for each growing step.

Network accomplishment (achievement)

Figure 4.7a shows recursive mirroring's cost compared with crossbar architecture. As we can observe, growing complexity is proportional as N^2 which

is not a good behaviour because we know (from Section 3.2) that one side of the bound between cost and scalability trade-off is the crossbar solution. Interestingly enough, we recall that there is no structure able to perform better than crossbar exhibiting a growing cost proportional as N^2.

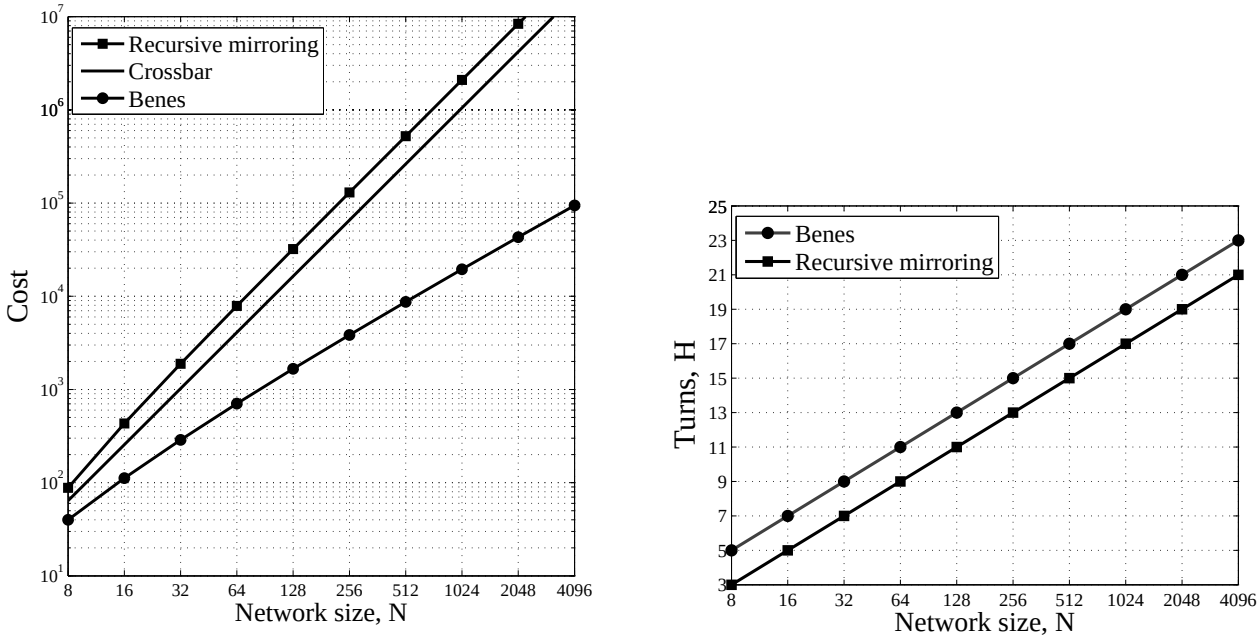

(a) Cost function of Benes and mirrored Benes networks

(b) Number of turns H of Benes network

Figure 4.7: Scalability characterisation of Benes network

Figure 4.7b shows the maximum number of HLS for several network sizes. As we have previously seen, two additional turns are added for each increasing step performing very similar as Benes network (see Figure 4.3b).

In conclusion, joining the high cost exhibited and the number of turns performed, make **Recursive mirroring construction rule** be considered as an unsuitable solution to the trade-off.

4.3 Benes-crossbar (HBC)

In Section 3.7 we have presented a hybrid network between Benes and crossbar structure (HBC network). Thereafter we have characterised a N=8 HBC

network in Figure 3.39 obtaining $H_{HBC}(N = 8) = 3$ and $C_{HBC}(N = 8) = 48$ as main results. Being that exhaustive characterisation the starting point, the aim of this section is to define two construction rules applied to reach higher N network sizes with a hybrid combination. First we explore a basic HBC construction rule, and secondly, we join mirrored property and HBC (M-HBC) in order to give a solution combining those new network architectures.

4.3.1 basic HBC

Construction rule

Figure 4.8 presents structures made using the HBC construction rule. Being N the total number of ports to be built and m the size of the inside crossbar structures, we can obtain with the ratio N/m the number of stages that are need to complete the network. Those stages are made using the Benes construction rule, and that implies N/m of crossbars inside. In fact, it is important to mention that due to logically construction must be satisfied $N \geq m \geq 2$, knowing that $N = m$ makes HBC become the crossbar structure and $m = 2$ degenerate into a Benes structure.

These networks answer the proposal of finding a compromise between the SE in HLS used and the complexity (in terms of number of rings used) for different sizes N. We set different sizes of the inside crossbar structure m in order to balance the load of Benes advantageous-cost with crossbar offered scalability. Indeed, the final network cost and exhibited number of turns are strictly related to the chosen m.

Scalability $H(N)$ and cost $C(N)$

Considering the HBC construction rule previously explained, we can obtain the expression for the cost applying recursively the following Equation 4.7: from the outer stages, every inner step is obtained as: twice the half-sized network cost plus the number of SEs to build that step (containing two microrings each). This can be expressed as follows:

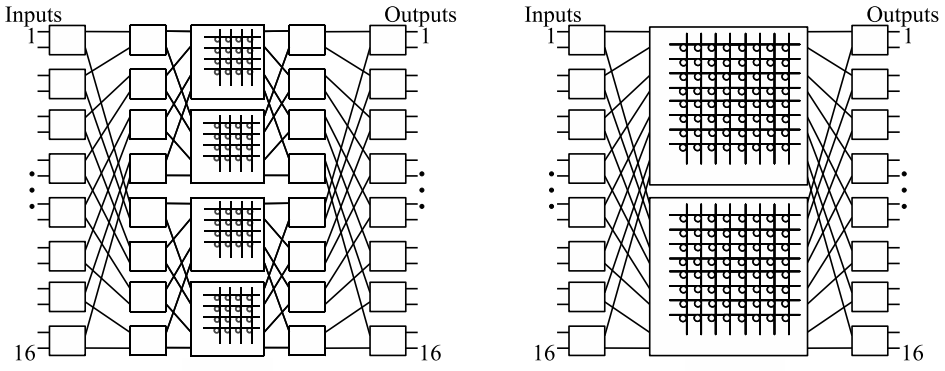

(a) Network with $N = 16$ ports and $m = 4$ Crossbar inside

(b) Network with $N = 16$ ports and $m = 8$ Crossbar inside

Figure 4.8: Two examples of Benes recursive construction from smaller crossbars inside

$$C(N) = 2N + 2C\left(\frac{N}{2}\right) \tag{4.7}$$

$$C(N) = 2N + 2\left(2\tfrac{N}{2} + 2C\left(\tfrac{N}{4}\right)\right) = 4N + 4C\left(\tfrac{N}{4}\right)$$

$$C(N) = 4N + 4\left(2\tfrac{N}{4} + 2C\left(\tfrac{N}{8}\right)\right) = 6N + 8C\left(\tfrac{N}{8}\right)$$

So we get that $C(N) = 2kN + 2^kC\left(\frac{N}{2^k}\right)$;

with the small crossbar inside $C(m) = m^2$; and $\frac{N}{2^k} = m$;

$$C(N,m) = 2Nlog_2(\frac{N}{m}) + N \cdot m \tag{4.8}$$

We can also find a closed expression for the number of turns. In fact, H_{HBC} is set by the number of stages built with the Benes procedure plus the turn performed by the crossbar structure. For instance, network 4.8a has five turns (four stages plus the crossbar) or network 4.8b has $H_{HBC}(16) = 3$. Concreting, as a function of N and m:

$$H_{HBC}(N,m) = 2log_2N - (2log_2m - 1)$$

$$H_{HBC}(N,m) = 2log_2(\frac{N}{m}) + 1 \tag{4.9}$$

Confirming our examples in Equation 4.9. Larger m crossbar sizes implies lower number of turns but a higher network cost (see Equation 4.8 proportional to $m - \log_2 m$).

Network accomplishment (achievement)

Figure 4.9 shows different cost functions for several HBC networks. We can observe that all the solutions are bounded by the crossbar structure at the top and by the Benes cost at the lowest part. Within that range, from one side, the smaller is the size of the m crossbars inside, the nearer is the cost of the function to the Benes limit. But from the other side, the higher is the m-sized crossbar inside structure, the closer is the cost to the crossbar N^2 function. Summarising, HBC exhibits a growing cost behaviour similar to the Benes network but now choosing the offset with the inside crossbar size.

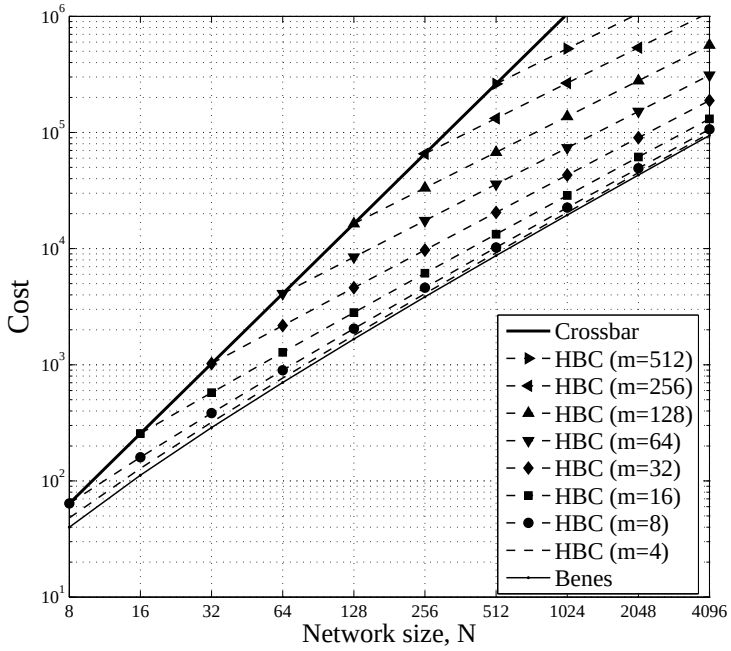

Figure 4.9: Complexity for different HBC networks

Figure 4.10 depicts the number of turns for several HBC networks. From the scalability point of view, these different m-sized HBC networks present the same growing pattern as the Benes structure. Moreover, for lower values of m the structure has a higher number of turns reaching the Benes curve. But for higher values of m the offset gets reduced obtaining a lower curve.

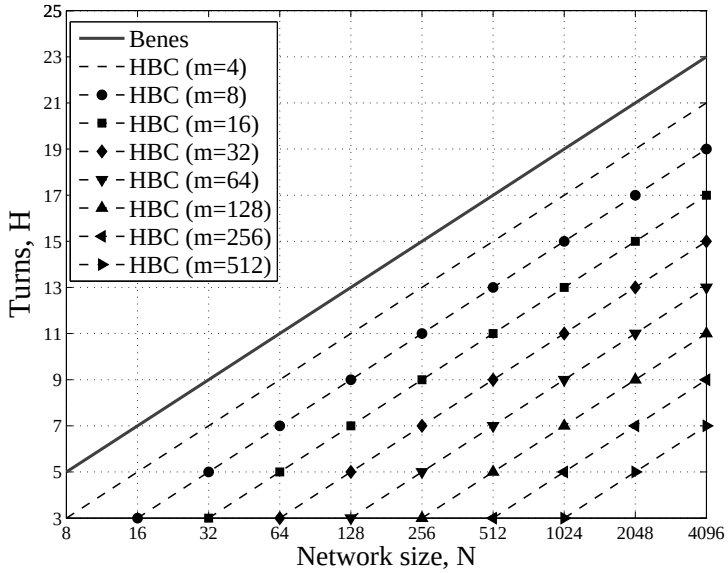

Figure 4.10: Scalability for different HBC networks

In conclusion, we have presented a structure where the advantageous characteristic of Benes and crossbar can be both exploited into a balanced solution. Nevertheless, we have seen that those HBCs with small m are cheaper but exhibit a poor scalability while HBCs with a higher m offer better scalability but also an expensive complexity.

4.3.2 mirrored HBC

With the aim at finding a better solutions for the trade-off between complexity and scalability, we define a construction rule that combines the HBC structure with the mirroring technique.

Construction rule

Figure 4.8 presents the mirrored hybrid Benes-crossbar (M-HBC). We can observe that the upper plane is equivalent at the HBC network depicted in Figure 4.8a. The lower plane is obtained changing all the 2B-SEs by 2M-SEs.

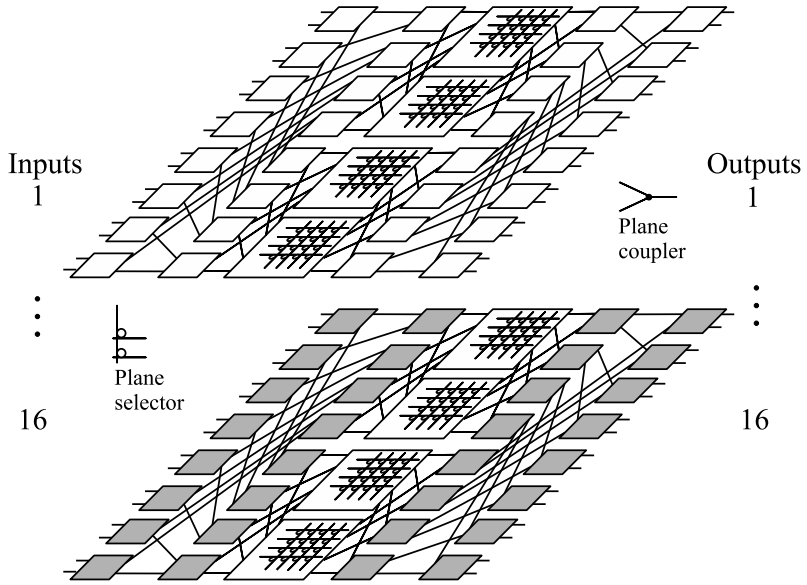

Figure 4.11: $N = 16$ HBC mirrored network $m = 4$ crossbar inside

Therefore, we can define the construction rule to obtain a M-HBC as:

1. Build a N-sized HBC network.
2. Add a plane topologically equivalent at the HBC previously build but now with 2M-SEs.
3. Incorporate plane selectors at the beginning of the network and plane couplers at the end.

Scalability $H(N)$ and cost $C(N)$

The cost for the M-HBC network can be obtained as twice the HBC plus the plane selectors.

$$C_{M-HBC}(N,m) = 2 \cdot [2Nlog_2(\tfrac{N}{m}) + N \cdot m] + 2N$$

$$C_{M-HBC}(N,m) = 4Nlog_2(\frac{N}{m}) + 2N(m+1) \tag{4.10}$$

We can obtain the closed expression for the scalability dividing H_{HBC} by two, applying the floor function and adding one turn due to the selector. In fact, these three operations are the result of applying mirroring to a network.

$$H_{M-HBC}(N,m) = \lfloor \frac{2log_2(\frac{N}{m}) + 1}{2} \rfloor + 1 \tag{4.11}$$

Network accomplishment (achievement)

Figure 4.12 shows different cost functions for several M-HBC networks. Now several networks are expensive than the crossbar structure due to the unsuitable result when mirroring a high m-sized inner crossbar. All the solutions are bounded by the the Benes cost at the lowest part, but now they suffer a offset because of mirroring property. Within the crossbar-Benes range, we still have that from one side, the smaller is the size of the m crossbars inside, the nearer is the cost of the function to the Benes limit. But from the other side, the higher is the m-sized crossbar inside structure, the closer is the cost to the crossbar N^2 function.

Figure 4.13 depicts the number of turns for several M-HBC networks. From the scalability point of view, these different M-HBC networks present the same growing pattern as the mirrored Benes structure (that is half growing of the basic Benes network).

In conclusion, when we exploit mirroring, the complexity of the HBC gets doubled but the number of turns gets reduced. And as the not mirrored case, those M-HBCs with small m are cheaper but exhibit a poor scalability while M-HBCs with a higher m offer better scalability but also an expensive complexity.

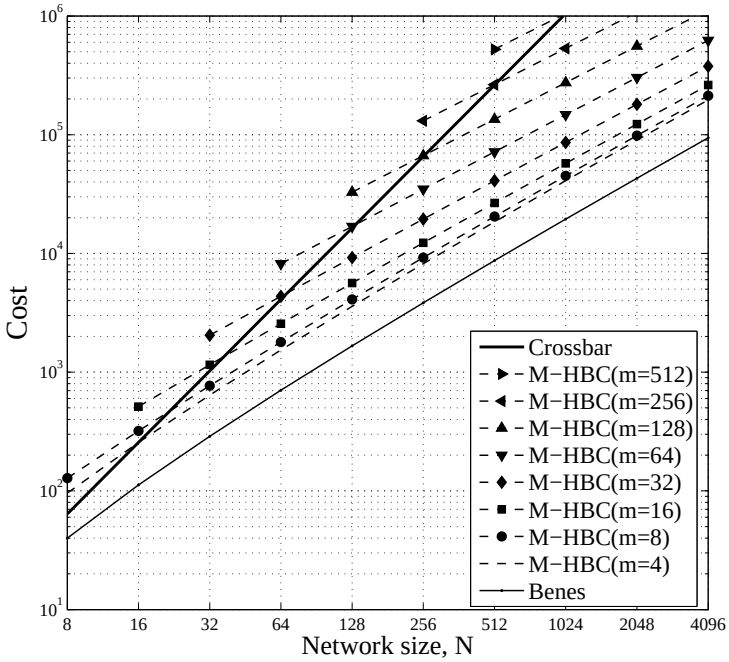

Figure 4.12: Complexity for different M-HBC networks

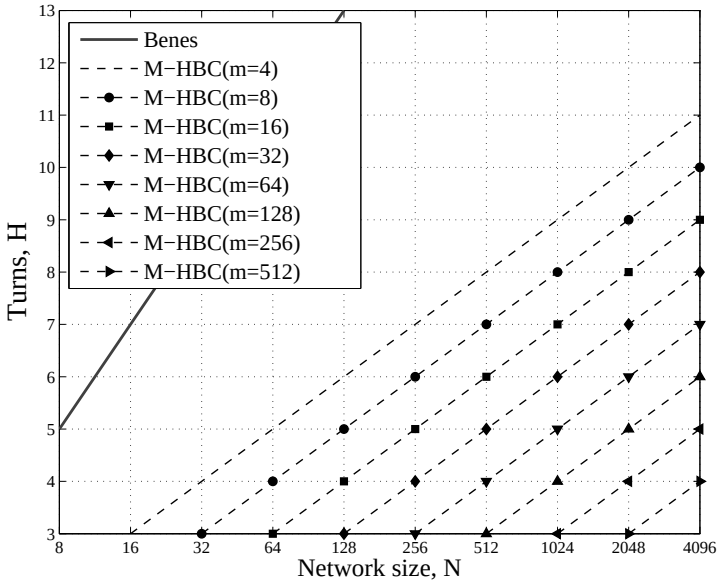

Figure 4.13: Scalability for different M-HBC networks

4.4 Clos

In this section we aim at analysing the scalability behaviour of the well-known Clos network. Firstly we present the Clos structure and its characteristics and secondly we assess several modifications of its construction rule to explore new solutions.

Construction rule

Figure 4.14 shows the construction procedure to obtain a generic three-stage network. The stages of this network are made with different sized interconnection matrixes instead of 2x2 Switching Elements. For instance, we can observe the non-squared matrixes having n inputs and p outputs in the first stage, and p inputs and n outputs in the last stage.

Therefore, it is also shown in Figure 4.14 that second stage is build considering p switching matrixes with the same number of inputs and outputs (k). Hence, squared switching matrixes can be implemented with different structures allowing us several freedom on the architecture design.

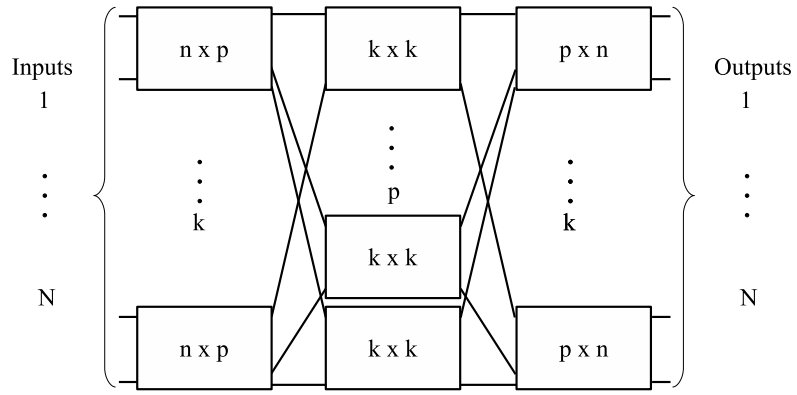

Figure 4.14: Three stage network construction detail

In Section 2.2 we have presented several properties for this type of network, now we recall those interesting properties to characterise the networks delimiting several parameters.

Rearrangeable non blocking (RNB) condition:

$$p \geq max(n_1,n_3) = n \quad p = n$$

Instead of strictly non blocking (SNB) condition:

$$p \geq n_1 + n_3 - 1 = 2n - 1 \qquad p = 2n - 1$$

Optimal n that minimises the network cost (for both RNB and SNB cases):

$$n \cong \sqrt{\frac{N}{2}}$$

We define ρ as a ratio between n and p to have a parameter that easily identifies the point that we are analysing in the range from rearangeable case to the strictly non blocking case. In fact, ρ is also the building ratio between inputs/outputs of the matrixes in first and last stages.

Three different values of ρ are considered during this network characterisation. From one side, we consider RNB case taking $p = n$. Then as an middle step, we set ρ with an intermediate value between RNB and SNB. And from the other side we take $p = 2n - 1$. Thus, Table 4.1 shows the values considered.

		$\rho = \frac{n}{p}$
RNB	$p = n$	$\rho = 1$
Intermidiate	$p = \frac{4}{3}n$	$\rho = 0{,}75$
SNB	$p = 2n - 1$	$\rho \simeq 0{,}5$

Table 4.1: Values for ρ in the range from RNB to SNB

At this point we consider diverse variations for this generic three-stage network. First we analyse the all crossbar three-stage solution finding its scalability and cost. We analyse that Clos-crossbar for different sizes of the first and last stage matrixes. Then, a three-stage with a Benes network in the middle is characterised by its metrics $H(N)$ and $C(N)$. And finally, we consider a solution using in the middle stage the mirroring technique for the switching matrixes with Benes networks.

4.4.1 Clos all crossbar

Lets consider the structure shown in Figure 4.15 whose switching matrixes are made with crossbar structures (named Clos for the rest of this work).

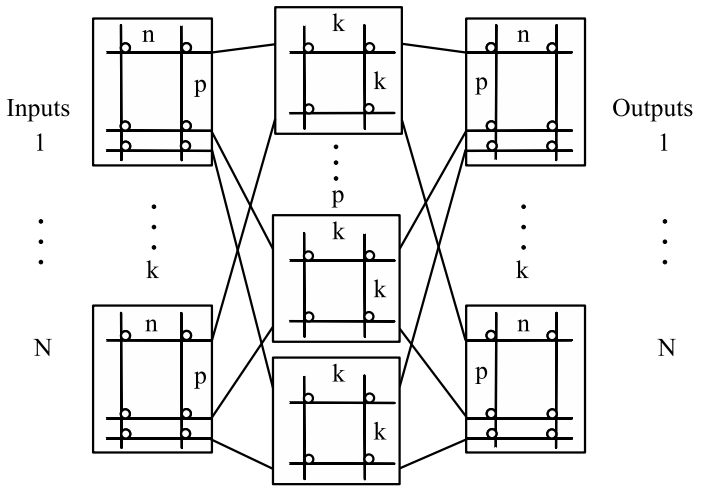

Figure 4.15: Three stage network with all crossbar switching matrixes

Scalability $H(N)$ and cost $C(N)$

We can easily obtain $H(N)$ for this specific structure made with three-stage of crossbar switching matrixes. Connections routed through this structure need to pass one 1B-SE in HLS at each crossbar to get the correct output. So, taking into account from Section 3.2 the examples presented, we can simply add one counter (number of SE in HLS) for each stage. Thus, we get the following expression:

$$H_{Clos}(N) = 3 \tag{4.12}$$

The cost for this structure can be extrapolated from the construction rule and considering that all crossbar switching matrixes have a microring at each cross point. So we obtain for this three-stage switching fabric:

$$C_{Clos}(N) = n \cdot p \cdot k + k^2 \cdot p + p \cdot n \cdot k \tag{4.13}$$

Equation 4.13 separates the contribution to the total cost of the network in three addends, one for each stage. As already mentioned n is $\sqrt{\frac{N}{2}}$ when possible, or the next integer value for those cases that do not give a feasible value (decimal). And finally, expressing k and p as a function of N, we obtain Equation 4.14 that gives us the total cost as a function of N and ρ.

$$C_{Clos}(N,\rho) = \frac{\sqrt{2}}{\rho} N^{\frac{3}{2}} \tag{4.14}$$

Network accomplishment (achievement)

Let us observe the behaviour of those expressions in Figure 4.16 where network cost is calculated with the three different values of ρ presented in Table 4.1, that is for $\rho = 0.5$ (SNB case), $\rho = 0.75$ (intermediate case) and $\rho = 1$ (RNB case).

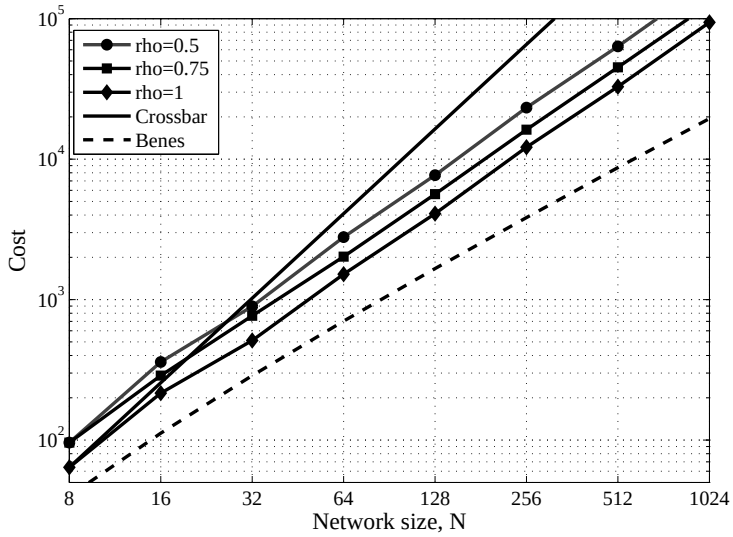

Figure 4.16: Cost for Clos networks with all crossbar switching matrixes

The cost of the SNB construction is about twice the cost of the RNB construction for almost all N sizes. For the first network size $N = 8$ we have that $\rho = 0.5$ (SNB) and $\rho = 0.75$ (intermediate) constructions correspond to the same building structure, so they exhibit the same cost. We can also observe two slightly curves for the cost at network sizes between 16 and 64

(of a expected straight behaviour) due to the infeasibility of building optimal switching matrixes for certain values N. For larger network sizes $N \geq 128$, the three alternatives present the same increasing behaviour, letting clearly be the SNB more expensive than the intermediate construction ($\rho = 0.75$) and the RNB having the cheapest cost.

Finally, since the three constructions perform with $H(N) = 3$, we can select the solution attending to the trade-off between cost and rearrangeability of the network.

4.4.2 Clos-Benes (HCB)

Figure 4.17 depicts a three-stage Clos structure whose switching matrixes in the middle stage are made with Benes networks (Hybrid Clos Benes HCB). For simplicity reasons, we consider from now on the rearrangeable condition, that is $n = p$. Thus, the ratio "ρ" remains equal to one for this network.

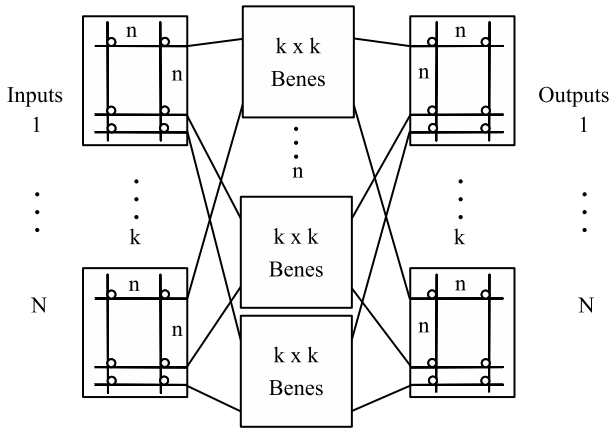

Figure 4.17: Clos-Benes network (HCB)

We can also infer from Figure 4.17 that first and last stages remain with crossbar switching matrixes as the structure characterised before in Section 4.4.1 (Clos all crossbar). As we already mentioned, squared switching matrixes in the middle can be easily build with diverse structures, e.g. Benes as follows. Therefore, we consider k squared switching matrixes of n inputs and outputs in the first stage made with crossbar structures; n squared Benes

sub-networks of size k; and as the first stage, the last third with k crossbar switching matrixes of n inputs and outputs.

It is important to mention that n must satisfy two conditions for a feasible construction: $n \leq \frac{N}{2}$ to do not degenerate the network into a double crossbar N^2 solution; and $n \geq 2$ because at least, the first and last stages of the HCB should be higher than the 2x2 SEs of the complete Benes solution.

Scalability $H(N)$ and cost $C(N)$

Let us proceed with the cost calculation for this network attending to the description presented above and recalling the Benes construction rule. Thus, we sum the three stages in the same way that we proceeded in Equation 4.13 but for this HCB case.

$$C_{HCB}(N) = n \cdot n \cdot k + C_{Benes}(k) \cdot n + n \cdot n \cdot k \tag{4.15}$$

Where $C_{Benes}(N) = 2 \cdot N \log_2 N - N$ (see Equation 4.2); and $k = \frac{N}{n}$

$$C_{HCB}(N,n) = 2N \log_2(\frac{N}{n}) + N(2n-1) \tag{4.16}$$

We can observe the similarity between Equation 4.16 (cost for a HCB) and Equation 4.8 (cost for a HBC). In both cases we have the degree of freedom given by the size of the crossbar structure (m in HBC and n in HCB respectively).

Regarding to the scalability performed, now $H(N)$ depends on the size of the Benes networks built at the middle stage. In fact, we must consider two turns due to the first and last stages respectively plus the turns in the middle Benes. We obtain the following expression:

$$H_{HCB}(N) = 1 + (2log_2(\tfrac{N}{n}) - 1) + 1$$

$$H_{HCB}(N) = 2log_2(\frac{N}{n}) + 1 \tag{4.17}$$

Network accomplishment (achievement)

Figure 4.18 shows the complexity for different HCB networks. We can observe that all the solutions are still bounded by the Benes cost at the lowest part. Nevertheless, the upper bound set by the all crossbar N^2 solution is crossed at the beginning of each network. In fact, this confirms the first previously feasibility condition presented ($n \leq \frac{N}{2}$), obtaining for each network:

- When $n = N$ does not satisfying the feasibility condition. Because of that, we obtain a cost equal to twice N^2 crossbar solution (see first cost of each network in Figure 4.18).
- When $n = \frac{N}{2}$, that is the second value for the cost of each network, we are on the bound set by the continuous line of the crossbar solution.
- Finally, this solution becomes complexity-advantageous when $n < \frac{N}{2}$.

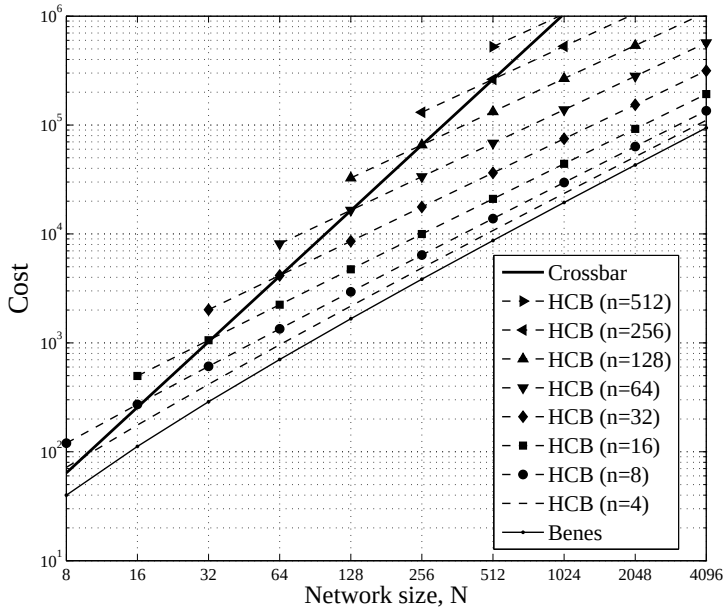

Figure 4.18: Complexity for different HCB networks

Figure 4.19 depicts the number of turns for several HCB (Hybrid Clos-Benes) networks. From the scalability perspective, this solution offers exactly the same behaviour as HBC (Hybrid Benes-Crossbar). Thus, we can observe

for all these networks the same growing pattern as the Benes network; for lower values of n the structure has a higher number of turns reaching the Benes curve; and for higher values of n the number of turns gets reduced.

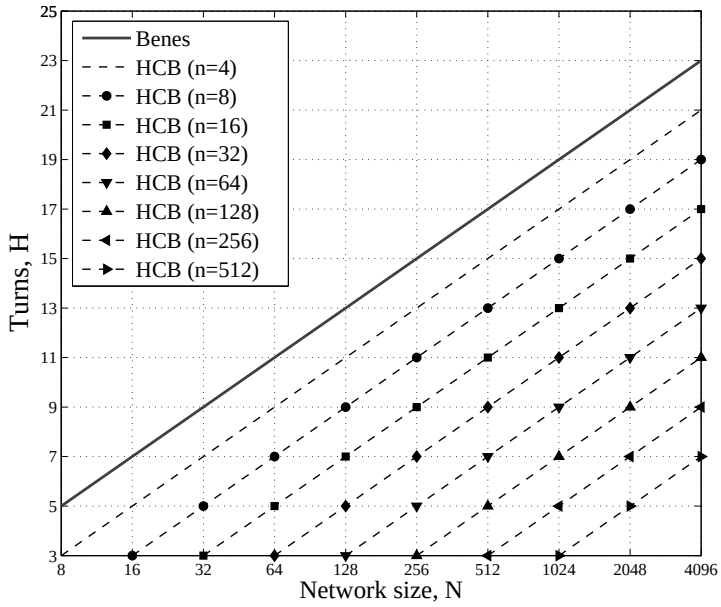

Figure 4.19: Scalability for different HCB networks

In conclusion, we have presented another structure where the advantageous characteristics of Benes and crossbar can be both exploited into a balanced solution. Nevertheless, in this case we have built first and last stages with crossbar-matrixes letting the inner part for a Benes network. We have seen that these HCBs present the same scalability as the HBCs but exhibiting a slight increased complexity. Finally, as in the previous section, for small values of n the network becomes cheaper but exhibits a poor scalability while HCB with a higher n offers better scalability but also an expensive complexity.

4.4.3 Clos-mirrored Benes (M-HCB)

Figure 4.20 presents the mirrored hybrid Clos-Benes (M-HCB). We can observe that several modifications are needed to apply the mirroring technique in the middle stages.

- First and last stage switching matrixes get double-sized. We need to select for each input between double number of switching matrixes in the middle. Thus, switching matrixes at first stage become n x $2n$ and switching matrixes at last stage become $2n$ x n.
- All Benes networks of size k x k get mirrored. That is built a lower plane changing all the 2B-SEs by 2M-SEs.
- Each switching matrix must be linked from first and last stages to all normal/mirrored planes in the middle. Links devoted to normal planes are dashed, and links devoted to connect mirrored planes are in continuous line (see Figure 4.20).

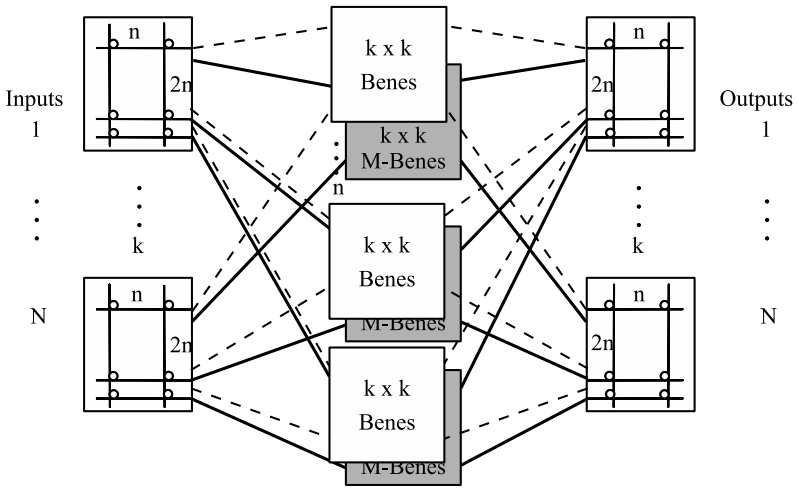

Figure 4.20: Clos-mirrored Benes network (M-HCB)

Scalability $H(N)$ and cost $C(N)$

The complexity presented by this M-HCB network is twice the HCB because of the mirroring technique. Moreover, there is no need to add plane selectors

(as we have previously seen) because the crossbar switching matrixes at first and last stages let us choose between both planes. Thus, we sum the three stages in the same way that we proceeded in Equation 4.13 and 4.15 but for this M-HCB case.

$$C_{M-HCB}(N) = n \cdot 2n \cdot k + 2 \cdot C_{Benes}(k) \cdot n + 2n \cdot n \cdot k \tag{4.18}$$

Where $C_{Benes}(N) = 2 \cdot N \log_2 N - N$ (see Equation 4.2); and $k = \frac{N}{n}$

$$C_{HCB}(N,n) = 4N \log_2(\frac{N}{n}) + 2N(2n-1) \tag{4.19}$$

We can observe the similarity between Equation 4.19 (cost for a M-HCB) and Equation 4.10 (cost for a M-HBC). In fact, both cost expressions double their basic network construction due to the mirroring technique. And as we mentioned in the basic HCB case, we still have the degree of freedom given by the size of the crossbar structure (m in HBC and n in HCB respectively).

Regarding to the scalability performed, now $H(N)$ is reduced to the half from the exhibited by the not mirrored network.

$$H_{M-HCB}(N) = \lfloor \frac{H_{HCB}(N)}{2} \rfloor + 1$$

$$H_{HCB}(N) = \lfloor \frac{2log_2(\frac{N}{n}) + 1}{2} \rfloor + 1 \tag{4.20}$$

Network accomplishment (achievement)

Figure 4.21 shows the complexity for different M-HCB networks. We can observe that all the solutions are still bounded by the Benes cost at the lowest part. But now, has increased the feasible restriction that should be satisfied by the crossbar upper bound. In fact, because of the mirroring application, the complexity has been slightly incremented obtaining the following:

- Now $n = N$ and $n = \frac{N}{2}$ do not satisfying the feasibility condition. Because of that, we obtain a cost equal to four times and twice N^2 crossbar solution respectively (see first cost of each network in Figure 4.21).

- When $n = \frac{N}{4}$, that is the second value for the cost of each network, we are on the bound set by the continuous line of the crossbar solution.
- Finally, this solution becomes complexity-advantageous when $n < \frac{N}{4}$.

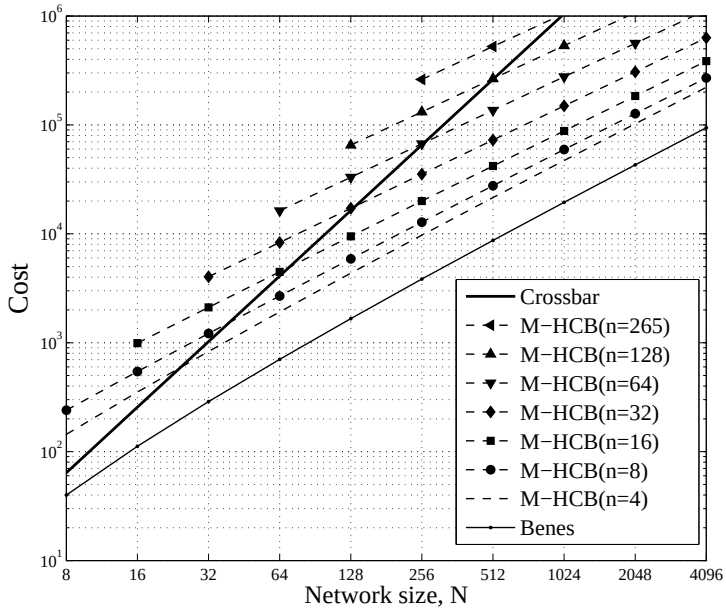

Figure 4.21: Complexity for different M-HCB networks

Figure 4.22 depicts the number of turns for several M-HCB (mirrored Hybrid Clos-Benes) networks. From the scalability point of view, these different networks present the same behaviour as M-HBC (mirrored Hybrid Benes-Crossbar). And at the same time, the growing pattern is the performed by mirrored Benes structure (that is half growing of the basic Benes network).

Concluding this 4.4Clos section, we have presented a different solution that combines Clos (with crossbar switching matrixes) and Benes networks (HCB). We have obtained similar results as in the HBC case in terms of complexity and scalability. Finally, we have applied the mirroring technique at the Benes-like part confirming the likelihood between M-HBC and M-HCB.

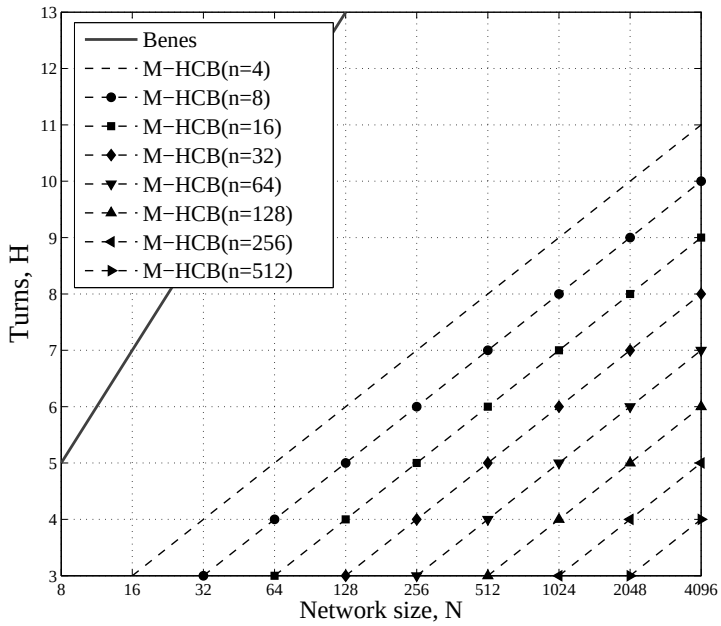

Figure 4.22: Scalability for different M-HCB networks

4.5 Vertical Replication

In this section we present a construction rule slightly different from the well-known vertical replication (VR). In fact, after recalling a rather similar exhaustive characterisations, we aim at presenting VR and defining mirroring-VR (M-VR) in order to give an alternative solution exploiting the vertical dimension. Then, we formulate the scalability $H(N)$ and cost $C(N)$ obtained and as we have done previously, we evaluate those expressions graphically.

Simulation results

We have analysed in Section 3.6.2 a four plane Benes network used to route 8x8 requested matchings (Figure 3.38 equal as Figure 4.23a). The main idea beyond that procedure is to obtain more benefit from the mirroring technique by considering an expensive network. Moreover, we can exploit the vertical dimension building Banyan mirrored networks instead of mirrored Benes.

Figure 4.23 depicts the three steps followed. From the first structure considered as a slight variation of the mirroring procedure to the last structure

that implicitly answers to the VR technique, we have that:

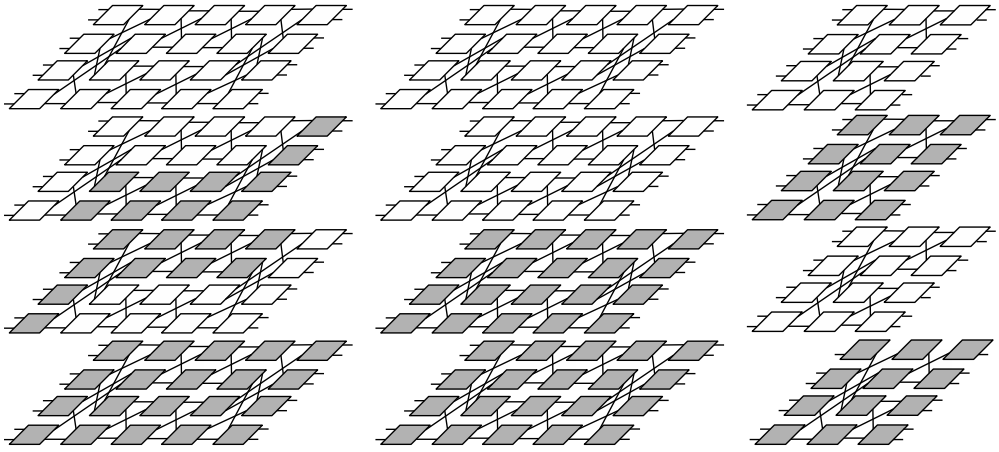

(a) First approach to the VR (b) Four Benes networks equal per pairs (c) Four Banyan networks

Figure 4.23: N=8 structures considered from mirroring partial planes (a) to Banyan VR (c)

1. Network 4.23a is the initial idea that explores a rather mirroring property already discussed in Section 3.6.2. As we have previously seen, there is a higher portion of matchings (near 39.000 of the existing 40.320) that need to pass through two SEs in HLS. Thus, adding the need of a plane selector at the beginning of the network gives us a worst case connection of three SEs in HLS for the most of the matchings, setting $H(8) = 3$.

2. Network 4.23b is an intermediate step between the first structure deduced from the mirroring property and the final Banyan VR. It consists of a VR and mirroring simultaneously applied to a Benes network (two planes with 2B-SE as a building element, and two planes made with 2M-SE). An analogous exhaustive characterisation of this network as the done for 4.23a does not exhibit a significant variation on the obtained result. Therefore, due to the plane selectors and the network depth, we still obtain $H(8) = 3$ as the number of turns for this network.

3. Network 4.23c results from the application of two building steps to a N=8 Banyan structure (half depth of a Benes network). First, we

make a two Banyan networks due to the value of the *Utilisation factor (Uf)* (explained in the following) for a N=8 structure. Both networks with white boxes as 2B-SE and then, two mirrored Banyan networks (one for each of the previous generated plane) both with grey boxes as 2M-SE. It is important to mention that for this third network there is no need to apply the exhaustive characterisation due to the noticeably reduction of the network's depth.

Construction rule

Figure 4.24 depicts basic VR and M-VR constructions. We can infer the following points:

- N plane selectors for both networks. These selectors are 1xk for the basic network (see Figure 4.24a), and 1x2k for the mirrored network (see Figure 4.24b) in order to let choose between all the available planes.
- k Banyan planes built in basic network.
- $2k$ Banyan planes in the mirrored network. k planes are devoted to the basic Banyan, and k planes are mirrored-type Banyan.
- The number of planes is taken considering the *utilization factor (Uf)* [16]. That *Uf* is defined as the maximum number of I/O paths that cross a generic interstage link. Thus, given a Banyan topology with size N including k planes is rearrangeable if and only if:

$$k \geq Uf = 2^{\lfloor \frac{\log_2 N}{2} \rfloor} \tag{4.21}$$

Scalability $H(N)$ and cost $C(N)$

Banyan vertically replicated network shown in Figure 4.24a presents a number of turns equal to the depth of the Banyan structure plus the plane selector.

$$H_{VR}(N) = \log_2 N + 1$$

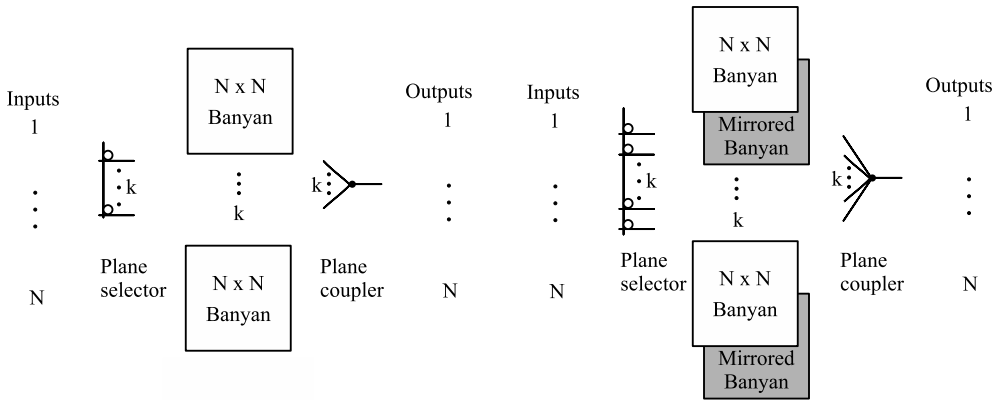

(a) Vertical replication of a Banyan network

(b) Vertical replication of a the pair Banyan and mirrored Banyan networks

Figure 4.24: VR and M-VR applied to a Banyan network

Regarding to the complexity, we can obtain a closed expression separating the contribution of two addends. The first one counts the number of microrings used at the plane selectors (for N inputs to choose from Uf planes). And the second addend considers the cost of Uf Banyan planes:

$$C_{VR}(N) = N \cdot Uf + N \log_2 N \cdot Uf$$

Now, we proceed to the calculation of $H(N)$ and $C(N)$ for the mirrored VR (see Figure 4.24). As we have seen in previous cases, mirroring the network we obtain half number of turns, but doubling the complexity. Thus, we obtain the following expressions:

$$H_{M-VR}(N) = \lfloor \tfrac{\log_2 N}{2} \rfloor + 1$$

$$C_{M-VR}(N) = 2 \cdot (N \cdot Uf + N \log_2 N \cdot Uf)$$

Network accomplishment (achievement)

Figure 4.25 shows the cost for the VR and M-VR networks compared with crossbar and Benes. We can observe that in this graph both logarithmic scales reach higher values than previously. In fact, the complexity exhibited by this network is higher than the cost seen by other solutions. It is important to mention that VR becomes cost-advantageous for $N \geq 128$ while M-VR

is cost-advantageous for sizes $N \geq 512$ both with respect to the crossbar. Moreover, the growing pattern of these two networks is nearer to the crossbar than to the Benes as a consequence of the Uf planes needed.

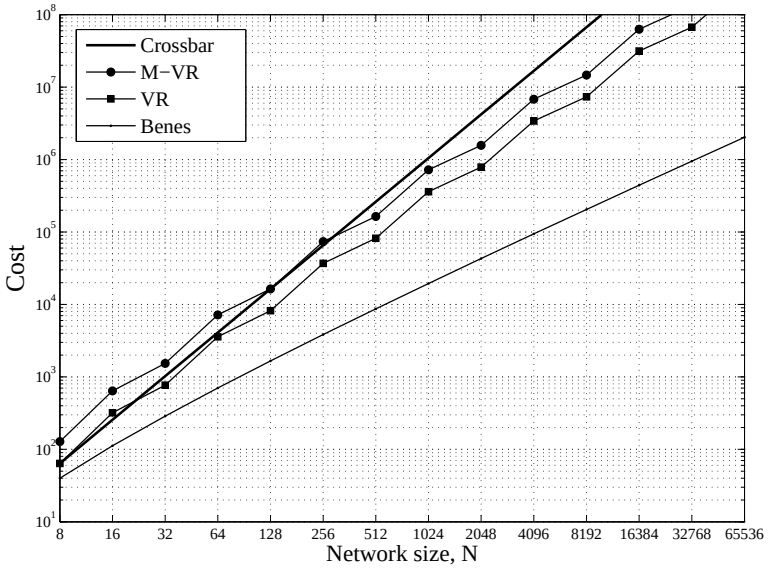

Figure 4.25: Cost for VR and M-VR networks

Figure 4.26 depicts the scalability behaviour for both VR and M-VR structures compared with Benes and M-Benes. We can observe that VR has a growing behaviour equal to the M-Benes because of its growing behaviour equal to $\log N$. Therefore, when we apply mirroring to the VR structure, we reduce twice the normal Benes scalability function. Consequently obtaining the addition of only one turn every two network sizes.

In conclusion, VR and M-VR presents possibly the highest complexity between all the networks presented in this chapter. But from the scalability perspective, the number of turns performed has reaches the lowest growing behaviour analysed.

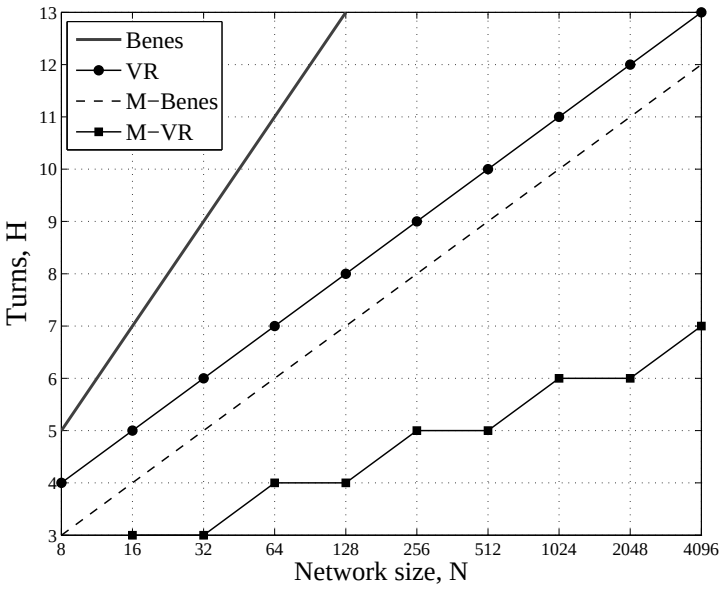

Figure 4.26: Turns for VR and M-VR networks

4.6 Discussion

In this section we aim at comparing all the network structures seen in this chapter. Firstly we point out their relevant characteristics regarding to the complexity. Secondly, we compare them from the scalability point of view. And finally, we conclude identifying the best solutions for the trade-off attending to the previous obtained observations.

Complexity

Figure 4.27 shows the cost for the most remarkable networks analysed in this chapter for sizes from 8 to 8.192 ports. Continuous lines depict basic structures while dashed lines and "M-" prefix are used to identify mirrored structures.

We can infer the following points:

I The cost exhibited by crossbar is the highest when we apply the feasibility condition to the M-HBC network. Therefore, despite $m = N$ M-HBC cases, crossbar is the upper bound for the cost.

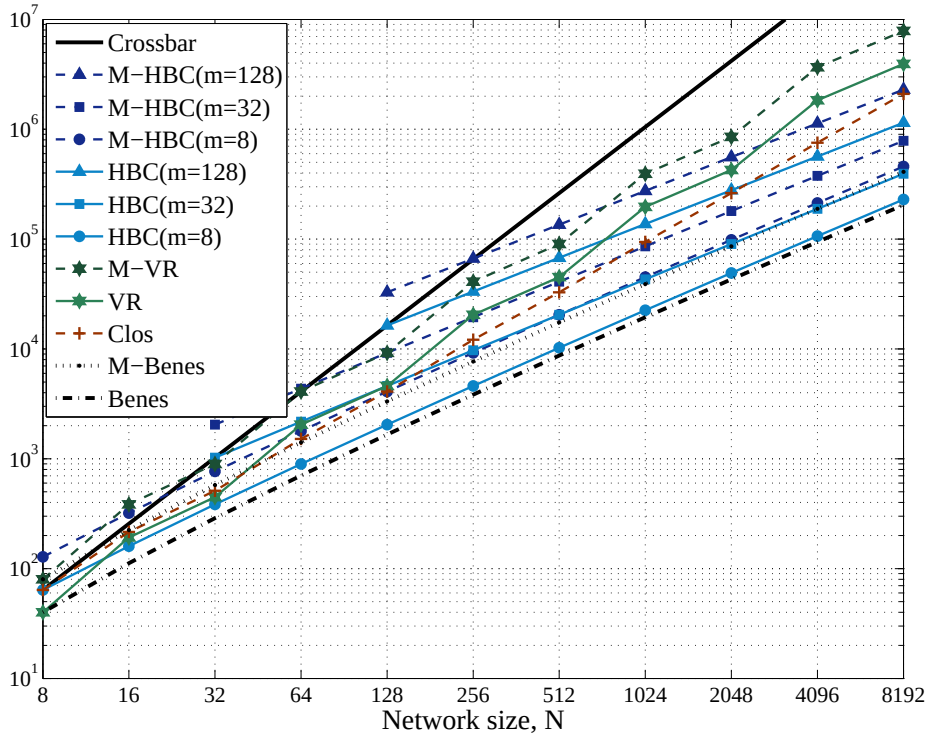

Figure 4.27: Complexity for several architectures as a function of N

II Benes network shows the lowest achievable complexity between all the architectures.

III Two hybrid solutions have been presented in Sections 4.3 and 4.4.2 (Hybrid Benes-Crossbar HBC and Hybrid Clos-Benes HCB respectively). Among both, HCB usually exhibits a higher complexity than HBC. Because of that we have depicted only the complexity for HBC architecture, letting HCB be considered as a slight cost-disadvantageous similar solution.

IV The approach used for HCB and HBC in the previous point holds for their mirrored solutions.

V Benes-based networks (e.g. HBC, M-HBC, HCB, M-HCB, Benes and M-Benes) present a similar growing behaviour, that is proportional to $N \log_2 N$. The cost offset of each Benes-based network depends on two

features: firstly, for higher values of crossbar matrixes (m or n) the network becomes expensive; and secondly, mirroring technique doubles the complexity (incrementing the starting point of the curve).

VI Clos network has an intermediate growing pattern between crossbar and Benes. For sizes $N \leq 128$ Clos network exhibits a similar cost as M-Benes network.

VII Accomplishing the crossbar upper bound, M-VR and VR architectures show the highest complexity for $N > 512$ and $N > 2048$ respectively,

Number of turns, H

Figure 4.28 shows the number of turns for the most remarkable networks analysed in this chapter for sizes from 8 to 8.192 ports. As in the cost analysis, continuous lines depict basic structures while dashed lines and "M-" prefix are used to identify mirrored structures.

We can infer the following points:

i The number of turns (H) cost of crossbar is the lowest (best) achievable. Due to the fact that this structure is made by a squared matrix of 1B-SEs, it performs constantly as $H(N) = 1$.

ii Benes network shows the highest (poorest) number of turns between all the architectures.

iii Hybrid HBC and HCB exhibit the same number of turns when $m = n$.

iv The approach used for HCB and HBC in the previous point holds for their mirrored solutions.

v Basic Benes-based networks HBC and HCB present a similar growing number of turns as Benes network, that is proportional to $2\log_2 N$. The offset of each basic Benes-based network depends on its m or n, for higher values of crossbar matrixes the network exhibits lower Hs.

vi Networks M-HBC M-HCB and VR present a similar growing number of turns as mirrored Benes, that is proportional to $\log_2 N$. The starting

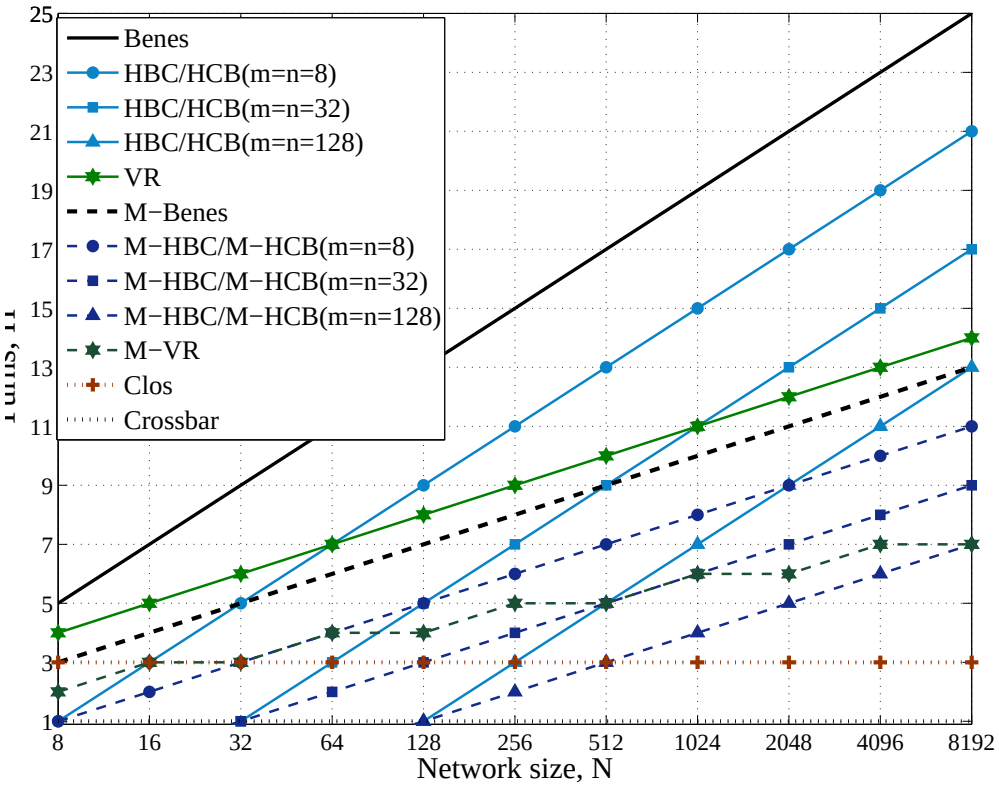

Figure 4.28: Number of turns for several architectures as a function of N

number of turns for each network still depends on its m or n, for higher values of crossbar matrixes the network exhibits lower Hs.

vii M-VR is the only network showing a number of turns proportional to $\frac{1}{2}\log_2 N$.

viii Accomplishing the crossbar lower bound, Clos network has the lowest number of turns exhibiting $H(N) = 3$.

Trade-off solutions

Previous points **I**, **II**,**i** and **ii** illustrate perfectly both limits of the trade-off between C and H. From one side, Crossbar network exhibits the highest complexity and the best number of turns, while from the other side, Benes network is the cheapest and poorest solution. Therefore, the following points of the previous cost-turns characterisations are devoted at offering intermediate and balanced architectures such as HBC or HCB.

Hybrid solutions can be designed to satisfy a specific requirement in number of turns by varying m and n. In order to characterise these networks, we should remain with a constant ratio $\frac{N}{m}$ or $\frac{N}{n}$ at every building step. This approach offers the possibility to select a constant number of turns for the hybrid solution but exhibiting a increased growing pattern. Instead, through this comparison we have considered constant-sized crossbar matrixes in hybrids construction.

Points **V**, **v** and **vi** show the mirrored technique allowing to go from N to a $\frac{N^2}{2}$ sized architecture with the same number of turns by doubling the complexity.

In conclusion, Clos network exhibits the best balanced solution for lower network sizes and for severe requirement in number of turns. When the number of ports increases (e.g. $N \geq 1024$) we can consider different alternatives if a higher number of turns is allowed.

Chapter 5

Conclusion

5.1 Main findings

We have analysed several solutions to the trade-off between complexity and scalability of interconnection architectures based on microring resonators.

Through the first part of this work, we have introduced microring resonators focusing on several features. We have defined basic 1x2 and two 2x2 SEs emphasising the asymmetric performance of these switching elements.

Then, using those SEs as a building elements, several $N = 4$ and $N = 8$ sized networks have been exhaustively analysed. This procedure has given the possibility to point out the best cost/scalability performances in small-sized networks.

- From one side, we have obtained interesting results in Section 3.4.2 Modified Benes for $N = 4$ network ($C_{mod.Benes}(4) = 12$ and $H_{mod.Benes}(4) = 2$) or in Section 3.7 HBC where hybrid solution exhibits $C_{HBC}(8) = 48$ with a number of turns $H_{HBC}(8) = 3$.

- But from the other side, we have obtained unsuitable solutions such as $N = 8$ modified Benes network ($C_{mod.Benes}(8) = 40$ and $H_{mod.Benes}(8) = 4$) or the four plane network in Section 3.6.2 $C_{4pl\ Benes}(8) = 192$ with $H_{4pl\ Benes}(8) = 3$.

Summarising, a considerable part of the work has been done in Chapter 3 in order to comprehend for small-sized architectures the challenge of this

trade-off.

After that study for small scenarios, we have faced the cost/scalability trade-off for large switching fabrics. It is important to mention that in this work construction rules are considered as results inferred from the exhaustive analysis.

Therefore, we have characterised the well-known crossbar, Benes and Clos architectures when using microring resonators as a building elements. Then, intermediate solutions have been presented in order to give a performance balanced between the bounds of the trade-off (highest complexity but lowest number of turns given by the crossbar structure, and cheapest but poorest solution achieved by Benes network).

We have aimed at proposing several new architectures, defining hybrid Benes-crossbar (HBC) and hybrid Clos-Benes (HCB) which enable an extra parameter on the network design. Hence, considering different m-sized crossbars inside the HBC or n-sized crossbar matrixes at the edges of the HCB, we are able to give intermediate architectures between crossbar and Benes.

Additionally, we have defined in Sections 3.6 and 4.2 the mirroring technique. As we have seen, by offering an extra plane (which doubles the complexity of the network), the number of turns gets reduced at the half. Moreover, mirroring can be used at any Benes-likely part built by changing 2B-SE into 2M-SE without modifying the topology.

Finally, in Section 4.6 we have compared and discussed all the obtained results for the large-sized networks analysed in Chapter 4. Pointing out the well scalability performance achieved by the Clos network for lower network sizes and letting consider for larger architectures different alternatives if a higher number of turns is allowed.

In conclusion, the impairment due to the asymmetric behaviour of the microring resonator can be partially solved with a suitable network design.

5.2 Future research lines

Several research lines can be faced in order to continue the analysis of interconnection architectures based on microring resonators. For instance, four of them are mentioned in the following:

Complex microring model

Microring resonator based SEs defined in Section 3.1 do not consider wavelength characteristics. Thus, we can take into account properties defined in Section 2.1 such as FSR or switching time. Moreover, the consideration of these features should allow switching at each microring as a function of the WDM channel used.

AWG involvement

Arrayed Waveguide Gratings (AWGs) are passive devices able to behave as wavelength routers (the information at an input port is forwarded to an output port which depends on the input wavelength and the input port). An optical switching fabric made with AWG uses tunable transmitters and receivers around it equally if we consider the previous research line to build a passive microring-based architecture. Thus, considering a complex microring model and knowing the offered possibilities by an AWG, can be faced a deeper research in this field.

Scheduling algorithms

Through Chapter 3, we have obtained a high value for the worst-case performance in several exhaustive characterisations caused by a reduced number of matchings. For instance, histograms 3.27b and 3.28b have a $H(8) = 4$ due to 113 and 165 matchings respectively of the existing 40.320. For these cases, we can consider a scheduling algorithm at the beginning of the network able to route slightly different those worst-case matchings.

Final layout

We have described several construction rules where a considerable number of links crossed to build the network (e.g. Figures 4.6, 4.8a and 4.8b). Those connections have several physical feasibility conditions. Through this work we do not have mentioned any of them, and consider physical impairments for the architecture design should be another promising challenge.

Bibliography

[1] J.M. Tendler et al.
Power4 System Microarchitecture
IBM J. Research and Development vol. 46, no. 1, pp. 5-26, Jan. 2002.

[2] P. Kongetira, K. Aingaran, and K. Olukotun.
Niagara: A 32-Way Multithreaded SPARC Processor
IEEE Micro vol. 25, no. 2, pp. 21-29, Mar./Apr 2005.

[3] S. Vangal et al.
An 80-tile 1.28 TFLOPS network-on-chip in 65 nm CMOS
In International Solid State Circuits Conf. Feb. 2007.

[4] A. Shacham, B. G. Lee, A. Biberman, K. Bergman, and L. P. Carloni.
Photonic NoC for DMA communications in chip multiprocessors
Proc. 15th Annu. IEEE Symp. High-Performance Interconnects (HOTI 2007), CA, Aug. 2007.

[5] C. Gunn.
CMOS photonics for high-speed interconnects
IEEE Micro, 26(2):58 to 66, Mar./Apr. 2006.

[6] A. Shacham, A. Biberman, K. Bergman, and L. P. Carloni.
Photonic Networks-on-Chip for Future Generations of Chip Multiprocessors
IEEE Transactions on Computers, CA, vol. 57, no. 9, Sept. 2008.

[7] M. Petracca, K. Bergman, and L. P. Carloni.
Photonic Networks-on-Chip: Opportunities and Challenges
IEEE International Symposium on Circuits and Systems, May 2008.

[8] M. Petracca, B. G. Lee, K. Bergman, and L. P. Carloni.
Design Exploration of Optical Interconnection Networks for

Chip Multiprocessors
IEEE Symposium on High Performance Interconnects 2008.

[9] Chao Li, and Andrew W. Poon.
Silicon Electro-Optic Switching Based on Coupled-Microring Resonators
paper JThD115 *Optical Society of America* 2007.

[10] Benjamin G. Lee, Aleksandr Biberman, Po Dong, Michal Lipson, and Keren Bergman.
All-Optical Comb Switch for Multiwavelength Message Routing in Silicon Photonic Networks
IEEE Potonics Technology Letters, vol. 20, Iss. 10, May 2008.

[11] Sai Tak Chu, Brent E. Little, Wugen Pan, Taro Kaneko, and Yasuo Kokubun.
Cascaded Microring Resonators for Crosstalk Reduction and Spectrum Cleanup in Add Drop Filters
IEEE Potonics Technology Letters, Vol. 11, no. 11, Nov. 1999.

[12] P. Dong, S. Preble, and M. Lipson,
All-optical compact silicon comb. switch
Opt. Express, vol. 15, no. 15, pp. 9600 to 9605, Jul. 2007.

[13] B. G. Lee, A. Biberman, N.Sherwood-Droz, Carl B. Poitras, Michal Lipson, and K. Bergman.
High-Speed 2x2 Switch for Multi-Wavelength Message Routing in On-Chip Silicon Photonic Networks
European Conference on Optical Communication (ECOC), paper Tu.3.C.3, Sep 2008.

[14] Benjamin G. Lee, Aleksandr Biberman, N.Sherwood-Droz, Michal Lipson, and Keren Bergman.
Thermally Active 4x4 Non-Blocking Switch for Networks-on-Chip
Annual Meeting of the Lasers and Electro-Optics Society (LEOS), paper TuBB3, Nov 2008.

[15] S. Mookherjea, and A. Melloni.
Chapter **Microring resonators in integrated optics** in **Micro and Nanofabrication for Optics**

J.-C. Chiao (ed.) McGraw-Hill, 2009.

[16] Achille Pattavina.
Switching Theory Architectures and Performance in Broadband ATM Networks
John Wiley & Sons Ltd, 1998, Politecnico di Milano, Italy.

[17] Paolo Giaccone.
Switching Architectures - Part 2
May 2008. Politecnico di Torino, Italy.

[18] Andrea Melloni, and Mario Martinelli.
The ring-based Resonant Router
ICTON, Mo.B2.3, 2003.

[19] Andrea Bianco, Davide Cuda, Roberto Gaudino, Guido Gavilanes, Fabio Neri, and Michele Petracca
Scalability of Optical Interconnects based upon Microring Resonators

[20] A. Bianco, D. Cuda, P. Giaccone, M. Garrich, R. Gaudino, G. Gavilanes, and F. Neri.
Optical Interconnection Architectures based on Microring Resonators
International Conference on Photonics in Switching, Sept. 2009. Pisa, Italy.